

Thesis submitted in partial fulfilment of the requirements
for the degree of

Master of Science

Offshore and Dredging Engineering at
Delft University of Technology
Faculties of 3ME and Civil Engineering.

***Assessment of Marine Pipelines Subjected to Impact
from Dropped Objects***

Dimitrios M. Karras

October 20th, 2017

Graduation Committee:	Prof.dr. A.V. Metrikine	TU Delft
	Dr.ir. F.P. van der Meer	TU Delft
	Ir. J.S. Hoving	TU Delft
	Dr.ir. P. Liu	Intecsea BV

An electronic version of this thesis is available at <http://repository.tudelft.nl>

Page intentionally left blank

Abstract

When damage assessment is needed for an operating pipeline due to impact with an accidentally dropped object, DNV standards treat this case with conservatism and thus fail to give a realistic estimation. Usually, damage is measured as the dent deformation that the pipeline will experience. Depending on the size of the dent, leakage, rupture or cease of production might occur. Thus, it is important to quantify how a pipeline behaves and interacts with its environment during an impact with a dropped object.

Initially, a simple finite element model has been developed in order to verify some laboratory experiments from Karamanos and Gresnigt that have been conducted under quasi-static conditions, where no inertia or velocity need to be taken into account. The falling object's geometry, external or internal pressure and different material models have been investigated in order to derive preliminary conclusions regarding the stiffness of the system and the shape of the dent.

Next, velocity and mass of the indenter and of pipeline are taken into account in order to simulate the previous experiments dynamically. It has been observed that there are significant differences when inertia is taken into account in the denting behavior of a pipeline for low-velocity impact scenarios. Moreover, the effect of strain-rate sensitivities of steel have been incorporated by using the Cowper-Symonds law and their importance is stressed out in the results especially for mild steel pipelines.

In an effort to model closer the reality, simplified fluid models have been created using both the Lagrangian approach and the acoustic element formulation. This way, the partial incompressibility of the fluids, their inertia and their pressure can be modeled more accurately in order to reach valuable conclusions as to how they contribute in the system behavior.

All the aforementioned analyses have been conducted under the assumption that the bed upon the pipeline is resting is completely rigid. However, in reality the pipeline rests on a soil bed which is flexible and deformable. This is the most significant aspect of this thesis. Specifically, the energy dissipation due to the soil deformation and the pipe penetration into the soil is investigated. A soil – structure finite element model has been developed, considering a simplified Mohr-Coulomb elastoplastic model of failure which is adequate to obtain a good estimate regarding the soil contribution. It has been shown that for a range of different soil profiles of clay and sand, the energy dissipation is significant resulting in decrease of the dent deformation compared to a rigid bed case. Sensitivity analyses have been carried out regarding the impact velocity, mass and the initial embedment of the pipeline into the soil where it is shown that for the same kinetic energy input different results are being derived.

A final model is considered, where pressure, soil and strain-rate of steel are combined. The system behavior can be explained based on fundamental physics which give additional confidence in the interpretation of the results. Useful conclusions are derived in the end, showing that in many cases current practice is over conservative when assessing damage from dropped objects and thus a more detailed analysis and approach should be used in the future when conducting a risk or integrity assessment.

Page intentionally left blank

Acknowledgements

The research reported in this thesis is mainly performed at INTECSEA Delft, the sponsor company. There are a number of people I wish to thank for making this thesis possible.

First and foremost, I want to thank INTECSEA, Delft for offering the interesting topic and supporting me with the space and knowledge which was needed throughout the writing of this thesis. Especially, I would like to express my sincere gratitude to Mr. Ping Liu (INTECSEA) for his guidance throughout the year as well as for the valuable time he spent for our countless discussions on the subject. Also, I would like to thank Prof.dr. A. Metrikine for his critical feedback and guidance along the way. Furthermore, I would like to thank Dr.ir. F. van der Meer for his valuable feedback throughout the duration of this thesis.

I would also like to thank Ruud Selker, Pedro Ramos, Andreas Georghiou, Rafael Rodriguez, Emilien Bonnet and Deng-Jr Peng, all from the Intecsea office in Delft, for their valuable time discussing critical aspects of this thesis and for sharing with me their knowledge.

After two hard and at the same time very interesting and productive years, this journey is coming to an end. However, this wouldn't be possible without the constant support and faith of my family and friends from Delft and Greece. I would like to thank my family for all these years of support and understanding. Their unconditional love, patience and encouragement has helped me evolve not only as a scientist but as a human as well.

I would also like to commemorate my dear friend Georgios Papageorgiou, who passed away during my first days in Delft in September 2015. He has been a mentor, teacher but also a valuable friend for me.

Karras Dimitrios

Delft, October 2017

Page intentionally left blank

To my family

Michalis, Venetia
Giorgos & Pavlos

Page intentionally left blank

Contents

1.	Introduction.....	1
1.1	Background.....	1
1.2	Problem Definition.....	3
1.3	Research Objective	3
1.4	Approach.....	4
1.5	Thesis Outline	6
2.	Denting of Tubes	7
2.1	Introduction.....	7
2.2	Denting Resistance Mechanism.....	8
2.3	DNV Treatment of Denting	10
3.	Finite Element Model	15
3.1	Model Set-up.....	15
3.2	Model Parameters	16
3.3	Boundary Conditions	16
3.4	Material Model	17
3.5	Normalization of Results	18
3.6	Element Selection	19
3.7	Analysis Procedure	20
4.	Quasi-Static Denting.....	23
4.1	Length Sensitivity of Model	26
4.2	Shape of Indenter	27
4.3	Presence of Internal Pressure	30
4.4	Effect of External Pressure	33
4.5	Effect of Young's Modulus	35
4.6	Effect of Material.....	36
5.	Dynamic Denting.....	39
5.1	Introduction.....	39
5.2	Preliminary analysis.....	41
5.2.1	Fixed Tube of Finite Length	41
5.3	Semi-Infinite Tube.....	42
5.3.1	Model Length.....	42
5.3.2	Gravity in Dynamic Analysis.....	42

5.3.3	Dynamic vs Quasi-Static Analysis.....	43
5.4	Velocity Dependence.....	45
5.5	Strain-Rate Sensitivity.....	47
5.6	Damping Investigation.....	51
6.	Pipeline-Fluid Interaction.....	55
6.1	Introduction.....	55
6.2	Gas Filled Pipelines.....	56
6.2.1	Results and Comparison.....	57
6.3	Liquid Filled Pipelines.....	58
6.3.1	Model Description.....	59
6.3.2	Acoustic Elements.....	60
6.3.3	Fluid with Zero Pressure.....	61
6.3.4	Fluid under Pressure.....	64
6.4	Conclusions.....	65
7.	Soil Modeling.....	67
7.1	Introduction.....	67
7.2	DNV Treatment.....	68
7.3	Soil Properties.....	68
7.3.1	Soil Basic Properties.....	69
7.3.2	Young's and Shear Modulus.....	70
7.3.3	Undrained Shear Strength of Clays.....	71
7.3.4	Undrained Sand Behavior.....	73
7.4	Failure Models.....	77
7.5	Wave Propagation in Soil.....	78
7.6	Soil Finite Element Model.....	79
7.6.1	Soil Domain Dimension and Boundary Conditions.....	79
7.6.2	Meshing.....	82
7.6.3	Geostatic Stress Field.....	82
8.	Pipeline – Soil Interaction.....	85
8.1	Introduction.....	85
8.2	Analysis Procedure.....	86
8.3	Investigation of Soil Profiles.....	87
8.3.1	Unburied pipeline.....	88
8.3.2	Half-Buried Pipeline.....	91
8.4	Effect of Velocity.....	93

8.4.1	Soft Soil	94
8.4.2	Stiff Soil	95
8.5	Conclusions.....	97
9.	Combined Model	99
9.1	Introduction.....	99
9.2	Soil – Filled Pipe Model	99
9.2.1	Soil – Gas Model	100
9.2.2	Soil – Liquid Model.....	103
9.3	Soil – Strain-Rate Yielding Model	104
9.4	Conclusions.....	105
10.	Conclusions and Recommendations	107
10.1	Conclusions.....	107
10.1.1	Static - Dynamic analysis differences	107
10.1.2	Contribution of Material	108
10.1.3	Contribution of Fluid	108
10.1.4	Contribution of Soil	109
10.1.5	Overall	110
10.2	Recommendations.....	111
11.	References and Bibliography	113

Page intentionally left blank

List of Figures

Figure 1.1 International Ship Traffic Map (Source)	1
Figure 1.2 Falling Container on a Marine Pipeline (Source)	1
Figure 1.3 Anchor Properties (Source)	2
Figure 2.1 Dented pipe after removal operation. (Karamanos, Pournara, 2013)	7
Figure 2.2 Denting derivation for a tube that is allowed to displace in the direction of denting. 7	
Figure 2.3 (a) Dent Proposed Theories (b) Theoretical arrangement for dent calculation	8
Figure 2.4 Ring-Generator Model (Wierzbicki and Suh)	9
Figure 2.5 Energy – Maximum dent relationship plot according to DNV relationship.	11
Figure 2.6 DNV - Energy - Permanent Dent relationship according to DNV -RP-F111	13
Figure 3.1 Initial finite element model set-up for quasi static analysis.....	15
Figure 3.2 DNV-RP-F111, Recommended Indenter Shapes	16
Figure 3.3 Engineering vs True Stress-Strain Curve	18
Figure 3.4 Shell (a) vs Solid (b) Element Modeling	19
Figure 3.5 Required energy per dent size diagram for shell and solid elements.....	20
Figure 4.1 Typical Force-Dent diagram	23
Figure 4.2 Von Mises stresses of a dented pipe	25
Figure 4.3 Vertical displacement component contour plot, for different stages	25
Figure 4.4 Force-dent diagram for different model lengths.....	26
Figure 4.5 Force-dent diagram for different transverse size of the indenter.....	27
Figure 4.6 Required energy - dent for different indenter lengths in the lateral direction.....	28
Figure 4.7 Deformed tube cross-section for indenter size equal to 0.66D.....	29
Figure 4.8 Deformed tube cross-section for indenter size equal to 2D.....	29
Figure 4.9 Force-dent diagram for different internal pressure levels.....	30
Figure 4.10 Required energy - dent diagram for different pressure levels.	31
Figure 4.11 Longitudinally cut of a deformed pipeline for different pressure levels..	32
Figure 4.12 Effect of depressurization on dent size of a pipe.....	32
Figure 4.13 Force-dent diagram for different external pressure levels.	33
Figure 4.14 (a) Required energy - dent diagram for different external pressure levels	34
Figure 4.15 Deformed pipe for $q = 0.2$	34
Figure 4.16 Force-dent diagram for different values of Young's Modulus.....	35
Figure 4.17 Force-dent diagram for different material models and different yield stresses.	36
Figure 4.18 Required energy - dent for different material models and yield stresses.....	37
Figure 5.1 Typical dent deformation versus time diagram. (Alsos et al, 2012).....	39
Figure 5.2 Dynamic model configuration.....	40
Figure 5.3 Force-dent diagram for a finite length tube resting on a rigid bed with fixed ends. .	41

Figure 5.4 Dynamic model length determination	42
Figure 5.5 Effect of gravity on load-dent diagram in a dynamic analysis	43
Figure 5.6 Comparison of quasi-static and dynamic force-dent diagrams.....	44
Figure 5.7 Transferred energy (work) versus time for a fixed kinetic energy	45
Figure 5.8 Force-dent relationship for different velocities and constant mass.	46
Figure 5.9 Energy-dent diagram for dynamic analysis.....	46
Figure 5.10 Stress-Strain curve for different strain-rate values according to Cowper-Symonds.	47
Figure 5.11 Strain-rates over time for different velocities of impact and constant energy input.	48
Figure 5.12 Force - Dent diagram for strain-rate model.....	49
Figure 5.13 Quasi-static (top) versus Dynamic (bottom) deformation pattern.....	51
Figure 5.14 Rayleigh damping components. Percentage of critical damping versus frequency	52
Figure 5.15 Force-dent diagram for different velocities and different mass proportional Rayleigh damping.....	53
Figure 6.1 Schematic representation of an operating pipeline when hit by an object.....	55
Figure 6.2 Schematic representation of finite element model assumptions.....	57
Figure 6.3 Force-dent diagram for different velocity and pressure levels.....	57
Figure 6.4 Maximum deformed tube for internal pressure level of $q=0.4$	58
Figure 6.5 Schematic representation of finite element model used.....	58
Figure 6.6 Force-dent curve for a filled pipe with no pressure.....	62
Figure 6.7 Pipeline - fluid interaction cross-sectional deformation over time.....	63
Figure 6.8 Force- dent diagrams for internal pressure level equal to (a) $q = 0.2$ and (b) $q = 0.4$	65
Figure 7.1 Soil types by clay, silt and sand composition as used by the USDA	69
Figure 7.2 Shear modulus of different soil versus the developed shear strain.....	71
Figure 7.3 Static shear strength of several clays as function of rate of shear strain.	72
Figure 7.4 Statoil's equivalent elastoplastic material model for clays	72
Figure 7.5 Schematic representation of the effect of high strain rate on the stress-strain response of sand in uniaxial compression	73
Figure 7.6 (a) Effect of saturation on uniaxial compression response of sand soils (b) Dynamic modulus ratio as a function of strain-rate	74
Figure 7.7 Effect of increase in strain-rate on stress-strain response and volumetric strains in (a) loose sand, (b) dense sand.	75
Figure 7.8 Equivalent undrained shear strength profile of sand for different approaches.	76
Figure 7.9 Soil failure models' comparison.....	77
Figure 7.10 Schematic representation of acoustic waves and how the soil domain shape affects their absorption.....	81
Figure 7.11 Connection detail of finite with infinite elements at the boundaries	81
Figure 7.12 Final finite element soil model	82

Figure 7.13 Geostatic stress field.....	83
Figure 8.1 Pipeline-soil interaction model.....	85
Figure 8.2 Maximum and permanent dent sizes for different surface values of S_u	88
Figure 8.3 The force-dent curve does not change when soil is introduced.	89
Figure 8.4 Absorbed energy as a fraction of the kinetic energy for the different clay profiles. .	90
Figure 8.5 Pipeline - soil interaction, deformed cross-section for different time intervals.	90
Figure 8.6 Half-buried pipeline model set-up.....	91
Figure 8.7 Force-dent diagram for half-buried pipeline.	91
Figure 8.8 Soil lateral movement for the half-buried pipeline.....	92
Figure 8.9 Maximum absorbed kinetic energy fraction for buried and half-buried cases.	92
Figure 8.10 Maximum (left) and permanent (right) dent size for unburied and half-buried cases and different soil profiles.....	93
Figure 8.11 Schematic representation of conversion of energy between global deflection and local denting	93
Figure 8.12 Absorbed kinetic energy - velocity diagram for unburied and half-buried cases. ..	94
Figure 8.13 Maximum and permanent dent size for different velocity input for buried and half-buried cases.	95
Figure 8.14 Fraction of kinetic energy absorbed versus the impact velocity for soil profile-5. 96	
Figure 8.15 Wave propagation in soil medium for the unburied pipeline case for 5 and 20 m/s impact velocities respectively.....	96
Figure 8.16 Maximum dent size for different velocities in the stiffer soil case for unburied and half-buried cases.....	97
Figure 9.1 Pipe-fluid-soil interaction model set-up	99
Figure 9.2 Absorbed energy versus the internal pressure level for buried and half-buried pipelines.	100
Figure 9.3 Maximum and permanent dent depth for different pressure levels of gas for half-buried and unburied case	101
Figure 9.4 Force-dent diagrams for different pressure levels for buried and half-buried pipeline	101
Figure 9.5 Top view of Von Mises stress field for (a) empty pipe (b) pressurized pipe with $q = 0.4$ at $t = 0.16$ sec.....	102
Figure 9.6 Absorbed energy comparison for unpressurized and pressurized pipelines on soil	102
Figure 9.7 Energy absorption for gas and water filled pipeline resting on soil for different pressure levels.	103
Figure 9.8 Maximum (left) and permanent (right) dent depths for a half-buried pipeline filled with gas or water.	103
Figure 9.9 Energy absorption for Soil-1 profile, for (a) no strain-rate yielding and (b) strain-rate yielding of steel.	104
Figure 9.10 (a) Maximum and (b) Permanent dent depth for Soil-1 profile without (left) and with (right) strain-rate yielding of steel.	105

Page intentionally left blank

List of Tables

Table 1-1 Container Properties	2
Table 2-1 DNV-RP-F107 Assumptions on Denting	10
Table 2-2 Damage levels according to DNV	11
Table 3-1 Model Parameters for quasi-static model.	16
Table 4-1 Model Input Parameters	23
Table 4-2 Maximum and permanent dent results for different yield stresses.	37
Table 5-1 Dynamic Load Cases.....	43
Table 5-2 Maximum and permanent dent results as derived from DNV, quasi-static and dynamic	45
Table 5-3 Comparison of dent depth between dynamic, quasi-static FEM and DNV	50
Table 6-1 Liquid input properties required for the analysis.....	60
Table 6-2 Results for Water filled pipeline with no internal pressure and different impact velocities.....	61
Table 6-3 Results for different pressure levels and different modeling of the enclosed fluid . .	64
Table 6-4 Summarized conclusions on different modeling of the pipe fluid and their capabilities.	66
Table 7-1 Soil Properties for (a) clay and (b) sand as given by DNV-RP-F105.....	69
Table 7-2 Soil elastic moduli for different types	70
Table 8-1 Base case input parameters.....	87
Table 8-2 Considered clay soil profile properties for the analysis.....	87
Table 8-3 Considered velocity-mass input cases for the sensitivity analysis.....	94

Page intentionally left blank

1. Introduction

1.1 Background

Over the last years, offshore oil and gas exploration has significantly increased, in order to meet the world's demands. Along with the exploration, the use of pipelines to transport the hydrocarbons between production facilities or to shore has been also developed dramatically.

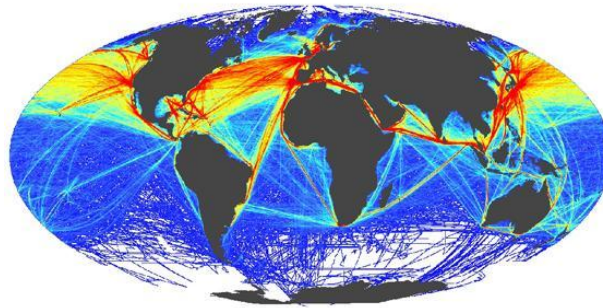


Figure 1.1 International Ship Traffic Map ([Source](#))

However, things do not go always as planned or as desired. Pipeline routing has to take into account several parameters, from the environment, the mammals and the bathymetry, to potential hazards from human activity. For the later, potential danger for the structural integrity of the pipeline can be trawling fishing gears, anchor dropping and dragging, container dropping or random small and large objects that can fall of a ship. It is important for the pipelines to be able to sustain potential impact from such objects and prevent leakage from occurring.



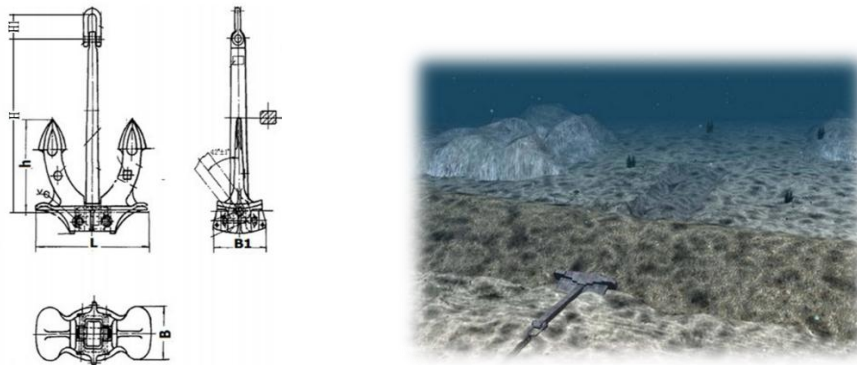
Figure 1.2 Falling Container on a Marine Pipeline ([Source](#))

Codes such as DNV, give a very rough and conservative estimate of the damage caused by falling objects, which makes them unpractical to use in situations where detailed assessment is required. Thus, it is important for the offshore industry, to properly assess this accidental scenario, in order to give reliable results of the damage and consequently take the right decisions for the economy and the environment.

Container Type	Max. Gross Mass (kg)	L (mm)	W (mm)	H (mm)
20 ft. Standard	24000	6100	2370	2590
40 ft. Standard	30500	12190	2440	2590

Table 1-1 Container Properties (Source)

A very important parameter of the problem is the velocity of the falling object. This is a standalone research topic that depends on various parameters. For instance, the terminal velocity of a falling object in water depends on the depth, the initial velocity of the object, the shape and weight of the object and the angle under which it goes into the sea.



Mass of Anchor (kg)	H (mm)	B1 (mm)	H1 (mm)	L (mm)	H (mm)
3060	1283	841	380	1832	2374
4890	1498	984	415	2135	2769
6900	1681	1105	480	2391	3100
10500	1934	1273	600	2752	3571
14100	2135	1404	660	3036	3939
20000	2399	1578	730	3411	4420

Figure 1.3 Anchor Properties (Source)

The kinetic energy of a falling object is not only function of its velocity but it has also to do with the mass of the object. Thus, this will not be investigated and instead some representative values of dropping velocity over a range will be chosen. DNV-RP-F105, gives some graphs for estimation of the terminal velocity and guidelines, but for a proper damage assessment this has to be calculated in more detail. For the sake of completion below the trajectory of a falling object can be seen.

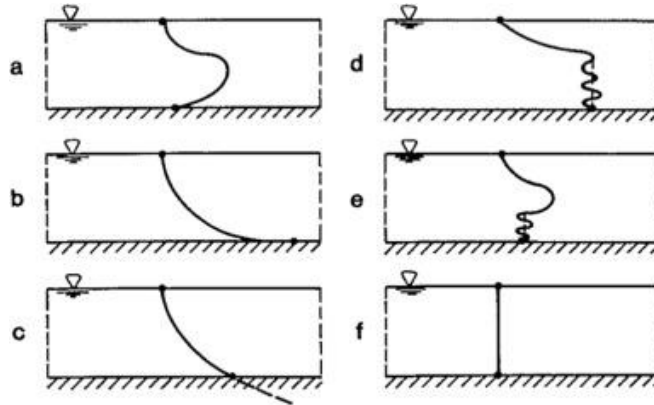


*Figure 1.4 Falling object trajectories for different shapes and initial angle when entering the water.
(DNV-RP-F107)*

1.2 Problem Definition

Despite the fact that denting damage of pipes has been investigated for many years, current practice only proposes conservative relationships between the kinetic energy of the falling object and the dent size, excluding all the other parameters like pressure, material behavior, soil bed or pipe fluid interaction.

This leads to conservative results that might be far away from reality. Thus, a study has to be conducted to investigate all of the parameters that participate in the impact of dropping objects with the pipeline and how energy of the falling objects dissipates in every component of the structure-fluid-soil system. A better understanding of this phenomenon, can help a lot in reducing the calculated risks related to leak.

1.3 Research Objective

Aim of the present study is to understand the physics behind the impact of dropped objects on operating pipelines and try to create a numerical model that can very accurately predict the behavior of the system by taking into account all the significantly contributing parameters such as:

- Shape, mass and velocity of the dropped object.
- Contribution of the soil in the dissipation of the total kinetic energy of the system and determination of the soil depth that participates in the impact.
- Contribution of the pipe fluid added mass and pressure to the denting resistance of the pipe.
- Contribution of material properties of the pipeline.
- Effect of surrounding water and hydrostatic external pressure.
- Comparison with existing guidelines.

1.4 Approach

In order to properly address the physics and the mechanics behind the impact of objects on marine pipelines, a fundamental understanding of all the different parameters is required.

Initially, the denting mechanism as explained in the relevant work and literature must be understood. The simplified theories, such as Wierzbicki and Suh are used in the DNV codes. The basic assumptions and simplifications should be understood as well as the reasoning behind them. By doing so, the research goals of this thesis can be established. Then, a brief explanation and analysis of the DNV approach on the matter will be done in order to understand how industry tackles this problem and what are the conservative and non-conservative assumptions that go with it.

Next, a dedicated Finite Element model will be developed in order to reproduce results from various published experiments and analyses found in the literature (Karamanos, Gresnigt, Palmer, Jones). This way, confidence can be gained on whether or not the model works properly and thus can be trusted. Simple, configurations that are used in the laboratories and match well with the assumptions made in the theoretical studies will be modeled and analyzed.

As soon as the model is established and verified it is possible to carry out investigations on a different set of parameters for quasi-static experiments on an infinite stiff bed. The parameters that will be investigated are the size of the denting object, the material yield stress and elastic modulus, the existence of internal and external pressure. Investigation of these parameters and examination of both the load-dent and energy-dent curves can give valuable insight onto how they affect the system behavior under quasi-static conditions, so for relative small terminal velocities.

However, by doing a quasi-static analysis the inertia terms are neglected and this can lead to wrong conclusions and results when quantifying a dent size and shape. The reason is that an impact depends not only on the stiffness of the parts but also on the ratio between masses. Moreover, strain-rate phenomena are also not taken into account during a quasi-static analysis. Numerous studies and experiments have shown that mild steel pipeline

behavior strongly depends on the strain-rate and thus this has to also be verified and implemented in the FEM model.

In the unfortunate event of an object falling on the pipeline, the most probable is that the pipeline will be operating during the impact. This means, that the pipeline is filled with either oil or gas and has an internal and external pressure acting on it radially. In a simple quasi-static analysis, only the pressure exerted on the wall can be studied, whereas the potentially added mass by the internal fluid or the transient pressure increase of fluids such as water or oil is not taken into account. An investigation will be carried out, in order to specify the order of magnitude that the inertia of the fluid affects the dent behavior of the pipeline.

Of course, the consideration of an infinite stiff bed (rigid) is not correct, as in reality the pipelines are either hanging in big spans or rest on a deformable seabed. The aforementioned studies and DNV, consider that all the kinetic energy of a falling object is dissipated in the form of dent deformation, which is very conservative. In order to determine and quantify the contribution of the soil in the dissipation of energy, it is necessary to understand the behavior and the properties of the soil whether it is sand or clay. DNV, very conservatively proposes linear springs for a dynamic loading case. This neglects the effect of soil plasticity which will have a major contribution in the dissipation of energy as permanent deformation. However, since purpose of this thesis is not to investigate the soil itself under such a loading but rather its response certain simplifications will be made.

By conducting now, the same simulations in a 3D model where soil-pipeline interaction is modeled properly it is possible to study the contribution of soil in energy dissipation. Different soil profiles will be considered with an effort to be as realistic as possible. By setting accordingly the parameters within an acceptable range it is possible to quantify the contribution of parameters such as the elastic modulus, the undrained shear strength and the density of the soil as well as the effect of embedment of the pipeline into the soil.

Concluding, all the different sets of analysis will be compared with the existing recommended practice and the simplified dynamic analyses in order to obtain valuable information on to which extend the DNV codes can be used when damage from dropped objects to pipelines must be evaluated and what aspects should engineer take into account when designing a pipeline with respect to accidental loading.

1.5 Thesis Outline

- Chapter 1 – Introduction: The introduction gives background information on the subject and the research goals and methods.
- Chapter 2 – Denting of Tubes: Basic theory for the indentation of tubes will be presented along with the DNV recommended practice.
- Chapter 3 – Finite Element Model: The first set-up of the finite element model will be presented with all the assumptions used to make the first set of quasi-static analyses.
- Chapter 4 – Quasi-static Analysis: Quasi-static analysis of tubes will be carried out, investigating key parameters like pressure, shape and material on the behavior of the pipe.
- Chapter 5 – Dynamic Analysis: For the same experimental set-up, a dynamic explicit analysis will be carried out to assess the differences with the quasi-static investigation. Strain-rate yield stress sensitivity will be also implemented.
- Chapter 6 – Pipe-Fluid Interaction: Modeling of the pipeline contents will be made here in order to capture their complete behavior and any inertia effects. Gas and water filled pipes are examined.
- Chapter 7 - Soil Modeling: Fundamental properties and theory for the soil behavior under dynamic loading will be presented along with the modeling techniques that have been followed to build a complete soil finite element model.
- Chapter 8 – Pipe-Soil Interaction: Based on the previous models from chapter 5 and 7, a combined model is created in order to study the effect of a flexible bed in the response of the pipeline when experience an impact.
- Chapter 9 – Combined Model: Based on all the previous developed finite element models, a combined study will be done in order to observe the interaction between the different reported phenomena.
- Chapter 10 – Conclusions and Recommendations: Conclusions are given for the research and the research questions are answered. Recommendations are given for the parts of this thesis that need further investigation.

2. Denting of Tubes

2.1 Introduction.

Dent is a depression in a surface made by pressure or a blow. By extending this definition to tubes, one could say that denting is the problem of large plastic deformations of pipes subjected to combined loading in the form of lateral indentation. Usually, the dent is described as a percentage of the tube diameter in order to have a feeling of the size of deformation.

Depending on the size of the dent the pipeline can be described from fully operational to critically damaged. Thus, it is important to understand how the denting resistance of a pipe is derived and what parameters contribute to it, before going to more sophisticated models and analyses.



Figure 2.1 Dented pipe after removal operation. (Karamanos, Pournara, 2013)

In order to refer to the dent depth without any confusion, the following definition that is derived geometrically will be introduced:

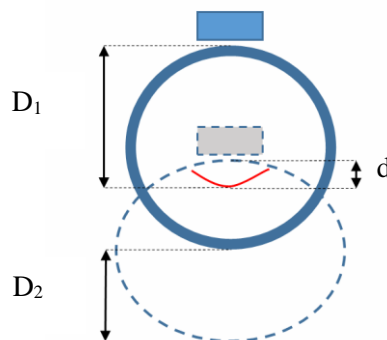


Figure 2.2 Denting derivation for a tube that is allowed to displace in the direction of denting.

From figure 2.2, the derivation of denting deformation is straightforward. By deducting the tube's global displacement from the upper point total displacement the denting depth is obtained. This can be written as:

$$d = D_1 - D_2$$

where D_1 is the maximum total displacement of the upper surface, and D_2 is the maximum displacement of the lower surface of the tube.

2.2 Denting Resistance Mechanism

Denting of a tube is a relatively complex phenomenon, which combines local yielding due to bending of the material, with a longitudinal stretching of the hoop generators. Excluding any of the aforementioned mechanisms will lead to wrong conclusions and results. For small deformations, the denting is almost elastic, meaning that after unloading the tube can retain its original shape and size. However, most often the denting is permanent at yielding of the material has occurred and the initial shape cannot be achieved again. From this point on a distinction will be made between the maximum (due to maximum loading) and the residual dent of a tube (permanent deformation after unloading).

Several analytical models have been proposed in the literature, in order to describe the denting of pipelines. Each model is based on different experimental set-up observation. The theories vary in the way that they introduce denting to the tube. This can be due to two plates that move simultaneously towards the cross-section center, or due to indenter that loads a specimen that is resting on a rigid surface. The only thing that they have in common is the 4-plastic-hinge deformation mechanism that is used in order to describe the denting. However, the position of the hinges is not the same for each model. Some of the proposed models can be found below.

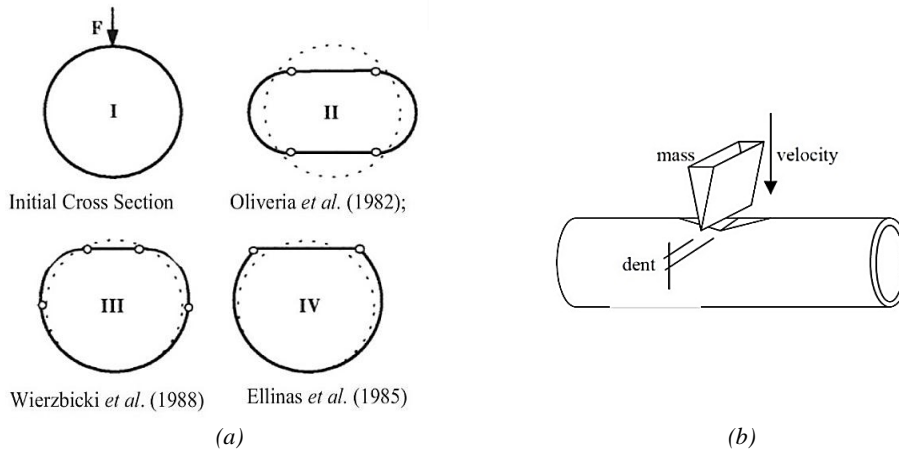


Figure 2.3 (a) Dent Proposed Theories (...) (b) Theoretical arrangement for dent calculation (DNV-RP-F107)

From the aforementioned models, tube response to denting has been adequately described by Wierzbicki and Suh, by observations from denting experiments, with a simplified yet very accurate analytic model based on the following premises and has been also implemented in the DNV codes:

- The plastically deforming zone that is undergoing severe shape distortion is restricted to a few diameters of the shell on both sides of the dent center. It is assumed that the extent of the locally damaged zone is finite.
- The cross-section at which the deformed part of the shell joins the undeformed part is taken to be plane and circular. Therefore, no ovalization and warping of the tube exist beyond the dent-affected zone.
- Inside the plastically deformed zone, the ovalization and its extreme form--the unsymmetrical shape distortion--are permitted.

The model involves the theory of plasticity, with the deformation energy of the system in order to connect the local response with the global deformation as a system of unconnected rings and unconnected generators as shown below. The rings and generators are loosely connected, so that lateral deformations are compatible, but there is no resistance to shear. The resulting coupled deformation, resembles the locally collapsed sections of actual tubes.

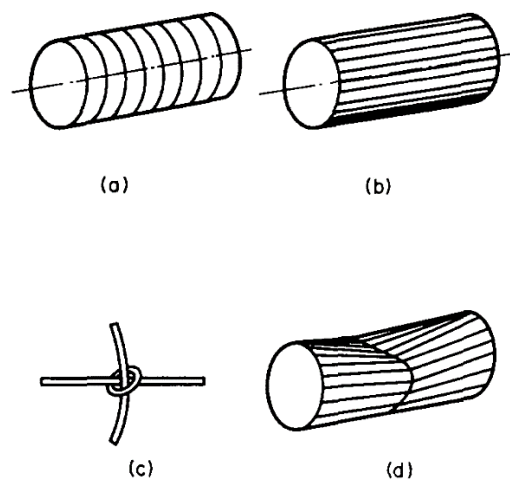


Figure 2.4 Ring-Generator Model (Wierzbicki and Suh)

The generators are treated in the model as rigid-plastic beams which can bend and stretch (or compress) as the depth of the dent increases. However, the change in the longitudinal curvature of generators is much smaller than the change in the circumferential curvature.

2.3 DNV Treatment of Denting

DNV, uses the theory and formulas that have been proposed by Wierzbicki and Suh written in a simplified manner. In this equation, a series of conservative assumptions are being made.

More specifically, DNV – F105, considers an infinite tube resting on a rigid bed which is being hit by a sharp object transversely. The object has a transverse length larger than the pipe diameter and its edge is practically a line and not an area. The effect of internal and external pressure is neglected. Internal pressure will have a positive effect on the dent as it provides the tube with extra capacity. On the other side, external pressure has a negative effect as it works together with the falling object reducing the capacity of the system dramatically. If the dent is large enough a propagation buckling may be initiated.

DNV Assumptions	
Conservative	Non-Conservative
No Internal Pressure	Falling Object Longer than D
No Fluid Mass	No External Pressure
No Strain-Rate Sensitivities	No Velocity/Mass distinction
Rigid Bed	-
All Energy absorbed as Dent Deformation	-
Absence of Coating	-
Falling object Rigidity	-
Object is very sharp	-

Table 2-1 DNV-RP-F107 Assumptions on Denting

Moreover, no dynamic phenomena such as strain-rate dependence of yielding are accounted or the velocity that the object may hit the pipe. Last but not least, the soil stiffness is not taken into account conservatively. Another parameter that in some cases might matter is the stiffness and the deformation capacity of the object that is falling. If the object is not rigid then additional kinetic energy will be dissipated in the form of deformation of the object. Goal of this thesis is to access all of the aforementioned assumptions and access how much they do or not affect the dent formation of a subsea pipeline.

The aforementioned can be described by the following equation, which gives the energy needed to produce a maximum dent depending on the diameter and thickness of the pipe. It is produced from the Wierzbicki force-dent equations. Thus, by assuming a critical dent depth, it is possible to find the energy that is needed to create this scenario. Then, this deformation energy, can be converted to a kinetic energy. Assuming that the total kinetic energy will be absorbed by the tube (due to the rigid bed and the rigid object) it can be further analyzed in a pair of mass and velocity for a given impact scenario in order to make the damage and probability assesment and of course it can also work in the other way around, if the energy is known and the dent depth is needed.

$$E = 16 \cdot \left(\frac{2\pi}{9}\right)^{0.5} \cdot m_p \cdot \left(\frac{D}{t}\right)^{0.5} \cdot D \cdot \left(\frac{\delta}{D}\right)^{1.5} \quad (1.1)$$

Where:

m_p : Is the plastic moment capacity of the wall equal to $0.25\sigma_y t^2$

δ : Is the pipe local deformation or dent depth

t : Is the wall thickness

σ_y : Is the characteristic yield stress

D : Is the tube outer diameter

E : Deformation Energy or Kinetic Energy Input

As can be seen from the equation, the dent depth depends directly on the yielding stress, the diameter and the thickness of the pipe. For the current formulation, the load-dent curve is a property of the pipeline and it is not affected by anything else. In reality as it will be shown later this is not entirely true.

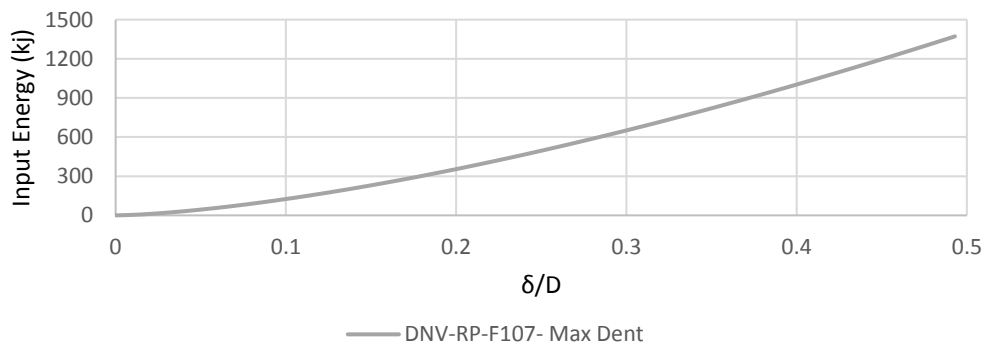


Figure 2.5 Energy – Maximum dent relationship plot according to DNV relationship.

Moreover, DNV sets damage classes for steel pipelines that have been subjected to impact depending on the ratio of the maximum dent with the diameter of the pipe. The damage classes are summarized in the table below:

Dent/Diameter (%)	Damage Description	Impact Energy
< 5	Minor Damage	Calculated by DNV equation for each case.
5 – 10	Minor Damage – Leakage Anticipated	
10 – 15	Major Damage – Leakage and Rupture anticipated	
15 – 20	Major Damage – Leakage and Rupture anticipated	
>20	Rupture	

Table 2-2 Damage levels according to DNV

In DNV-RP-F111, for trawling gear interference, an additional relationship can be found for denting. More specifically, this relationship predicts the residual or permanent dent on the pipeline. As it will be explained later more thoroughly, during an impact the tube obtains a maximum dent depth which reduces later after unloading. The dent depth after the impact will from now on be called residual or permanent dent.

The importance of distinguishing the dent depth in maximum and residual/permanent is the following.

- **Maximum Dent:** This value is important in order to access whether or not a pipeline will suffer fracture, puncture or any other mechanical brittle damage.
- **Residual/Permanent Dent:** This value is important when the pipeline is not critically damaged. In order to be able to operate regularly with a dent, the permanent dent must have an acceptable size not only for flow assurance problems but for other maintenance operations such as pigging.

The proposed relationship for residual or permanent dent according to DNV for bare steel pipes is:

$$\delta_p = \underbrace{\left(\frac{F_s}{5 \cdot f_y \cdot t^2} \right)^2}_A - \underbrace{\left(\frac{F_s \sqrt{0.005 \cdot D}}{5 \cdot f_y \cdot t^2} \right)}_B \quad (1.2)$$

Where δ_p is the estimated plastic permanent dent depth.

And F_s is the maximum impact force experienced by the pipe shell equal to:

$$F_s = \left(\frac{75}{2} E_{loc} \cdot f_y^2 \cdot t^3 \right)^{\frac{1}{3}} \quad (1.3)$$

where E_{loc} is the impact energy absorbed locally by the pipe shell.

As can be easily observed the relationship for the residual/permanent dent depth, comprises of two terms. Term A describes the loading path and the relationship between load and dent depth. As will be seen later, the force-dent curve is quadratic for the loading phase and almost linear for the unloading phase.

Indeed, term B correlates linearly the dent depth with the force and it is deducted from the first term. This means, that the first term calculates the maximum dent that will occur for a given energy input whereas the second term will determine the permanent dent size.

Based on this relationship, the permanent dent depth is affected by the absorbed energy, the diameter, the thickness and the yield stress.

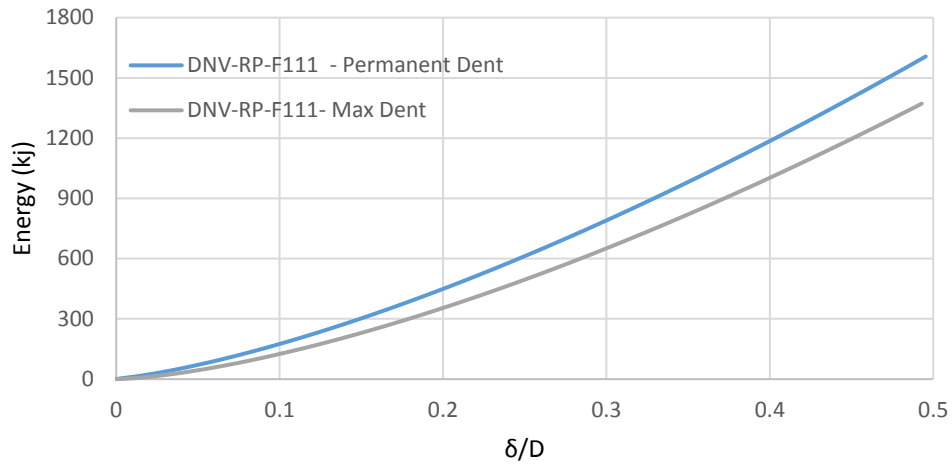


Figure 2.6 DNV - Energy - Permanent Dent relationship according to DNV -RP-F111

The ratio between permanent and maximum dent depth, is not constant. As the maximum dent increases the ratio of permanent over maximum dent decreases. This is mostly correlated with the material behavior, and its strain-stress curve. Denting exhibits the same behavior. For instance, $\delta_{perm}/\delta_{max} = 0.85$ for an input energy of 800kj whereas $\delta_{perm}/\delta_{max} = 0.81$ for 400kj.

Page intentionally left blank

3. Finite Element Model

Having explained the basic principles of tube denting and their response, it is important to extend these results to more complicated loading conditions in order to match as much as possible the reality. To this end, a dedicated Finite Element Model in ABAQUS, serving as a numerical laboratory will be used to simulate a series of problems, in order to better understand and explore the denting of pipes and how it is affected.

3.1 Model Set-up

For the preliminary investigations of the present thesis, the following model has been considered. A tube specimen of various lengths, resting on a rigid horizontal plate, compressed by an indenter at the center. This case does not model a realistic in place marine pipeline, however it can be used to derive some general results that will be used later in a more sophisticated analysis. Because the problem that is considered is double symmetrical only one quarter of the tube will be modeled in order to reduce the CPU time and allow the model to handle more complex phenomena that otherwise would require a lot of RAM and CPU power.

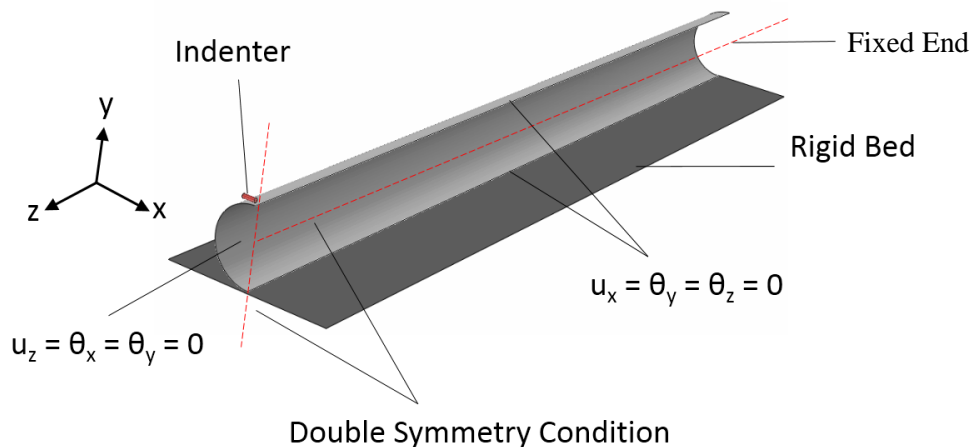


Figure 3.1 Initial finite element model set-up for quasi static analysis.

The inventor dimensions have been chosen according to the provisions of DNV-RP-F111. Two main inventors are considered, one very sharp and one rounded as can be seen below.

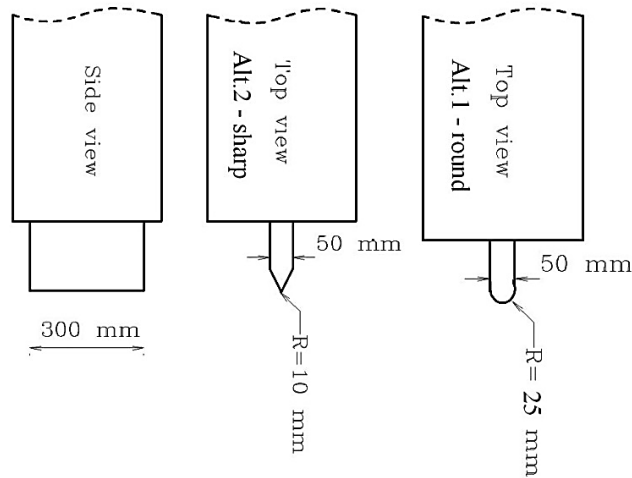


Figure 3.2 DNV-RP-F111, Recommended Indenter Shapes

3.2 Model Parameters

The parameters that are taken into account during the analysis are the following

Steel Young's Modulus	E
Steel Yield Stress	Sy
Diameter	D
Wall Thickness	t
Tube Length	L
Slenderness	D/t
Indenter Shape	Type A/B

Table 3-1 Model Parameters for quasi-static model.

3.3 Boundary Conditions

To this end, the following model has been constructed for both solid and shell elements. As aforementioned, due to double symmetry, it is necessary to consider appropriate boundary conditions so that the model will behave correctly. For the sake of notation, we will refer as the end section of the pipe the section at the top right corner of the figure and mid the section where lies on the symmetry plane (bottom left). Side of the pipeline will refer to the two longitudinal edges that emerge from the symmetry cut and are connecting the mid and the end cross sections. Having defined that, the following boundary conditions are applied in order to obtain symmetry (the notations used are in accordance with the ABAQUS coordinate system):

- End section: When the model is referred as “free” it means that no BCs are imposed to the end section. However, when the model is referred as “fixed” the end section is completely fixed (modeling a rigid steel plate at the end). Thus, no ovalization is allowed and no other displacement or rotation.
- Middle section: The longitudinal displacement is fixed, along with the rotations around x and y axes. Thus, $u_z = \theta_x = \theta_y = 0$
- Side edges: The transverse horizontal displacement is fixed, along with the rotations around y and z axes. Thus, $u_x = \theta_y = \theta_z = 0$
- The plate is completely fixed in all degrees of freedom.
- The indenter is fixed in all degrees of freedom except the vertical one $u_y \neq 0$

As the load is imposed through contact and not as a concentrated load, it is convenient, to achieve contact by prescribing the vertical displacement of the indenter towards the tube. This way the solution is in general more stable, and the user of the FEM software has a better feeling of the magnitude of deformation that he is expecting.

3.4 Material Model

The adopted material model is in line with the case study pipeline properties presented later. Minimum specified properties are assumed to characterize the pipeline’s material. The following function shows the Ramberg-Osgood relationship:

$$\varepsilon = \frac{\sigma}{E} + A_r \left(\frac{\sigma}{E} \right)^v \quad (3.1)$$

Here ε defines the acting (engineering) strain, σ the acting (engineering) stress and both A_r and n are fitting coefficients. The fitting coefficients can be uniquely defined when the following is known:

- Two points on the stress-strain curve, and;
- Young’s (elastic) modulus E .

It is assumed that the yield stress can be fitted at 0.5 % strain and the ultimate tensile strength occurs at 10.0 % strain. To perform Finite Element Analysis, typically, the true (logarithmic) stress-strain curve is required as input. This can be calculated from the engineering stress and strain values, σ_{eng} and ε_{eng} using the relationships presented here:

$$\varepsilon_{true} = \ln(1 + \varepsilon_{eng}) \quad (3.2)$$

$$\sigma_{true} = \sigma_{eng} (1 + \varepsilon_{eng}) \quad (3.3)$$

The engineering and true stress-strain curves calculated using the procedure described above are presented in Figure 3.3. For small values of strain, both curves are effectively the same. For larger values of strain, the true curve is larger than the engineering curve. The true stress-strain curve in this figure is used to characterize the material strength in the FE analysis performed for this study.

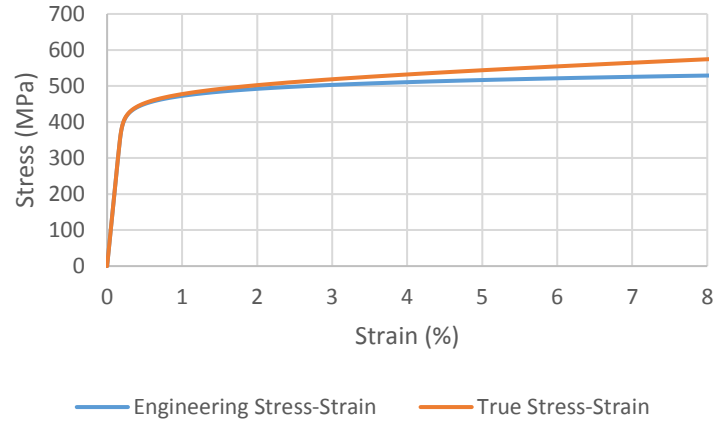


Figure 3.3 Engineering vs True Stress-Strain Curve

3.5 Normalization of Results

From this point on, the results presented in order to keep a constant notation will be normalized in the following manner.

- Denting load F will be normalized by F_p so that $f = F/F_p$, where:

$$F_p = f_y \frac{t^2}{4} \sqrt{\frac{D}{t}} \quad (3.4)$$

Where F_p is the force needed to create the four-plastic hinge mechanism on the tube cross section.

- Denting displacement will be normalized by the diameter (D).
so that $\chi = \delta/D$
- Internal and External Pressure will be normalized by the fully plastic pressure given by:

$$p_0 = \frac{2f_y t}{D} \quad (3.5)$$

so that $q = p/p_0$.

3.6 Element Selection

Generally, other researchers on the topic usually use shell S4R elements (4-node general-purpose shell, reduced integration with hourglass control, finite membrane strains) to model the tube.

However, for the purposes of this thesis also C3D8R (8-node linear brick, reduced integration with hourglass control) 3D elements have been used in order to identify and quantify the difference in the results and how these match with experiments found in the literature. Due to the reduced integration, the locking phenomena observed in the C3D8 element do not show. However, the element exhibits other shortcomings:

- **S4R:** Uniformly reduced integration to avoid shear and membrane locking. The element has several hourglass modes that may propagate over the mesh. Converges to shear flexible theory for thick shells and classical theory for thin shells. S4R is a robust, general-purpose element that is suitable for a wide range of applications
- **C3D8R:** The element tends to be not stiff enough in bending. Stresses, strains, are most accurate in the integration points. The integration point of the C3D8R element is located in the middle of the element. Thus, small elements are required to capture a stress concentration at the boundary of a structure.

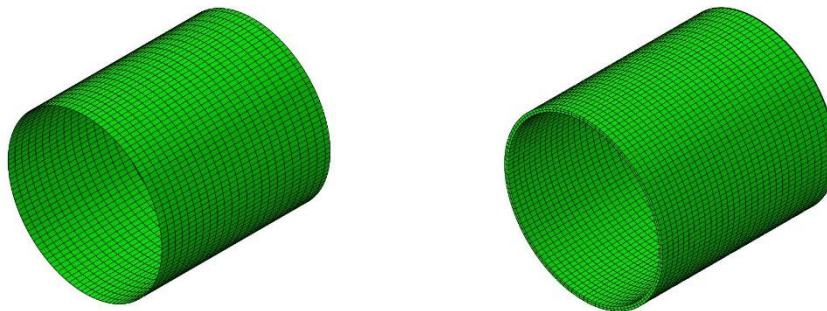


Figure 3.4 Shell (a) vs Solid (b) Element Modeling

Moreover, refinement of the mesh is necessarily needed in a region of approximately one diameter away from where the dent occurs. The elements in that region must not only be small enough but it has been observed that in the models where the elements were having a square shape, the convergence was achieved much more easily than those with just rectangular shape. This matters especially for large denting deformation. Moreover, for the C3D8R elements two elements have been found to suffice to capture the radial stresses accurately.

Beforehand, it is known that by using shell elements S4R, the radial stresses are omitted, thus resulting in a more favorable yielding condition (one stress component is neglected in the Von Mises criterion). Having said that, it is expected that especially for small D/t

ratios yielding will occur earlier in the brick model than in the shell, resulting in a smaller resistance of the system.

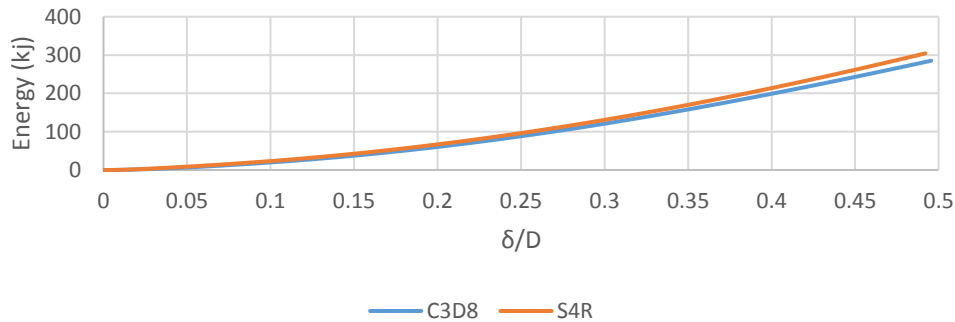


Figure 3.5 Required energy per dent size diagram for shell and solid elements. As can be seen the results are in a good agreement.

3.7 Analysis Procedure

For the analysis, a frictionless contact-pair algorithm has been utilized in order to model the experimental set-up. In the analysis, initial conditions as well as the step order is of great importance. Because non-linear geometry and material are used, the time-history of loading is significant and thus violating the order as it would have happened in nature will lead to wrong conclusions. The analysis consists of the following steps in the presented order:

- First the model is assembled and the indenter-cylinder-rigid plate parts are connected together.
- Next, the gravity is applied to the system in order to reach the initial equilibrium, as it would have happened in reality. It is expected, that some small stresses will develop at the bottom of the tube, in the interface with the plate, as all the weight is concentrated there.
- If the specific analysis included external or internal pressure, the pressure load is applied again until an equilibrium is reached.
- After this equilibrium has been achieved, the indenter starts moving with a prescribed displacement condition towards the cylinder where the denting starts.
- In the final step, the indenter starts to move upward (away from the tube specimen) in order to observe and measure the residual/permanent dent of the cylinder when it will reach its final equilibrium state.

The denting will continue, until the indenter will reach the vertical displacement that has been prescribed by the user. Note, that if the gravity is neglected in this analysis, the results do not match reality. This is very important especially for long specimens, where their weight counter balances their need for uplift.

The results are obtained by measuring the reaction force of the indenter, as the denting is already known. Then it is possible to create the Load – Dent curve for each experiment and determine the stiffness of the system for the given load combination and make the necessary comparison. The dent, will be measured as described from the previous chapter where the global displacement will be filtered out.:

Additionally, for every simulation, the deformation work done by the indenter is measured by integrating the load – dent curve until the maximum dent depth. This equals to the maximum absorbed energy of the pipe during impact. It is a critical part of the research, as it will serve as an input in a later stage for the dynamic analysis.

$$E = W(\delta) = \int_0^{\delta_{\max}} F(\delta) d\delta \quad (3.6)$$

Page intentionally left blank

4. Quasi-Static Denting

In this chapter, the so called quasi-static dent will be investigated. Quasi static means that the loading of the specimen happens slowly enough in order for inertia effects to be excluded. Practically, there is no rule that specifies when a load is quasi-static or dynamic. This depends highly on the geometry, the material and the boundary conditions. So, it is the purpose of this thesis to also investigate when the quasi static analysis becomes inadequate to properly describe the real situation. Before moving to more complicated model formulations and analyses it is important to investigate different parameters that affect the denting behavior of a steel pipe.

The parameters that will be investigated are: length of the model, effect of internal and external pressure, geometry of indenter, material properties. The conclusions and results from these investigations will be used as reference for later analyses in more sophisticated dynamic models and in models that account for a full fluid-soil-structure interaction.

Parameter	Value	Unit
Diameter (D)	914.4	mm
Thickness	20.9	mm
D/t	43.8	-
$f_{y,0.5\%}$ (X65)	450	MPa
Density	7850	kg/m ³

Table 4-1 Model Input Parameters

The initial FEM model has been verified with published work from Karamanos et al (2006) for different cases, in order to gain confidence in the results of the analysis. Before proceeding further, it is also important to have a look at a dent-force diagram analytically in order to understand the behavior of the pipe.

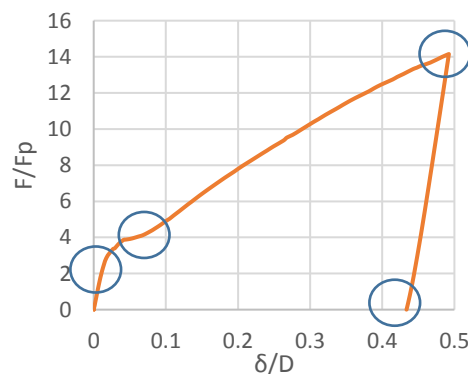


Figure 4.1 Typical Force-Dent diagram

As can be seen from the force-dent diagram, four points have been selected as representative of the situation. The first point, represents the pipe initially. After the indenter starts moving towards the pipe, an almost linear path is observed. At the end of this path, the second point is found, where yielding of the material takes place at the area that is in direct contact with the indenter.

Moreover, for thin walled pipes it has been observed that yielding is followed by a snap-through local buckling of the wall. The derivative of the curve at this point becomes equal to zero, which is equal to an instability in the system. This phenomenon, can be observed in this example as well, as for $F/F_p = 4$ there is a small region of practically zero stiffness.

After, yielding and local buckling of the cross section, a residual stiffness is observed in the system. This residual stiffness occurs due to the mobilization of the surrounding material. More specifically, this is the flexural resistance of the generators that has been well described by the research community and practically represents the resistance of the generators to bending.

Upon reaching the maximum prescribed dent, the indenter is slowly being removed. At this point, a decaying linear path is observed where the force is reduced to zero and the dent is also reduced to the so called residual or permanent dent depth. This is the dent that will be observed after an impact incident and which will be evaluated as to the workability of the pipe.

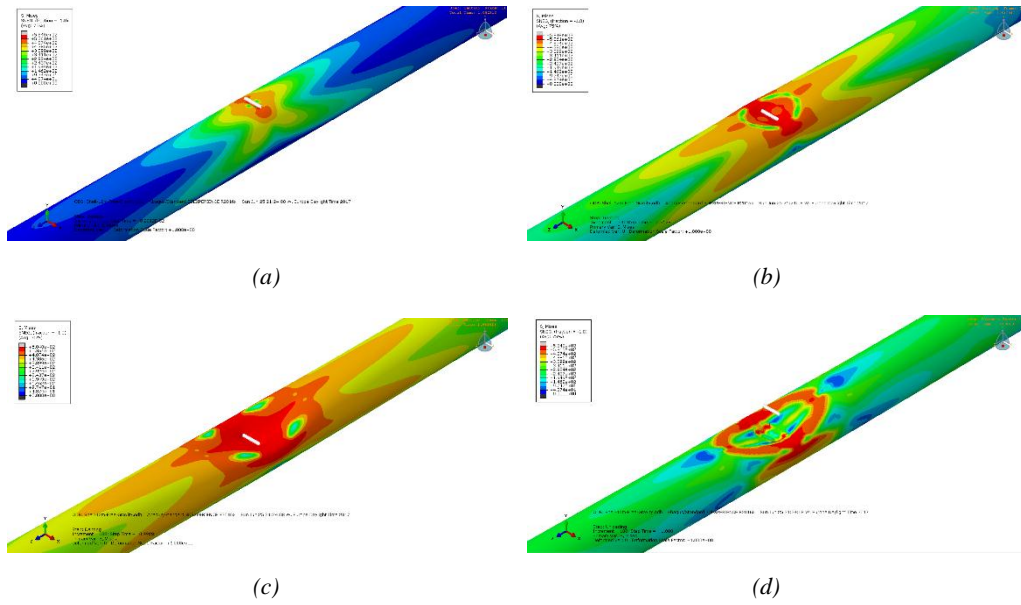


Figure 4.2 Von Mises stresses of a dented pipe at (a) elastic region (b) first yielding (c) maximum dent deformation (d) permanent dent deformation

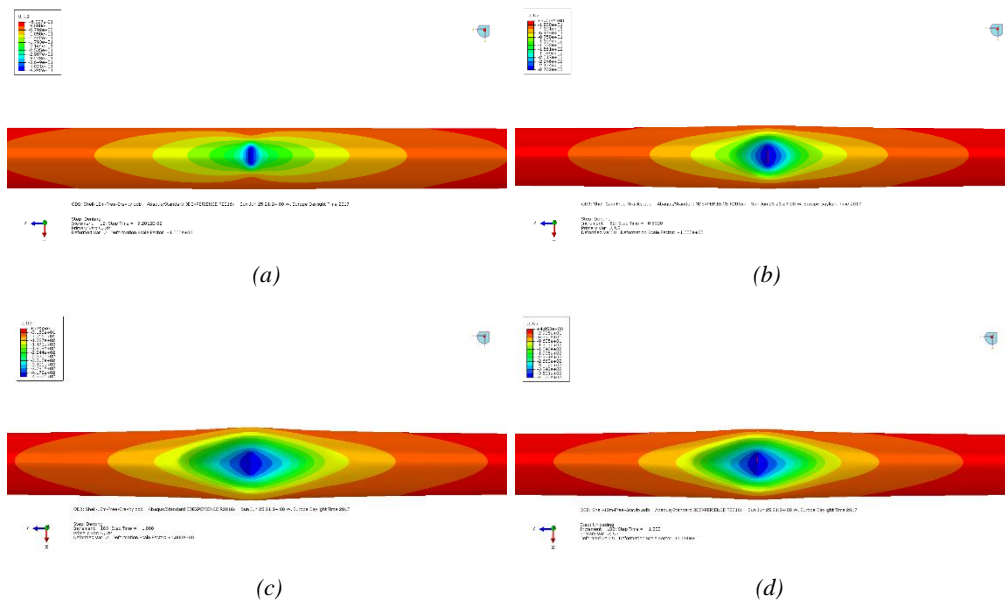


Figure 4.3 Vertical displacement component contour plot, for different stages of loading and unloading.

4.1 Length Sensitivity of Model

In this section, the length of the static model has been investigated. The reason, is that because in place pipelines are of interest for this thesis, small constrained specimens do not have value. Thus, it is important to investigate what length would be adequate to properly model this problem. In order to remove the effect of boundary conditions, two convergence criteria have been used. First, the point that lies on the other end of the denting must not have any upward vertical displacement throughout the analysis and secondly, the load – dent curves must agree.

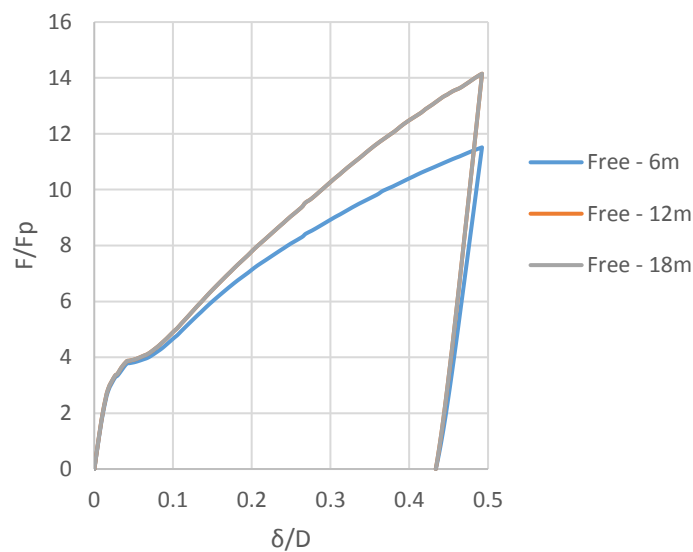


Figure 4.4 Force-dent diagram for different model lengths.

As can be seen from the above results, a half-model of 12m (24m in total) suffices to model properly the quasi-static denting. The difference between 6m and 12m analyses, is that the shorter specimen does not have enough weight to counterbalance the upward movement of the far end, thus resulting in a smaller stiffness. However, for dents up to $0.1D$ the prediction for all the models is the same, since this is a localized deformation that is not affected by any boundaries.

Moreover, it can be observed from the comparison of the residual stiffness path between the models that the longer the model the more resistance to denting the system has. This is natural since the system weight acts as a fixity not allowing rotation of the cross section after a certain length and thus a higher bending stiffness of the generators is obtained. This means that practically an in-place pipeline will act as a fixed pipeline of a certain length depending on the diameter. However, the residual dent is also not affected by the boundary condition as it is the same.

4.2 Shape of Indenter

As aforementioned, the dimensions of the denting hammers used for the investigations have been taken from the DNV-RP-F111. However, in reality the shape and size of the falling objects on the pipeline will differ. This means that the effect of size and sharpness of the object must be studied. The conclusions of this investigations will be very useful to understand the denting physics.

The first step would be to change the length of the DNV inventors, from a small size to a big one. At this point, it would be convenient to express the transverse length of the hammers by normalizing them by the diameter D . This will give a dimensionless character in the investigation. Rigid indenters with an edge of Type A and a length that varies between 0.16-2.0 diameters will be used in the analysis of the typical pipe section that has been chosen.

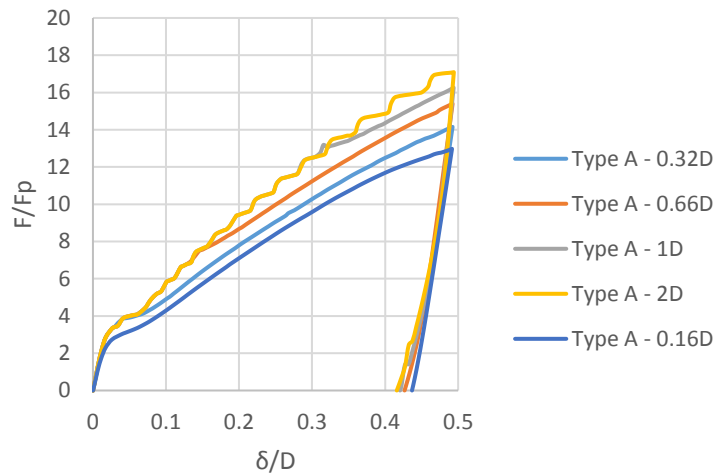


Figure 4.5 Force-dent diagram for different transverse size of the indenter.

As can be observed from the graph above, the transverse length of the indenter affects the behavior of the pipe against denting. More specifically, for smaller lengths yielding occurs faster. This is due, to the concentration in stresses, as the same force is applied through a smaller area. However, the difference is relatively small and could be neglected. For bigger dent sizes, larger than 10% of the diameter, the residual stiffness path the slope is generally stable for the different indenters as they curve remain almost parallel.

Moreover, the curve that belongs to the indenter with length equal to 2D and to 1D, presents small anomalies as the denting increases. This is not a numerical instability but it can be simply explained as follows: Initially the contact between the indenter and the specimen is restricted to a small area which is only a small fraction of the diameter in length. As the denting progresses, a bigger area of the hammer comes in contact with the pipe. This utilizes more material and activates a bigger region around the dent, which is responsible for the residual stiffness of the system. So, the bigger the object, the bigger

the area around the dent it activates resulting in a higher residual stiffness. Thus, behind every small jump of stiffness the reason is the increased contact area.

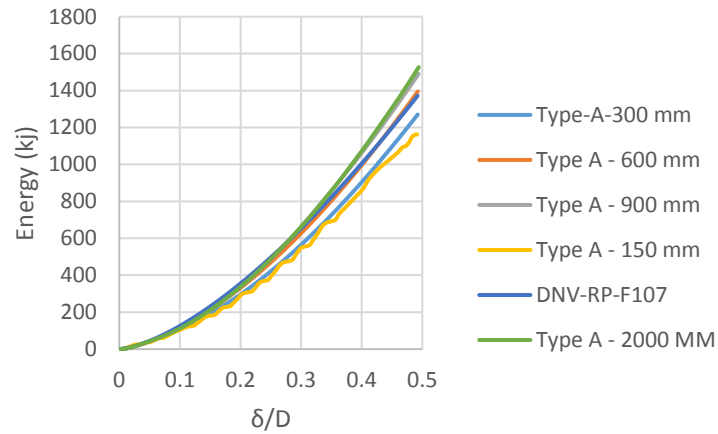


Figure 4.6 Required energy - dent for different indenter lengths in the lateral direction.

For the unloading path, not significant difference is observed. This, means that unloading of the pipe is a property of the cross section, as it tries to find equilibrium. Thus, the material properties and the D/t ratio seem to dominate the unloading response when no other loads are accounted. The residual dent depth, for all the aforementioned cases is similar with a difference of less than 5%, which makes it negligible.

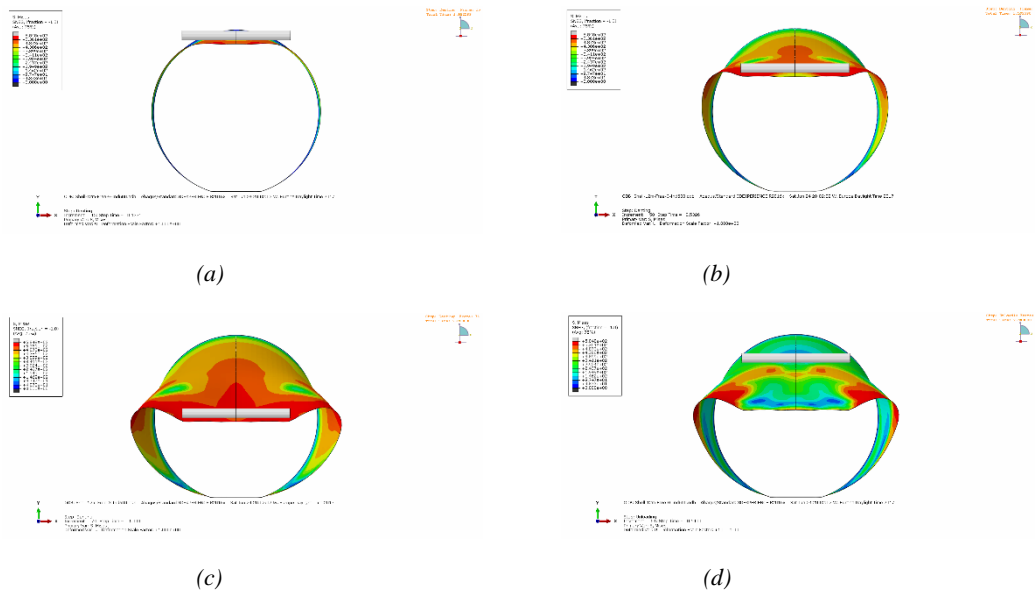


Figure 4.7 Deformed tube cross-section for indenter size equal to $0.66D$. (a) elastic region (b) first yielding (c) maximum dent (d) permanent dent

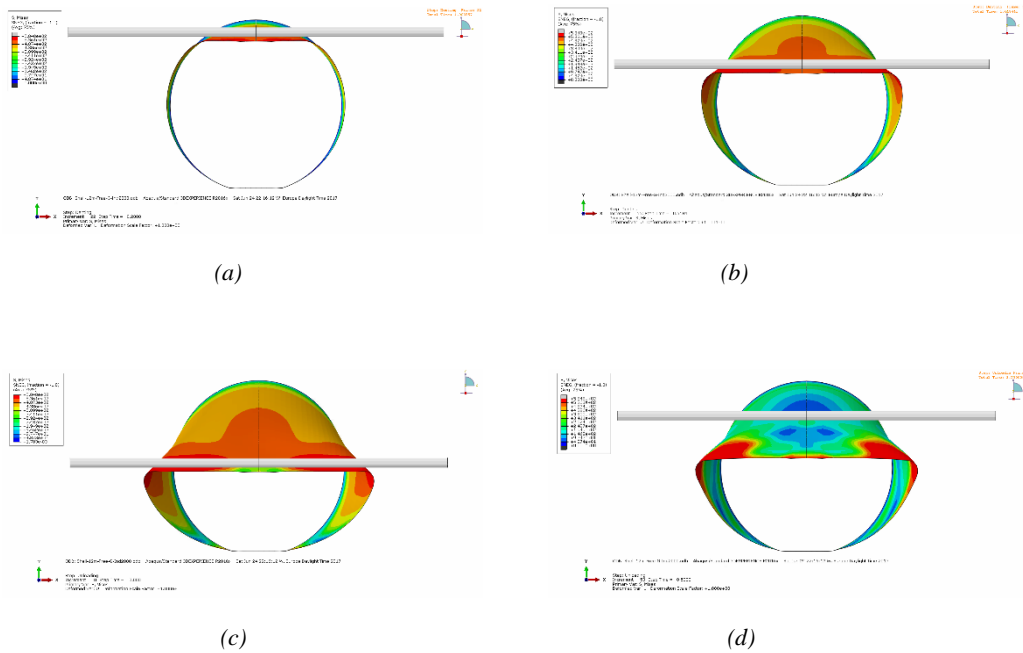


Figure 4.8 Deformed tube cross-section for indenter size equal to $2D$. (a) elastic region (b) first yielding (c) maximum dent (d) permanent dent

4.3 Presence of Internal Pressure

In this section, the effect of the internal pressure will be studied. This investigation is necessary, as it is very likely to be encountered when the pipeline is operating. The work done by internal pressure will have a positive effect in the system capacity, as it counteracts the denting force. In this section, we assume that the pressure gradient is zero and the pressure does not change with a volumetric change (locally). Moreover, due to the quasi-static nature of the analysis the inertia of the fluid and the added mass cannot be modeled here. This effect will be investigated later in the dynamic transient analysis, where the dynamic response of the system will be examined.

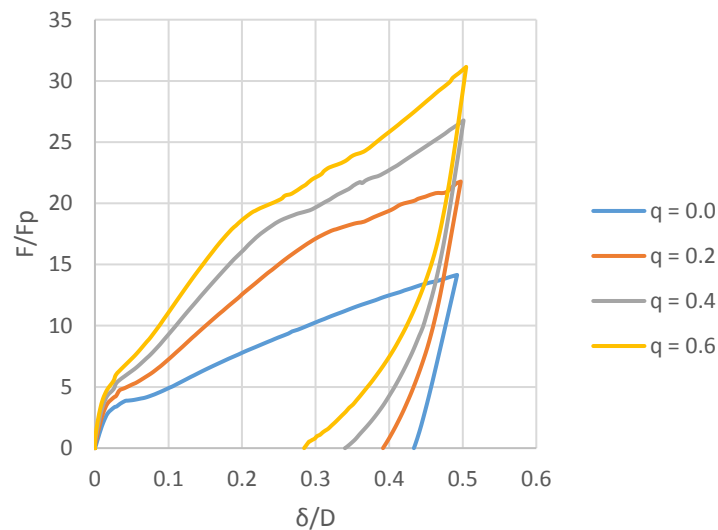


Figure 4.9 Force-dent diagram for different internal pressure levels.

More specifically, from the above graph, it can be easily observed the significant effect of the internal pressure in the quasi-static denting response of a pipe. As the internal pressure increases, although the hoop stresses get closer to the yielding stress, the system becomes stiffer.

For small dent sizes, it is observed that the yielding (change of slope) takes place for slightly higher loads, which means that the pressure provides extra stability to the system in the early stages of the deformation but yielding dominates this region. Next, the residual stiffness slope also becomes steeper with increased pressure. This, verifies the initial statement that was made: The internal pressure has a negative work against denting, which means that it acts beneficially and in the opposite direction of the dent.

In the unloading step of the analysis, something interesting is observed. Each specimen follows a different slope in the unloading path. As the internal pressure increases, the residual dent tends to decrease analogously. Specifically, the initial unloading path is governed by the material of the tube, but when the external force is about to drop to zero, the internal pressure affects the path and makes it curved rather than linear. This result is

very important, as most of the time pipelines work under internal pressure. Here, the extremely beneficial effect of a pipe under internal pressure is presented.

The effect of internal pressure can also be understood by the following graph, where the energy per dent depth is presented. For example, for a pressure equal to 60% of the yielding pressure, the energy needed is almost 2.5 times the energy of the empty pipe in order to reach the same deformation.

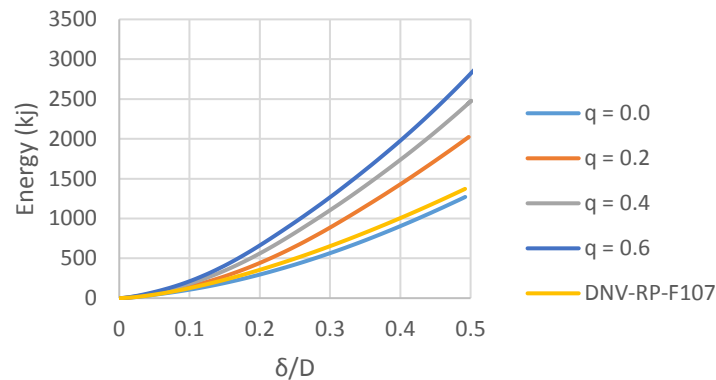


Figure 4.10 Required energy - dent diagram for different pressure levels.

Existence of pressure has an immediate effect on the size and shape of the dent. The dents, now are more localized around the contact area, whereas the nearby regions remain relatively untouched. This is a very important feature when the damage of the material has to be investigated in order to capture rupture and perforations of the pipe. A paradox takes place here. Although, the system in general is stiffer in terms of the load-dent curve, the so-called perforation energy is lower.

This can be explained, because due to the presence of the liquid (oil, gas or water) the deformation is localized to the area under the indenter. This means that all the energy that the falling object induces will be absorbed by a smaller area which in the end will lead to perforation or rupture. The amount of this energy will be less than the energy needed for an empty pipe because in that case the deformation will be more equally spread out resulting in smaller strains and stresses locally.

Moreover, in order to take into account, the fact that operating pipelines are shut down often for maintenance and inspection purposes, the internal pressure has been removed after the unloading of the tube specimen. The reason behind is to measure how much depressurization of the pipe affects the residual dent depth. As aforementioned, the internal pressure has a negative work, which makes the whole system stiffer and thus for the same energy input a smaller maximum and residual dent depths are derived.

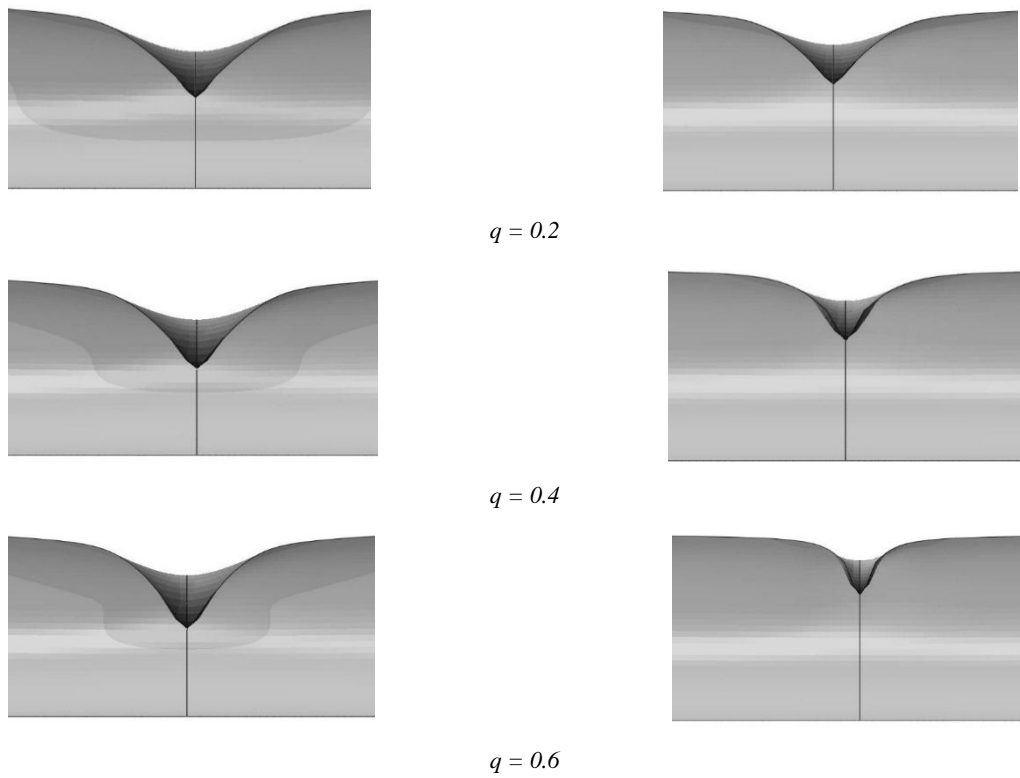


Figure 4.11 Longitudinally cut of a deformed pipeline for different pressure levels. (Left) maximum dent, (Right) permanent dent.

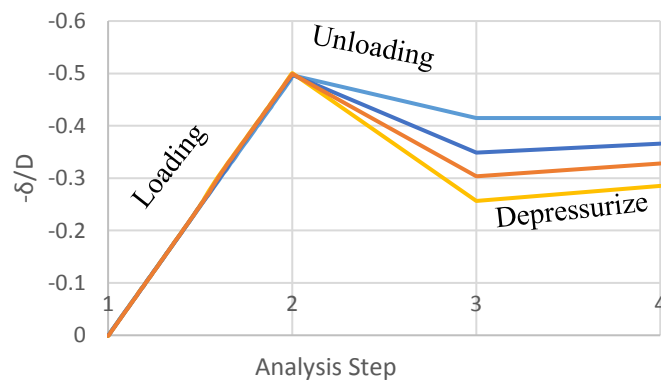


Figure 4.12 Effect of depressurization on dent size of a pipe.

4.4 Effect of External Pressure

In this section, the effect of the external pressure will be studied. This investigation is necessary, as the worst-case scenario would be that the pipeline has stopped operation and thus there is no internal pressure to counter the effect of the hydrostatic pressure.

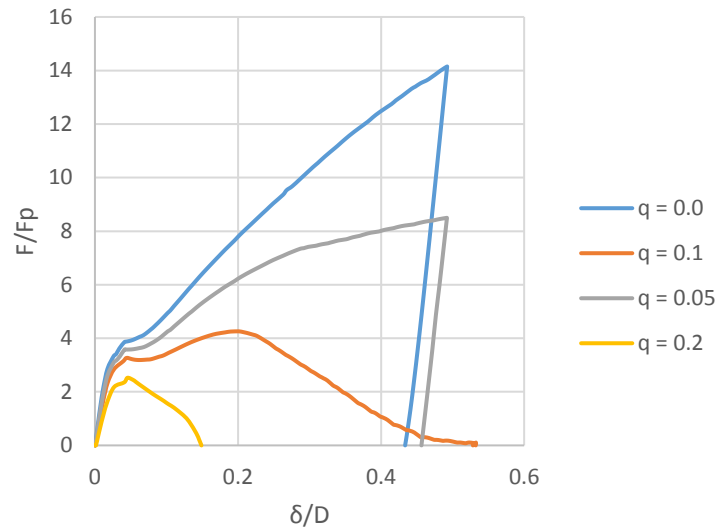


Figure 4.13 Force-dent diagram for different external pressure levels.

The work done by the external hydrostatic pressure will be added to the work done by the indenter, which will result in a reduced system capacity. To this, end several analyses have been carried out with the external pressure as the main parameter for investigation. The results will be compared with the empty pipeline case.

As expected, with a small increase of the external pressure, the system becomes a lot softer in terms of stiffness. The work needed by the indenter to reach the prescribed dent depth is less when external pressure exists. However, an additional phenomenon occurs here.

By denting the pipeline out of roundness conditions are introduced in the cross section and the circular shape starts to ovalize as the dent size increases. This acts as an imperfection and thus the work done by the external pressure is no longer in an equilibrium.

It has been observed, for a given indenter shape every cross section can initiate a propagation buckling for a pair of dent depth and external pressure. In order for this to happen, the pipeline initially shows a normal behavior against denting until a maximum value. After that, the system becomes unstable and the cross-section collapses. The collapse then is propagated towards the neighboring cross-sections until infinity or until the external pressure drops at some point. In practice, buckle-arrestors are positioned at specific points of the pipeline route in order to stop the propagation of collapse. Buckle-

arrestors have practically increased stiffness and thus they are not sensitive to buckling under the existing pressures of the site.

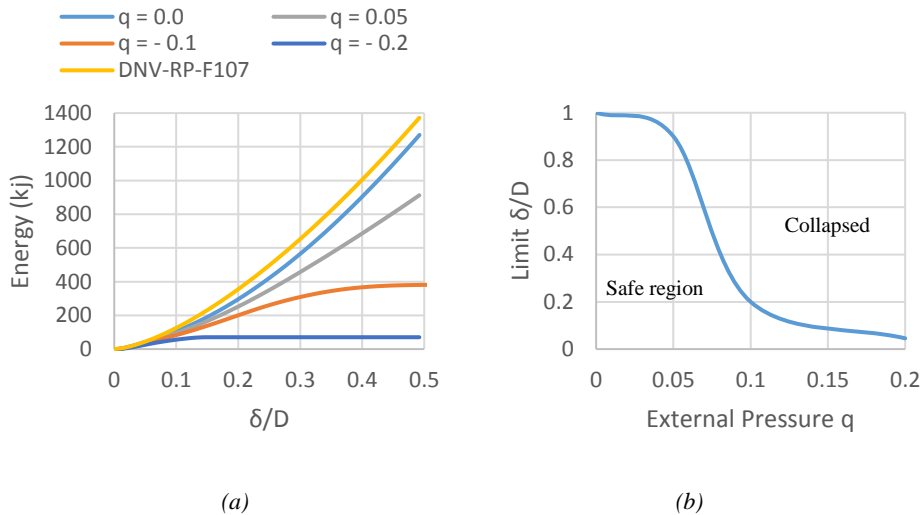


Figure 4.14 (a) Required energy - dent diagram for different external pressure levels, (b) allowable dent size for a given external pressure level.

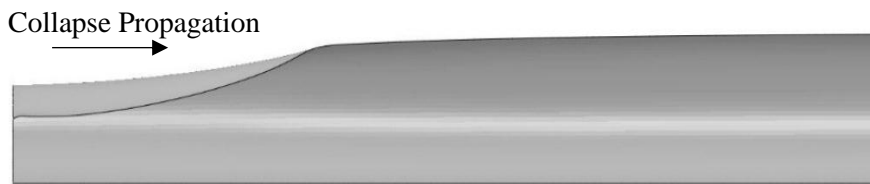


Figure 4.15 Deformed pipe for $q = 0.2$. The longitudinal deformation has been propagated further and the pipe is about to collapse.

Although, the implicit quasi-static algorithm can describe adequately the behavior of the pipeline, it breaks down as soon as the collapse buckling occurs. If a dynamic solver is used, the propagation buckling can be captured in its entirety, giving a better estimate and visualization of the phenomenon, and capture the propagation speed of the buckling. The findings of this investigation are very interesting, as it shows that in case of such a scenario, outcome could be devastating. DNV, does not take this into account based on the assumption that pipelines usually will be either buried or filled with contents. Thus, excluding internal and external pressure is considered a balanced assumption. In the required energy per dent depth graph, the significance of external pressure can be easily observed. Especially for dent depths beyond $0.1D$, DNV fails completely to give a reliable estimation.

4.5 Effect of Young's Modulus

One state of the art topic of research nowadays, is the value of Young's Modulus for steel and how it is affected by the loading rate. Some experiments (Selker & Liu, 2016) have been already conducted by researchers and academics on this topic, however the deviation from the standard value of $E = 210$ GPa is small. It is important so, to investigate how much even a small change of a few giga-pascals affects the behavior of the system. Some researchers claim, that this slight increase is due to viscoelastic phenomena that occur within the microstructure of the steel and add a viscosity term for very high velocity loading. Moreover, as reported from Selker et al, there is an elastic anisotropy of the pipe material that is attributed to the manufacturing process but will not be investigated here.

To this end, three cases have been considered for analysis, where the Young's Modulus takes values between 207-213 GPa in order to investigate the sensitivity of the system. These values, have been taken from the work of *M. Radovic et al* where the values of E were measured experimentally for several high-speed loads with different measurement techniques. This means, that we do not expect a big fluctuation of the E value but still if any it is important to quantify what the effect would be.

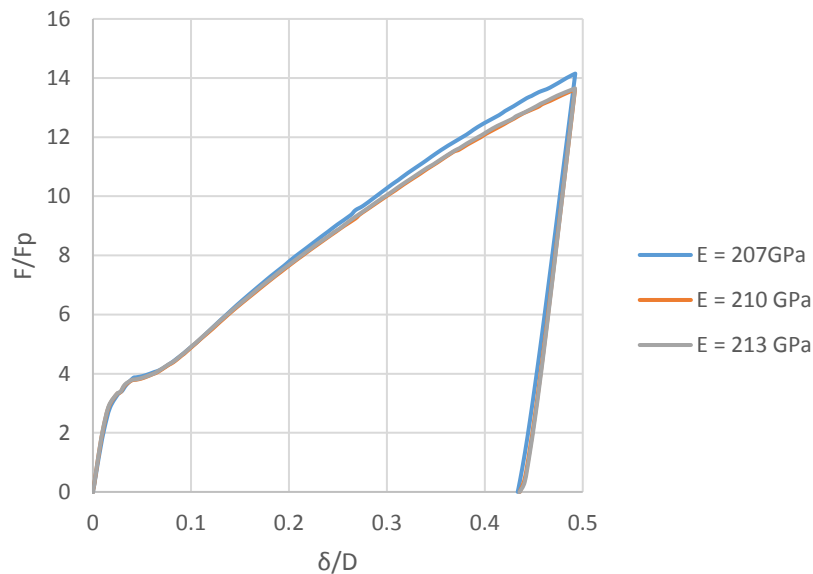


Figure 4.16 Force-dent diagram for different values of Young's Modulus

The effect of Young's modulus for the range that has been specified is trivial. This means, that even if a more sophisticated material model that accounts for viscoelastic behavior of steel is implemented, the results will not differ. Thus, it is safe to say that viscoelastic phenomena can be neglected for the range of velocities that the present thesis is interested in. It is possible that for different loading conditions and loading rates, viscoelasticity might play a significant role. For example, in pile-driving where the tube is loaded very fast axially, transmitting acoustic waves in the longitudinal direction.

4.6 Effect of Material

The effect of the yielding stress has also been considered for investigation. The reasons for this are two. First, it is desirable to check how higher steel grade pipelines will respond compared to lower grades. Secondly, for the dynamic impact analysis that will follow, strain-rate phenomena will play a significant role in the response of the system. This phenomenon, tends to increase the yield-stress of the system for very high strain-rates. So, it is important to see how an equivalent static model with increased yield stress can compare to the more realistic dynamic analysis.

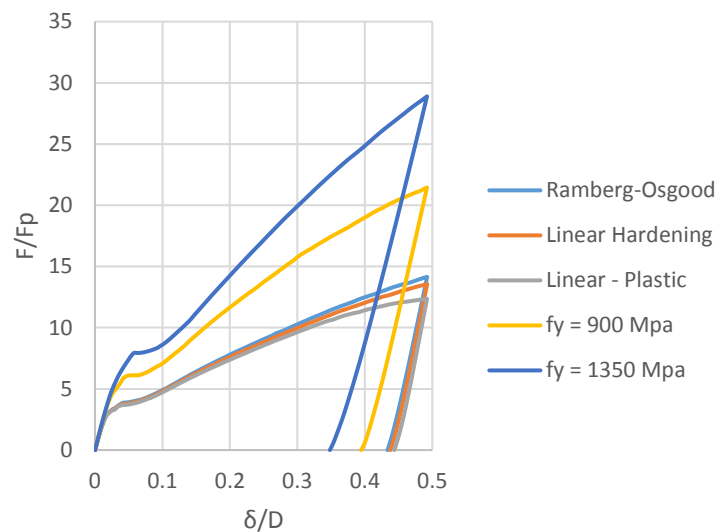


Figure 4.17 Force-dent diagram for different material models and different yield stresses.

By observing the load-dent curves of the above graph, the following can be safely concluded. Initially, for small dent size where the phenomenon is local and it is dominated by yielding, the hardening behavior doesn't play any role. On the other side, for increased yielding stress of the material, it is observed that the stiffness reduces for a bigger dent size as the yielding stress increases.

For the path of reduced stiffness, again, the material hardening does not seem to play significant role in the results. Only a small underestimation of the denting is observed for dent equal to $0.5D$. For the specimens, with increased yield stress, the residual stiffness is higher (steeper slope of the curve), as the yield stress increases. This results in forces up to two times higher than the ones that are calculated for the simple Ramberg-Osgood material with $f_y = 450$ MPa.

For the unloading path, yet again the behavior of the system differs for different yield stress values. The slope of the path for all of the cases is the same, however the residual dent depth is not. As the yield stress increases, the residual dent depth decreases. The difference between the measured residual dent and the maximum dent size is significant.

However, the deformation patterns of the cross-section and the longitudinal direction for all cases are completely the same as they are material insensitive. Specifically, the deformation profile has to do with the external parameters that act on the system as: the indenter shape, the length of the pipe, the boundary conditions for small pipelines, the existence of internal or external pressure.

Material	Max. Dent	Residual	Reduction
fy = 450 MPa	0.5 D	0.44 D	12%
fy = 900 MPa	0.5 D	0.4 D	20%
fy = 1350 MPa	0.5 D	0.35D	30%

Table 4-2 Maximum and permanent dent results for different yield stresses.

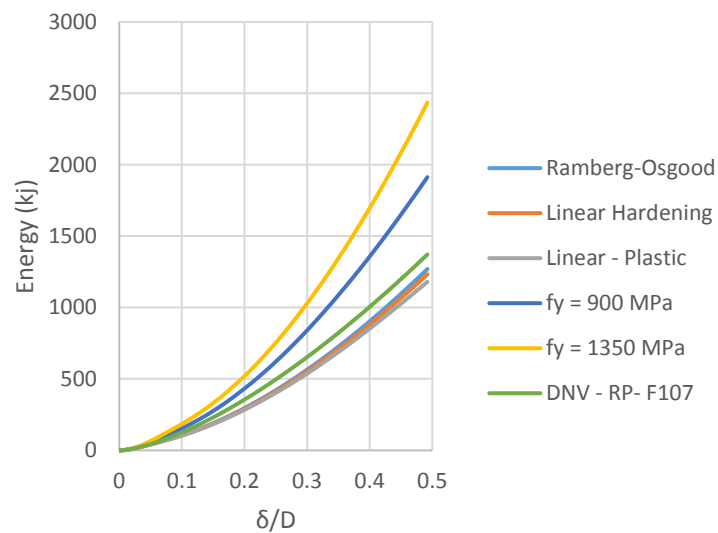


Figure 4.18 Required energy - dent for different material models and yield stresses.

Page intentionally left blank

5. Dynamic Denting

5.1 Introduction

In the previous chapter a simplified quasi-static denting model has been thoroughly investigated. However, this analysis does not take into account mass or velocity of the object that hits the pipe. Thus, it is important to quantify how much these parameters, affect the denting and the energy distribution in the system.

The physics of impact necessarily involve conservation of energy and momentum. When a moving object strikes a structure the force which decelerates the mass satisfies conservation of momentum. The kinetic energy of the impacting body will be partially converted to strain energy in the target and partly dissipated through friction and local plastic deformation and strain energy ‘radiated’ away as stress waves. The details are very difficult to predict, but some simple estimates based on first principles can usually result in reasonable estimates for response. Practically, the problem that has to be solved here is an impact transient problem with non-linear contact, as the contact area and the force that is introduced to the pipe vary with time. This means, that for different mass-velocity combinations the impact duration will change and together the behavior of the system.

Below a representation of the impact duration can be seen, in order to understand the physics of a realistic impact. The peak force is in phase with the peak dent displacement, which means that they happen simultaneously. Moreover, the whole phenomenon, lasts less than 0.1 of a second. This means, that due to the very high velocity loading and wave propagation that the system generates, the analysis has to be calibrated correctly in order to capture adequately all the aforementioned. Moreover, in the current investigation no Rayleigh or is taken into account initially, only a uniform 5% structural damping.

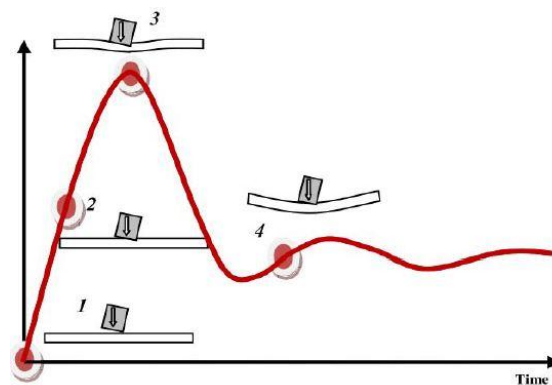


Figure 5.1 Typical dent deformation versus time diagram. (Alsos et al, 2012)

By bringing in mind a bullet –small mass, large velocity - that hits a steel plate, it is possible to imagine how the pipe will respond in such a case. The bullet will induce a very local dent to the system and thus the energy absorption will be local as well, resulting

in a more localized dent than if the bullet would have bigger mass and smaller velocity but same kinetic energy. In general, the dent shape and size will differ with different mass-velocity combinations. However, this is just an observation that has to be quantified and measured with the computational tools that are available.

To this end, the comparison and the investigation will be conducted in the following manner. For a given deformation energy from the quasi-static analysis a series of mass-velocity pairs will be created, where always the same kinetic energy will be derived. After that, a dynamic analysis will be performed where the rigid indenter will be assigned each time to these properties and the response of the pipe will be measured.

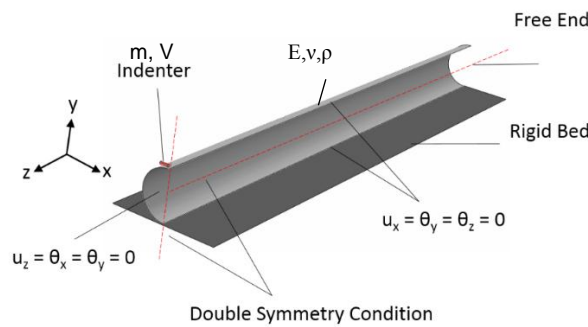


Figure 5.2 Dynamic model configuration

The important results will be the maximum and residual dent, the shape of the dent and the force-dent diagram as well as the time that is required in order to reach the peak load. Through the force-dent diagram it is very easy to understand how stiff the system has responded for a given excitation and based on the observations of the quasi-static analysis it is possible to understand what every behavior means practically.

Since now, the problem is not displacement controlled, is not possible to measure the force of the indenter directly. To overcome this issue, by recalling the Newton's 2nd law of motion, the force of a moving body is equal to its acceleration times its mass. Since the acceleration can be measured, the problem is solved by multiplying each time the acceleration time history of the indenter with the prescribed mass.

$$\Sigma \vec{F} = M \cdot \vec{a} \quad (5.1)$$

For the purposes of investigation, several different cases will be considered. Initially, for a fixed mass the velocity and thus the kinetic energy will increase, to observe how the system will react. This is due to the large uncertainties in the calculation of the terminal velocity. Moreover, for the same kinetic energy input several mass-velocity combinations will be tested in order to see what is the effect of the velocity in the deformation of the pipeline.

For the mass, no distinction has been made between real and added mass, as in the end the kinetic energy is calculated as follows:

$$E = K = \frac{1}{2}(M + M_a) \cdot V^2 = \frac{1}{2}(M_T) \cdot V^2 \quad (5.2)$$

The combinations have been derived by simply substituting the mass or the velocity in the equation above and solving for the other one, for a given energy.

5.2 Preliminary analysis

5.2.1 Fixed Tube of Finite Length

Before proceeding on the semi-infinite case of 50D length which is closer to reality, a model which can be easily configured in a laboratory will be tested to examine any differences between the quasi-static and the dynamic analysis. Then, it is possible to have a better understanding of the larger model which corresponds to the real situation.

The model is comprised of a double symmetric finite tube of 5D length, resting on a rigid bed where it's far end is fixed against all displacements and rotations. It is expected that due to the small length the effect of the boundary conditions will be significant. Initially, a quasi-static analysis is being performed followed by dynamic analyses with different velocities but for a fixed amount of kinetic energy input. Here, damping will be introduced as structural damping ξ , with values between 0 and 5%. Damping will be discussed again at the end of this chapter.

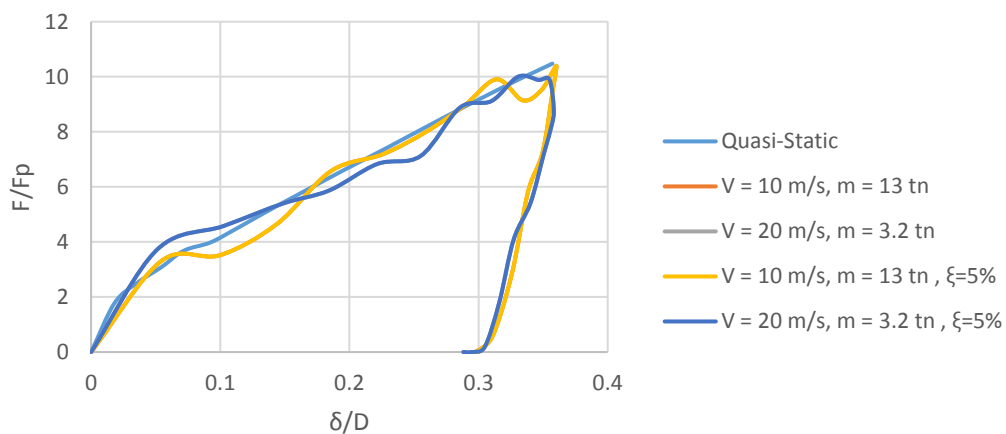


Figure 5.3 Force-dent diagram for a finite length tube resting on a rigid bed with fixed ends.

As can be seen from the above graph for an input kinetic energy of 645 kJ and for different input velocities the force-dent diagram between the dynamic and the quasi static cases are almost identical. This gives confidence in the results as no strain-rate effects are considered. Additionally, when structural damping equal to 5% is introduced to the model

not significant difference is observed. Since the results are reasonable for this simplified case of a fixed tube of finite length the semi-infinite pipeline will be analyzed next.

5.3 Semi-Infinite Tube

5.3.1 Model Length

The model length is chosen after an iterative procedure, based on two parameters. The first one is that the pipeline mass will always be larger than the dropped object's mass in order to account for the infinite mass that the pipeline has. The second one, is that the far end of the pipeline will not affect the solution of the problem. This can be easily obtained either by considering different lengths and check the convergence of the solution or by imposing fixity conditions at the far end of the pipeline and increase the length to the point that the boundary conditions will not affect the results anymore. In the end an approximate length for the symmetric model is considered to be $50D$ (or $100D$ for a full model with no symmetry).

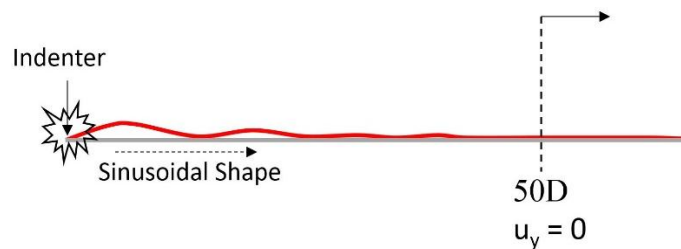


Figure 5.4 Dynamic model length determination

It is observed during the preliminary dynamic analyses, that besides the dent deformation, the pipeline vibrates as a one-dimensional beam in a global sinusoidal mode. This low-frequency global vibration of the pipeline as a beam is probably due to the absence of low-frequency damping in the finite element model. However, due to the difficulty that the calculation and estimation of damping has this will be treated separately later in this chapter. It is thus expected, that the stiffness of the system against dent will be a priori lower than in reality, however how much cannot be answered.

5.3.2 Gravity in Dynamic Analysis

During, modeling of the dynamic problem gravity has to also be taken into account. Gravity affects the system in two ways. First, it creates an initial stress state for the pipeline on the seabed (even with the effect of buoyancy) and secondly it acts as a permanent distributed force downwards during the impact duration. Of course, this force is equal the mass of the pipeline per meter times the gravitational acceleration which is equal to $1G$ (9.81 m/s^2).

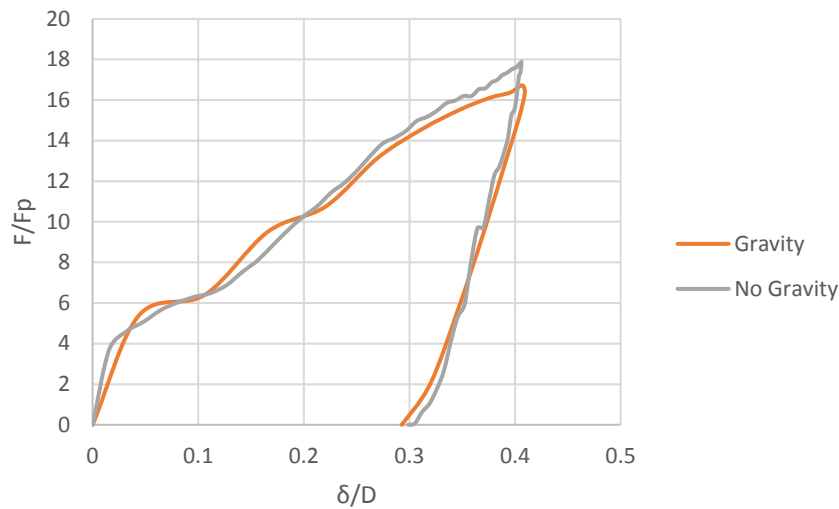


Figure 5.5 Effect of gravity on load-dent diagram in a dynamic analysis of a semi-infinite pipeline

One interesting thing has been observed about gravity, during the investigations of this thesis. The acceleration that is measured on the pipe and on the object during the impact duration are orders of magnitude higher than the 1G. This practically means, that gravity does not actually affects the impact but by 1-2%. This finding can be used to reduce a lot the computational time needed, as gravity in an explicit analysis needs a sufficiently big-time step in order for the system to reach equilibrium and this is not computationally efficient. Thus, in some cases for the duration of the impact the gravitational acceleration will be neglected, but not the initial stress state of the pipeline due to gravity before the impact.

5.3.3 Dynamic vs Quasi-Static Analysis

So far, all the analyses were considered quasi-static and thus no inertia was taken into account in both the developed FEM model and in the DNV formulas. However, the real-life situation is dynamic. It is desirable to compare, if in a dynamic analysis a specific energy input would give results similar to the quasi-static case. The following cases will be considered for the dynamic analysis for a fixed energy input:

Energy	Velocity (m/s)	Mass (kg)
670 kJ	5	53600
	10	13400
	15	5956
	20	3350

Table 5-1 Dynamic Load Cases

For the examined pipe $D = 914.4$ mm, $t = 20.9$ mm, energy equal to 670 kJ is chosen which corresponds to a normalized dent size of $0.306D$ from the DNV equation. Of course, the energy magnitude depends to the pipe diameter, D/t ratio and length. Smaller pipes can absorb a smaller amount of energy before reaching failure. In this investigation, no pressure is taken into account external nor internal and the bed is considered perfectly rigid and again no damping is taken into account. However, the qualitative results and conclusions should apply to all pipes.

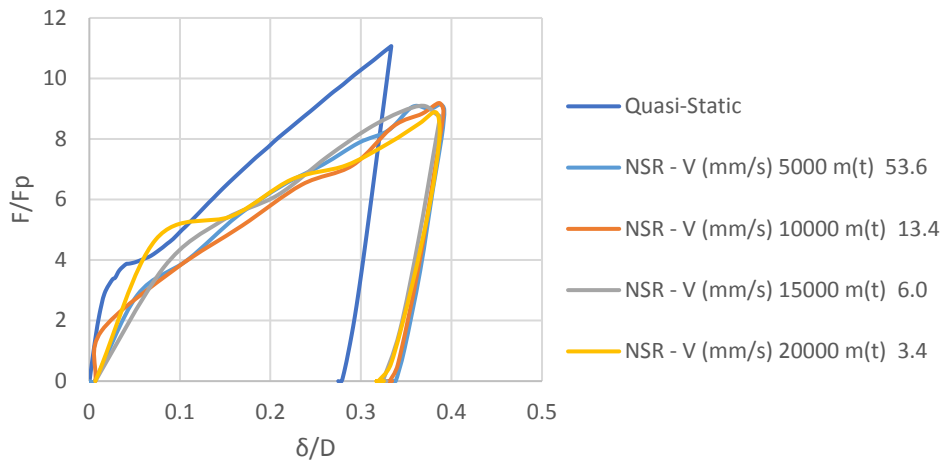


Figure 5.6 Comparison of quasi-static and dynamic force-dent diagrams for the same input energy.

By performing the dynamic analysis, the following are being observed:

- In contrast with the fixed tube in the preliminary analysis, now the dynamic cases without any strain-rate effects and damping included, do not correlate well and additionally the dynamic behavior is softer which seems to be counter-intuitive.
- For the prescribed kinetic energy input, both the maximum and permanent dent size are increased by 15% both and this applies also for smaller and larger input energy levels. The unloading path is not affected.
- The velocity magnitude does not affect the results for the dynamic analysis for values from 5 to 20 m/s. The area covered by the quasi-static and dynamic cases and equals to the work done by the indenter is the same. Until the first yielding the curves match.
- By not including any strain-rate effect on yielding, the resulting denting deformation is bigger than the quasi-static case. This would be the case for very slender cylinders with other than steel material.

- The load – dent curve is less steep (smaller stiffness) in the dynamic analysis, which means that the resistance of the pipe against denting is decreased when loaded dynamically and no strain-rate yielding is taken into account. The exerted force from the indenter is smaller as well. By observing the deformed structure longitudinally, it is evident that the denting in the dynamic case, is a lot steeper than the quasi static one. This indicates, that the flexural resistance of the system is not fully utilized when loaded dynamically, as the generators do not contribute fully in the resistance when stretched.

	Input Energy	Max. Dent (δ/D)	Perm. Dent. (δ/D)
DNV-RP-F111	670 kJ	0.306	0.267
Quasi-Static FEM		0.334	0.278
Dynamic FEM		0.386	0.322

Table 5-2 Maximum and permanent dent results as derived from DNV, quasi-static and dynamic FEM models.

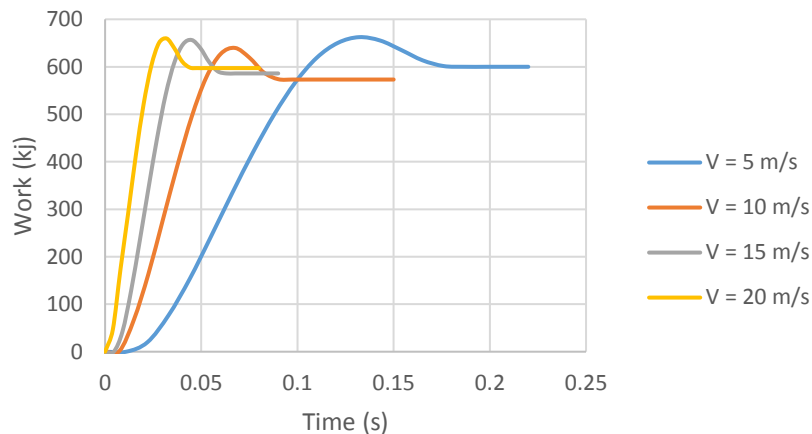


Figure 5.7 Transferred energy (work) versus time for a fixed kinetic energy and different velocities.

5.4 Velocity Dependence

In this section, the effect of the velocity for a given mass will be investigated for an empty pipe. This is considered to be an important investigation, because as aforementioned the terminal velocity calculation of an object cannot be predicted very accurately as it depends on the depth, the size, the angle that the object falls and its weight.

Here, the effect of strain-rate in yielding has been neglected in order to observe how good the dynamic results correlate with the quasi-static analysis. In a later stage, the strain-rate will be taken into account in order to observe how it affects the analysis. To this end, a pipeline resting on a rigid bed will be investigated for an impact with a Type A indenter.

Generally, the curves follow the same trend and as it has been already observed the unloading path is the same as it depends mostly on the material properties. The percentage difference between the maximum and residual dent size is roughly the same as in the quasi-static case.

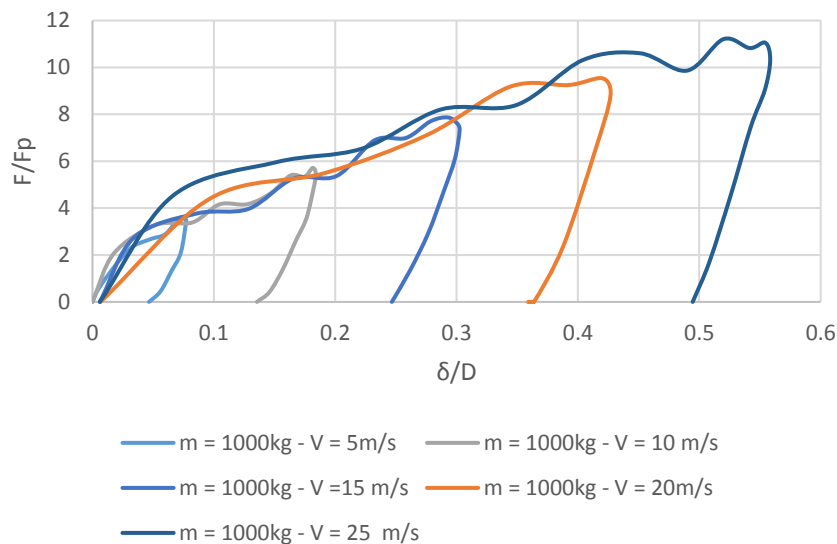


Figure 5.8 Force-dent relationship for different velocities and constant mass.

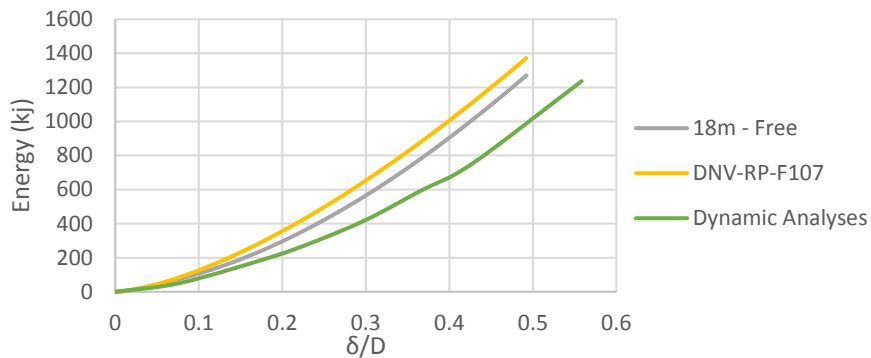


Figure 5.9 Energy-dent diagram for dynamic analysis.

By plotting, the results in the energy-dent diagram, it is clear that the dynamic analysis behaves a lot “softer” than the predicted response from the quasi-static analysis and from the DNV equations. There is no doubt that, inertia and velocity play significant part in the deformation of the pipeline during an impact and neglecting them is not conservative if no strain-rate is taken into account. This analysis verifies that even the material used is not strain-rate sensitive (like aluminum) the impact and consequent dent cannot be treated as a static loading.

If damping was accounted in this set of analyses, small differences would occur for different velocities as the damping excited forces are proportional to the velocity magnitude.

5.5 Strain-Rate Sensitivity

As aforementioned, up to this point no effort has been made to take into account the strain rate dependence of the yielding stress of the material. Thus, this must be investigated as it might affect the denting behavior and values of both maximum and residual/permanent dents.

The pipeline material might be almost strain rate insensitive (e.g., aluminum alloys), or strongly strain rate sensitive (e.g., mild steel), and this phenomenon might be more significant at higher impact velocities and less important, but not negligible, at lower impact velocities, which are often taken as quasi-static.

Palmer et. Al have estimated strain rates of 0.3 to 4.6 s⁻¹ in eight tests on concrete-coated pipelines impacted at velocities between 5.91 and 8.23 m/s. The pipeline wall curvatures in the longitudinal directions were calculated from the final internal radial displacement profiles of the pipelines and used to estimate strains of 0.002 to 0.067. The strain rate was then estimated when dividing these values by the recorded response duration for each test specimen. The yield stress increased reportedly up to 1.7 times of the characteristic value.

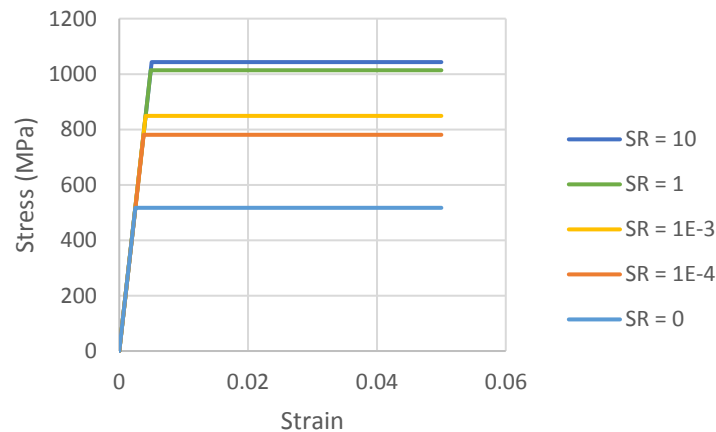


Figure 5.10 Stress-Strain curve for different strain-rate values according to Cowper-Symonds power law.

In common practice, the Cowper Symonds law is used in strain-rate sensitive problems in order to evaluate the yielding stress as a function of the strain rate. The equation has the following form:

$$\sigma_d = \sigma_y \left(1 + \left(\frac{\dot{\epsilon}}{D} \right)^{\frac{1}{n}} \right) \quad (5.3)$$

Where $\dot{\epsilon}$ is the strain rate for a time interval, and n, D are parameters that are obtained from experience and experiments and are not defined in a strict mathematical or engineering way. σ_y is the characteristic value of yield stress of the material.

One drawback of the Cowper-Symonds equation is that it considers an elastic-perfectly plastic material. This means that strain-hardening after yielding is not considered and the true stress-strain curve cannot be used.

Palmer et. al. examined the influence of material strain rate sensitivity with the Cowper Symonds equation having the usual coefficients for the yield stress of mild steel ($D = 40.4 \text{ s}^{-1}$, $n = 5$).

Following the values measured by Palmer et al for the strain-rate in a range of 0.3 to 4.6 s^{-1} , a comparison is being made for a velocity of 5, 10 and 15m/s to observe if indeed the derived values of strain rate are within an acceptable margin.

Indeed, the following graph represents the strain-rate of the $D=914.4\text{mm}$, $t=20.9\text{mm}$ pipeline for a dropping mass of 4000 kg, modeled with the type A indenter on a rigid bed. Strain rate values especially at the beginning of the impact correspond to values from 5 to 50 s^{-1} . However, the yield increase for these values is roughly the same and of course the biggest strain rate is observed for velocities up to 30m/s (108km/h).

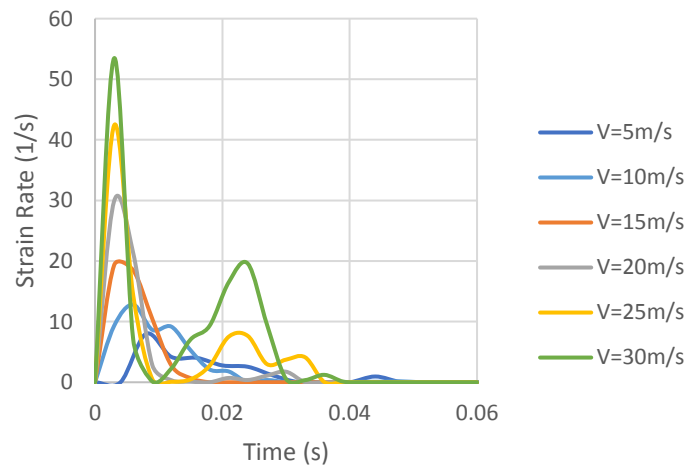


Figure 5.11 Strain-rates over time for different velocities of impact and constant energy input.

Now, by making use of the strain-rate dependence of the yielding stress in the FEM model, the previous analyses are conducted again. As aforementioned, the input energy is 670 kJ and several combinations with different mass and velocity will be considered.

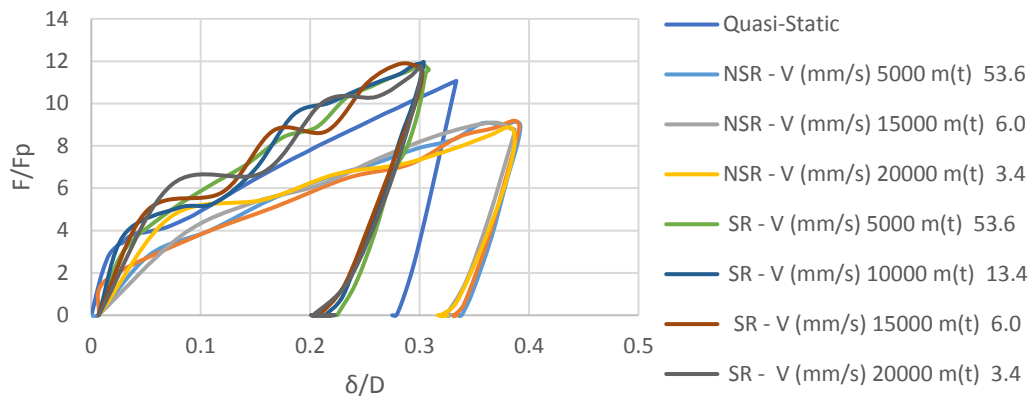


Figure 5.12 Force - Dent diagram for strain-rate model

By observing the above figure, we can conclude the following:

- The pipe presents a stiffer behavior against denting as the increased slope of the loading path suggests.
- Moreover, for the same input energy the maximum dent depth is reduced by 15% compared to the quasi-static case and 25% for the dynamic.
- The residual/permanent dent depth decreases by 25-30% compared to the quasi static case and 45% compared to the dynamic FEM.
- The absorbed energy remains unchanged, and it does not depend on whether or not strain-rate yielding is taken into account.
- The deformed pipeline again, exhibits a more local denting longitudinally compared to the quasi-static case. However, the denting itself is smaller due to the increased yield stress which adds an additional resistance to the system, as it will plastify for higher stresses.
- The unloading force – dent path is not affected by either the strain-rate or the dynamic nature of the loading, as all three displayed cases have almost parallel unloading paths.

It is concluded, that by including strain-rate dependences of the material in the model beneficial results are derived and it is closer to the reality as the experiments in the literature have showed. However, this must be used with caution in order not to reach

unrealistic high increase of the yielding stress. Strain-rate is very difficult to measure and also in Explicit analyses the time increment can affect the measured strain rate.

In the present work, the results have been also verified with the Implicit solver of Abaqus for a very small-time increment. This gives confidence in the presented results as the Implicit solver enforces a strict energy equilibrium to the system for each increment. However due to the fact that it consumes a lot of CPU and RAM, it is not convenient to use implicit algorithms in impact problems if it is not absolutely necessary.

	Input Energy	Max. Dent (δ/D)	Perm. Dent. (δ/D)
DNV-RP-F111	670 kj	0.306	0.267
Quasi-Static FEM		0.334	0.278
Dynamic FEM		0.386	0.322
Strain-Rate FEM		0.3	0.2

Table 5-3 Comparison of dent depth between dynamic, quasi-static FEM and DNV

From the comparison between the DNV equation, the quasi-static model and the dynamic with and without strain-rate effects the following are concluded:

- The DNV equation, is close with the strain-rate model for the calculation of the maximum dent depth. However, for the permanent dent depth this is not the case as there is a big difference.
- On the other hand, there is a very good agreement between the permanent dent as calculated from the quasi-static FEM and the DNV equation.
- The rest of the results show significant differences, in both the maximum and permanent dent depth.

Depending on the velocity and the energy input as well as the material behavior and the conditions that exist the dent depth can significantly vary. Moreover, this chapter is an idealized analysis with a rigid bed and with no contents. In real life, this most probably will not be the case. The DNV equations are already starting to break down compared to the detailed FEM calculations and thus more investigation is needed.

5.6 Damping Investigation

Until now, the analyses and investigations on the model behavior did not include damping or in some cases structural damping of 5% did not had any effect. As has been shown in the finite length fixed tube, the dynamic analysis was in good agreement with the quasi-static case when no damping or strain-rate sensitivities were included. However, for the semi-infinite pipeline which is of interest in the current thesis, it has been observed that the response against denting was softer compared to the quasi-static case, when dynamic analysis was performed. Of course, such a thing is counter-intuitive and despite some observations have been made, it was not possible to fully explain why the tube behaves in such a way.

After careful and thorough investigation on different parameters of the analysis it is concluded that damping seems to be critical in this specific case. More specifically, it has been observed that for the semi-infinite pipeline case the sinusoidal global deformation pattern especially of the upper generator is causing this softening of dent resistance.

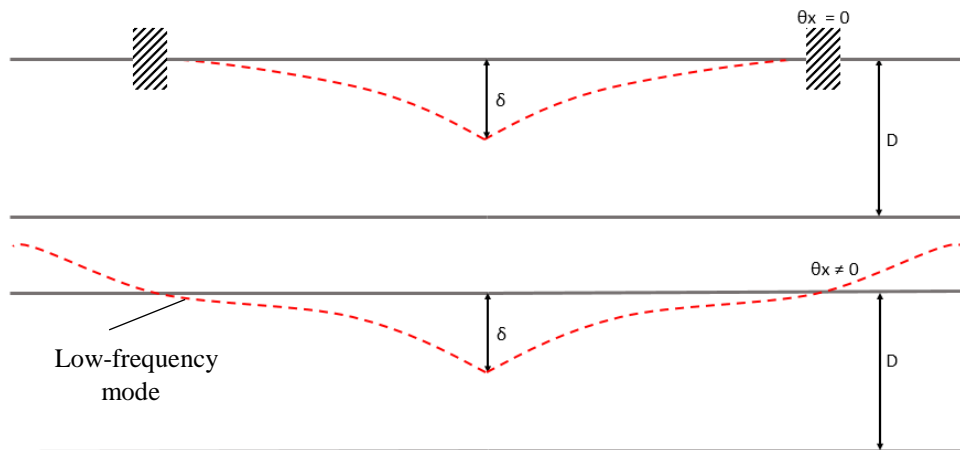


Figure 5.13 Quasi-static (top) versus Dynamic (bottom) deformation pattern. Grey solid line represents the undeformed pipeline and the dashed red line represents the deformed structure. This is a schematic representation and the scale of the drawing does not correspond to reality.

As can be seen in Figure 5.14, the deformation patterns for the quasi-static and dynamic case differ not only near the impact region but also several diameters away. When the experiment is conducted under static conditions, the upper generators of the tube are practically bended and for a length λ displacement and rotations are observed. The generator for a distance greater than λ from the impact point can be considered practically fixed and thus no rotation or displacement is observed. This happens due to the action of gravity that holds practically down the pipeline against any upward movement.

On the other hand, in the dynamic analysis of the semi-infinite pipe a smaller resistance was calculated. It appears that the global sinusoidal beam mode that was observed is causing this reduction of resistance. As can be seen in Figure 5.13, due to the global deformation, the fixity point of the upper generator ceases to exist as there is a global rotation of the cross section. So practically, it is not the global deformation of the whole cross section that plays a significant role, but rather the deformation of the upper

generators. This has also been examined during the process of this thesis, for a pipeline that was completely attached to the rigid bed without allowing separation. However, when damping was not introduced the results did not differ significantly. This happened because the upper generator was still vibrating in low-frequencies in a global sinus mode. As denting is a bending dominated phenomenon, this allowable rotation decreases a lot the resistance of the pipeline against denting compared to a fixed case.

The sinusoidal deformation pattern that has been observed is practically a low-frequency vibration of the pipeline. As has already been mentioned, impact is a high-frequency phenomenon. There is a strong indication that these global sinusoidal low-frequency modes that are present during the analysis do not correspond to reality as it is rather difficult for an infinite pipeline to deform that much globally in a few milliseconds, especially for higher velocities where it is expected to have a more localized response (case of a bullet).

It is thus evident that the low-frequency modes have to be canceled out by introducing low-frequency damping. The same practice has been already used in one of Abaqus benchmarks and specifically in an underwater explosion analysis of a pipeline. Explosions and impacts are both high-frequency phenomena which means that the analysis and model calibration between the two should be similar. In the Abaqus benchmark, the researchers have used a mass proportional Rayleigh damping, in order to remove all low-frequency responses of the pipeline so that the FEM analysis would match well with the conducted experiments that they have done.

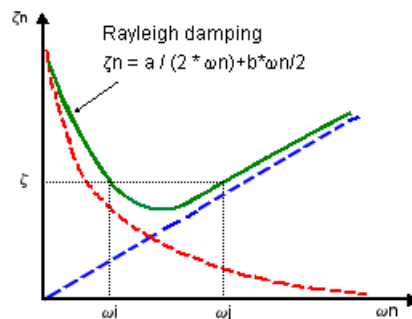


Figure 5.14 Rayleigh damping components.
Percentage of critical damping versus frequency of excitation.

Specifically, an alpha value equal to 750 s^{-1} has been chosen which results to damping values several orders of magnitude larger than the critical damping of each frequency, for frequencies less than 50Hz. At this point it should be highlighted, that Rayleigh damping is just a mathematical tool and does not have a physical interpretation. This means, that the alpha and beta values need to be carefully selected for each analysis and for each structure in an independent way.

Now that low-frequency damping has been identified as the main reason why the semi-infinite pipelines behave softer, an effort will be made to observe how the system behaves for different alpha values of the Rayleigh damping. This means that a mass proportional damping will be introduced. Different velocities for the same amount of energy will be checked without accounting for any strain-rate effects. However, Rayleigh damping is

only a mathematical tool to model the dissipation of energy known as damping in a structure that can be caused by different reasons. So, it is not possible to determine the alpha and beta parameters in the Rayleigh formula without verifying them with experimental data and results.

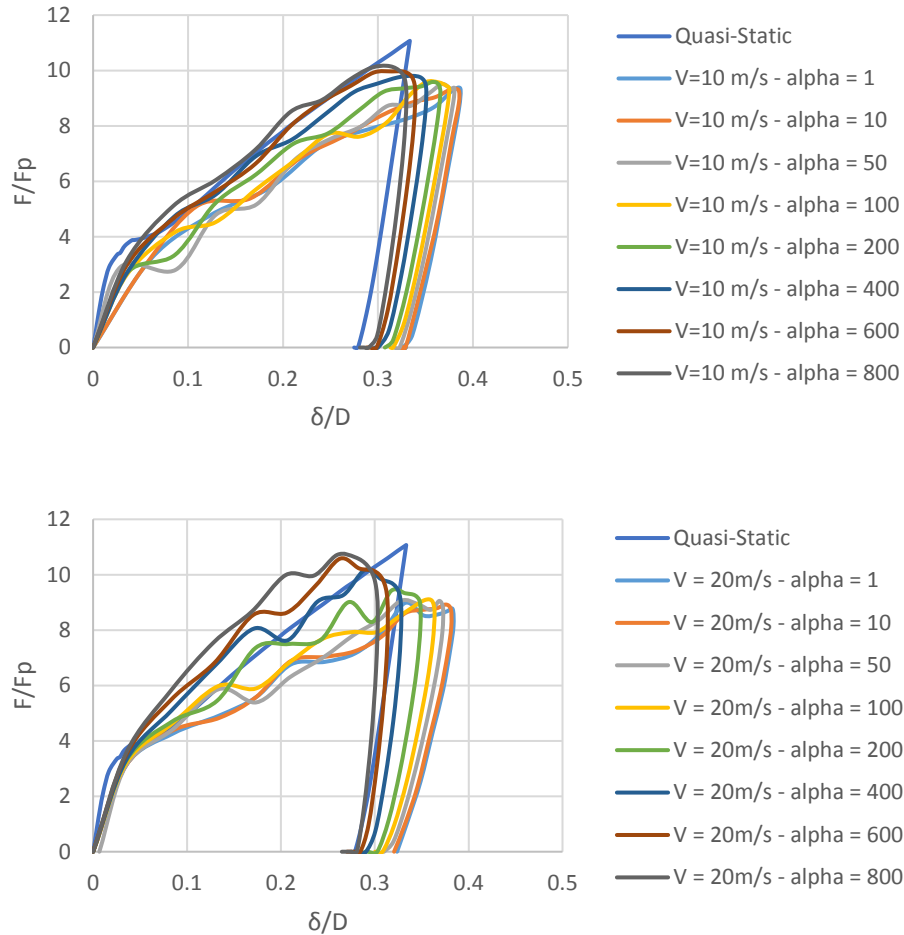


Figure 5.15 Force-dent diagram for different velocities and different mass proportional Rayleigh damping.

For only mass proportional Rayleigh damping, values for alpha between 1 and 800 s^{-1} and velocities between 10 and 20 m/s, several dynamic analyses are conducted. As can be seen from the above graph, as the value of alpha increases the resistance of the pipeline against denting increases as well converging more towards the quasi-static case. Additionally, for the same damping values and different velocities the response is different as expected, as damping forces are proportional to velocity.

However, not a clear estimation of the correct damping coefficient can be made only with FEM. It is possible that by using more sophisticated material models that can account for viscoelasticity of steel under high strain rates, the generated damping forces might be closer to reality. To the best of our knowledge, no published paper tackles the semi-infinite pipe problem, as most of them consider a fixed pipeline of relatively small length, which does not have any low-frequency induced behavior that compromises the results.

Page intentionally left blank

6. Pipeline-Fluid Interaction

6.1 Introduction

Any contents of a pipeline would provide an inertial resistance to the deformation of a pipeline wall through the “added mass” effect. The effect of this phenomenon increases as the density of the contents is increased, and is in addition to the inertial resistance of the pipeline wall material.

This plethora of variables is responsible for several authors reaching conclusions from their work which appear to conflict with the results of earlier studies on filled pipelines. In any event, the experimental investigations find that the addition of any contents in a pipeline (liquid, gas or granular), whether pressurized or not, causes smaller deformations to develop in the vicinity of the impact site when compared with the behavior of similar empty tubes, i.e., the deformation profile becomes more localized. This localization of the damaged area is due likely to the additional inertial resistance offered by the contents of a pipeline. Thus, the impact energy is absorbed in a smaller volume of the tube material which is responsible for a decrease in the perforation energy. This is a very important observation when the damage and fracture of the tube is investigated.

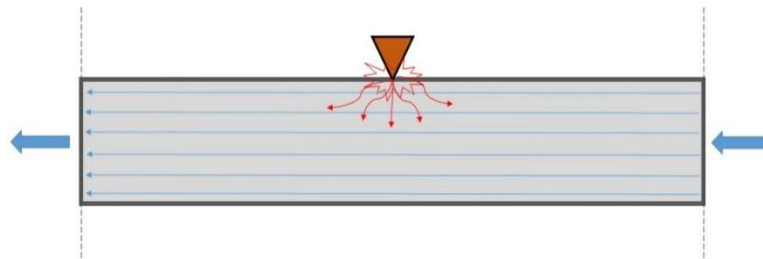


Figure 6.1 Schematic representation of an operating pipeline when hit by an object

Water inside the tube stiffen the wall and disperse some of the energy imparted to the wall within the contact region. These filling media increase the impact speed, and thus the input kinetic energy, required to obtain any specified central deflection. Although the increased stiffness concentrates the dishing of thin tubes around the point of impact, plug formation occurs at an in plane radial stretch.

Having said that, it is obvious that for gas content the added mass in the pipe wall will be negligible and thus only the pressure term will be of significance. On the other hand, oil pipelines will affect denting by their added mass, their internal pressure and because of the incompressibility assuming that they occupy the whole section of the pipe. It is straightforward though that for gas filled pipes a simplified model can be used without inertia effects.

In reality however, a pipe is not confined neither has a fixed volume, as it spans over hundreds of kilometers. Moreover, the liquid inside is not stationary but it is moving with

a certain velocity. This further complicates the physics that describe the problem. The most proper way would be to use Computational Fluid Dynamics in order to completely capture the flow within the pipe and how it will affect the denting and the energy dissipation. However, this is not in the scope of this study and a simplified manner for both gas and liquid filled pipelines will be followed in order to estimate how much they do affect the pipe denting.

6.2 Gas Filled Pipelines

For gas filled pipelines a simplified approach will be followed that does not account for inertia effects on the pipe wall. The modeling works under the assumption that if the temperature remains constant and leakage does not occur, the gas pressure is inversely proportional to the gas volume. This can be easily derived by using the ideal gas equation:

$$p_f V = M_{gas} RT \quad (6.1)$$

where p is the absolute pressure, V is the volume, M_{gas} is the mass R is the specific gas constant and T is the absolute temperature.

$$p_f = f(V_f) = -K \left(\frac{V(p) - V_0}{V_0} \right) \quad (6.2)$$

Where:

$$\Delta p_f > 0 : \Delta V_f < 0$$

$$\Delta p_f < 0 : \Delta V_f > 0$$

Interpreting this simple relation between pressure and volume, it's straightforward that for a very big volume of fluid, a small volumetric change will yield a very small change in pressure locally. For denting, the local deformation, will not reduce the enclosed volume of the pipeline if hundreds of kilometers are considered.

However, as has been mentioned earlier, due to the transient nature of this problem it would be wrong to consider that the volume of the fluid that participates in the impact would be practically infinite. Engineering judgment must be implemented here in order to consider a reasonable length of the pipe and the enclosed volume in order to measure any local overpressure that might be beneficial compared to considering a stable pressure throughout the analysis. There is not a straightforward answer to this as it is a very complicated problem which would most certainly require experimental verification.

ABAQUS includes a family of elements that can be used to represent fluid-filled cavities under hydrostatic conditions. These elements provide the coupling between the deformation of the fluid-filled structure and the pressure exerted by the contained fluid on the boundary of the cavity. In order to properly model the gas inside the pipe, special elements have to be used. F3D4 fluid cavity elements will be used within the Lagrangian framework. The hydrostatic fluid elements appear as surface elements that cover the cavity boundary, but they are actually volume elements when the cavity reference node is accounted for resulting in a pyramidal shape.

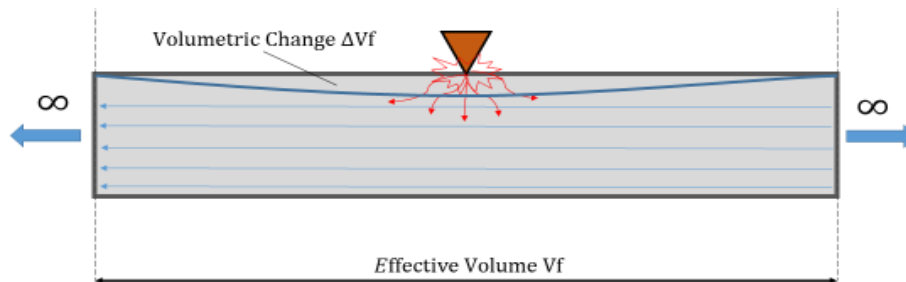


Figure 6.2 Schematic representation of finite element model assumptions.

6.2.1 Results and Comparison

The effect of internal pressure has been investigated. For the same kinetic energy input, as in the previous chapter (670 kJ), different pressure levels and different velocities have been investigated.

As expected, from the quasi-static study, with the increase of the internal pressure, the stiffness of the system is increased as well after local yielding occurs. The deformed shape of the pipeline, is now even more localized than the one in the quasi-static study as due to the inertia the flexural resistance is not fully mobilized. Again, the yielding point of the force-dent diagram is not affected by the pressure but rather the residual stiffness path.

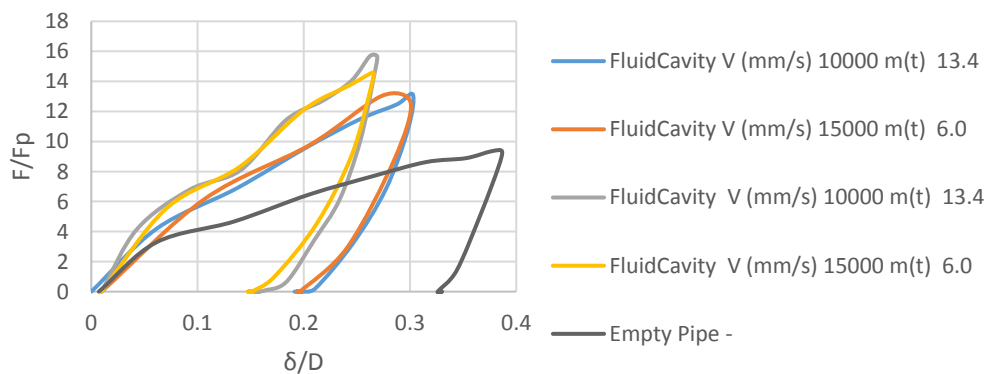


Figure 6.3 Force-dent diagram for different velocity and pressure levels.



Figure 6.4 Maximum deformed tube for internal pressure level of $q=0.4$. Localization of denting is observed.

For the two pressure levels examined, the decrease of maximum dent depth compared to the empty pipeline is 22 and 30% for $q = 0.2$ and $q = 0.4$ respectively. As for the permanent dent, the decrease is 40% and 55% for the two pressure levels. Same as in the quasi-static study, the unloading path exhibits a change of slope at the point where force is about to reach zero. This is the effect of the internal pressure that gives an extra push during unloading.

6.3 Liquid Filled Pipelines

Modeling gas is relatively straightforward with ABAQUS, whereas modeling of a liquid phase medium is not. More specifically, in order to account for the inertia and partial incompressibility of the fluid, fluid cavity elements do not suffice. A simplified approach to this problem has been presented from Yu & Jeong of the Volpe National Transportation System Center US.

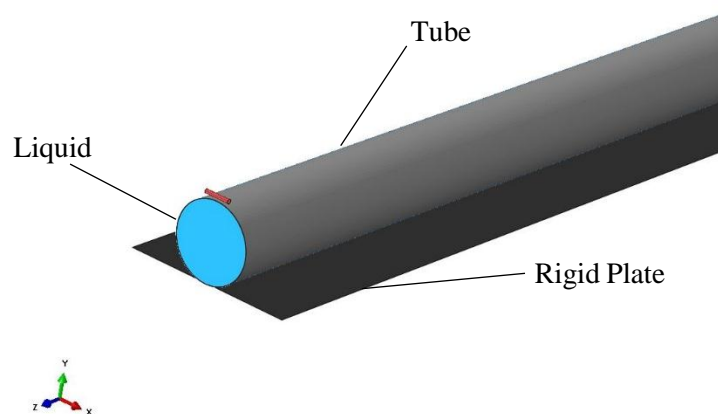


Figure 6.5 Schematic representation of finite element model used.

6.3.1 Model Description

The two authors, when studying the impact dynamic of pressurized tank cars in railways have developed a framework in order to model accurately fluids within the Lagrangian framework (C3D8R elements). The alternative to this would be to use Coupled Eulerian-Lagrangian analysis (CLE) or even Computational Fluid Dynamics codes which are both time consuming in terms of modeling and computational resources.

Their work has been verified by real scale field experiments of train impacts on pressurized tanks and thus is considered reliable and safe to use. Of course, certain limitations exist in this procedure as the velocities used did not exceed 7m/s. Namely, this method works well for relatively small displacements where no sloshing or turbulence is expected. It works for pressurized vessels like pipelines or tanks where the fluid is under pressure and the interior of the vessel is completely filled with liquid.

The hydrostatic behavior of the liquid phase can be depicted by equations of state that express the pressure p as a function of the density ρ and the specific energy

$$E_m : p = f(\rho, E_m) \quad (6.3)$$

where p is positive in compression and E_m measures the internal energy per unit mass. Further, a linear U_s-U_p Hugoniot form of the Mie-Grüneisen equation of state was employed as an effective method to model the behavior of liquids such as water or oil. The initial density ρ_0 and wave speed c_0 are required material parameters from which the elastic bulk modulus is calculated as:

$$K = \rho_0 \cdot c_0^2 \quad (6.4)$$

The deviatoric behavior of the liquid was assumed to be uncoupled from its volumetric response and governed by either a linear isotropic elastic model or a Newtonian viscous fluid model. The shear viscosity also acts as a penalty parameter to suppress shear modes that could tangle the mesh. The shear viscosity chosen should be small because water or oil is inviscid; a high shear viscosity will result in an overly stiff response.

An appropriate value for the shear viscosity can be calculated based on the bulk modulus. To avoid an overly stiff response, the internal forces arising due to the deviatoric response of the material should be kept several orders of magnitude below the forces arising due to the volumetric response. This can be done by choosing an elastic shear modulus that is several orders of magnitude lower than the bulk modulus. This method is a convenient way to approximate a shear strength that will not introduce excessive viscosity in the material.

Liquid	Density (kg/m ³)	Speed of Sound C0 (m/s)	Bulk Modulus (MPa)
Crude Oil*	1412	882	1100
Water	1000	1480	2200

Table 6-1 Liquid input properties required for the analysis.
(* Yu & Jeong, 2012)

The initial fluid pressure p_0 was defined as an initial hydrostatic stress state assigned to the fluid elements:

$$\sigma_{11} = \sigma_{22} = \sigma_{33} = -p_0 \quad (6.5)$$

$$\sigma_{12} = \sigma_{23} = \sigma_{31} = 0 \quad (6.6)$$

Along fluid-to-solid interfaces, even if we defined exactly matching geometries for the fluid and solid phases, the meshing process can still result in either overclosures or gaps between fluid and solid elements. Mesh overclosures can adversely affect stability and convergence of contact, so it is decided to define geometries with sufficiently large initial gaps to completely eliminate mesh overclosures in preprocessing giving an initial adequate step time for the fluid to expand and reach equilibrium before moving forward to the impact.

Moreover, due to the wave reflection within the fluid, it has been observed that if the fluid length is not adequate mesh distortion occurs due to excessive wave reflection. For this reason, a length sensitivity has been also carried out, by increasing the length until the mesh is not distorted. This is observed for a length of 70D, instead of the 50D which was used until now.

6.3.2 Acoustic Elements

In the absence of experimental data on pipe fluid interaction under pressure, acoustic elements (AC3D8R) have also been considered in order to test their behavior and also compare them with the elastic solid element approach that was presented earlier. Generally, with the acoustic elements the effect of the added mass can be captured approximately and also it is possible to account pressure without having excessive distortion in the mesh. This is accomplished in Abaqus, by utilizing a special purpose script which gives displacement degrees of freedom in the fluid nodes that are in contact with the structure. Specifically, the displacement field is achieved by using shape functions to connect this pseudo-displacement to the closest structure nodes and thus acceleration. However, the node displacement is constrained by the structure always, not allowing the fluid to move freely. This is just a computational approach and is not considered accurate enough for problems where added mass plays an important role.

However, the fluid’s inertia in a rigid body motion cannot be captured when using these elements which is a drawback when a flexible bed is used instead of a rigid one. The acoustic elements, will be modeled using exactly the same mesh as the solid elastic elements. Their behavior is defined by the density and the bulk modulus of the material. Since it is a closed volume, an iterative procedure is needed in order to determine the length in order for the results to converge and in order to not get a very stiff response due to very small volume. Impedence boundary conditions are not considered, as the wave propagation in the medium itself is not of interest.

6.3.3 Fluid with Zero Pressure

Initially, the case of a fluid with no internal pressure is considered. The fluid in an enclosed volume should resist to deformation due to two reasons. First, is the incompressibility of the liquid itself and the magnitude of its bulk modulus and secondly is the inertia of the fluid which acts as an added mass on the pipe wall.

As aforementioned, due to the fact that the solid elements work within the Lagrangian framework, a deviatoric stiffness will also contribute due to the added small shear modulus as penalty parameter to avoid excessive distortion of the mesh due to shearing. It is thus expected, that a small error will be present in the results.

After performing several analyses using both the solid elastic elements and acoustic elements it has been shown that there is a good agreement in the results. Specifically, using as a liquid both the oil and the water properties, the maximum and permanent dent sizes exhibit an error of less than 3%. The analyses included the benchmark kinetic energy input of 670kj formed as different combinations of mass and velocity, in order to observe the effect of the velocity in the dent.

		Maximum Dent (δ/D)			Permanent Dent (δ/D)		
Empty Pipe		0.386			0.328		

		Maximum Dent (δ/D)			Permanent Dent (δ/D)		
Impact Velocity (m/s)	Solid	Acoustic	Error (%)	Solid	Acoustic	Error (%)	
5.0	0.342	0.354	3.395	0.255	0.278	8.268	
10.0	0.324	0.336	3.420	0.241	0.248	3.084	
15.0	0.308	0.323	4.407	0.238	0.264	4.301	

Table 6-2 Results for Water filled pipeline with no internal pressure and different impact velocities

Two conclusions can be easily derived from the results. Initially, as the velocity increases the system exhibits increased stiffness which consequently leads to small maximum and permanent dent size for both the element types. This occurs mainly because of the incompressibility of the fluid and the bulk modulus and secondarily

because of the inertia of the fluid itself and the added mass effect. For oil filled pipelines the results were similar. Also, the maximum force and maximum dent go out of phase, resulting in a “softening” effect in the curve. This happens due to the fluid inertia during its movement.

The reduction of the maximum dent compared to an empty pipe case ranges from 10 - 18 % which is a significant reduction whereas for the permanent dent size the average reduction is about 25%.

Moreover, the acoustic elements show a softer behavior which leads always to an increased dent depth in all cases. However, the average error is about 3.5% which gives confidence in the results of the analysis.

By making an investigation two are the possible reason that can be distinguished that lead to this difference. The first one is that the acoustic elements do not properly take into account the inertia of the enclosed fluid and thus the added mass effect is underestimated.

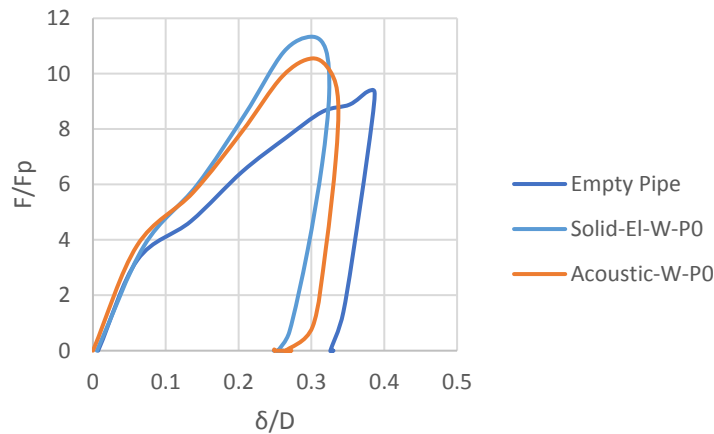


Figure 6.6 Force-dent curve for a filled pipe with no pressure

The second reason is that due to the penalty parameter of viscosity or shear modulus that the elastic solid elements have, an additional stiffness is introduced to the system which eventually leads to smaller dent sizes. In any case, because the results are in a good agreement it can be concluded that the combined effect of the inertia and the incompressibility of the fluid has a significant effect on the dent size and its shape and should be taken into account.

Moreover, the kinetic energy absorbed is the same in both the empty and filled pipe. However, what changes is the distribution of the deformation energy. In the empty pipe, all of the energy goes directly into the pipe as denting deformation, whereas in the filled tube, the energy is divided between the liquid and the pipe. Here, the load-dent curve resembles the system stiffness against denting (meaning the pipe plus the internal liquid) and not only the tube’s resistance. This is because in the derived force-dent curves the effect of the work done by the internal fluid is present.

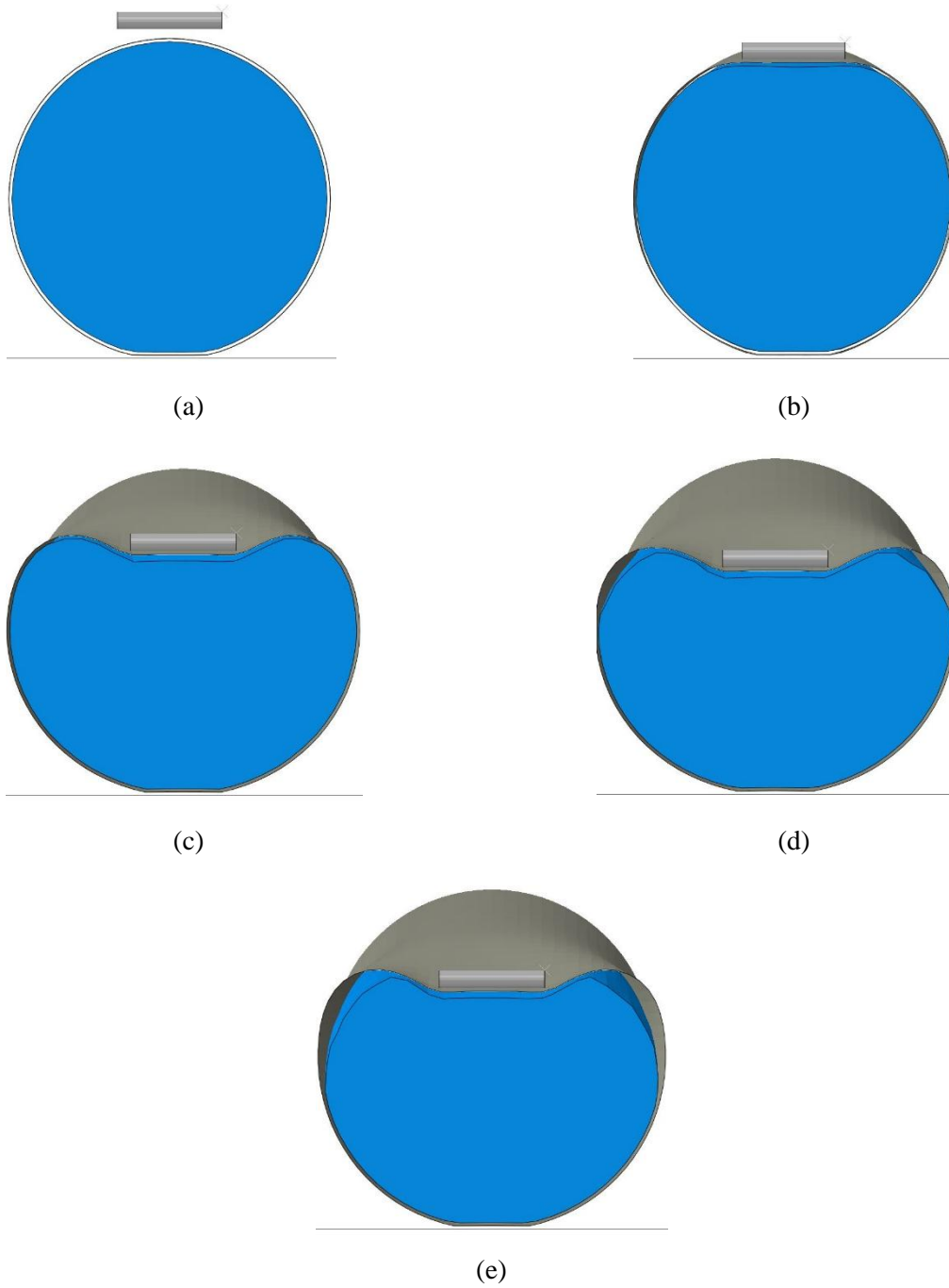


Figure 6.7 Pipeline - fluid interaction cross-sectional deformation over time.

6.3.4 Fluid under Pressure

The next question that arises is, what is the combined effect of pressure and liquid to the denting behavior of a tube. To this end, an investigation will be considered to assess how much this affects the response and how it compares to the unpressurized case of a liquid filled pipe. Again, the bed is considered rigid and no strain-rate yielding is accounted.

Since pipelines, operate under huge pressures it is possible that for these kind of pressures, the effect of added mass will be reduced as the primary reason of the added resistance to denting will be the pressure itself. This is why, in this section the results will also be compared with Fluid Cavity elements which do not account for any inertia but account for the bulk modulus and the pressure within the enclosed volume. For the current investigation, again water filled pipeline has been considered.

	Input Energy (kj)	Mass (kg)	Velocity (m/s)	Max. Dent (δ/D)	Perm. Dent (δ/D)
q = 0.2					
Solid				0.292	0.208
Acoustic	670	13400	10	0.303	0.198
Fluid Cavity				0.303	0.206
q = 0.4					
Solid				0.272	0.184
Acoustic	670	13400	10	0.269	0.152
Fluid Cavity				0.266	0.154

Table 6-3 Results for different pressure levels and different modeling of the enclosed fluid of the pipe.

When the fluid is under pressure, the positive effect on denting resistance is significant. The reduction of the maximum dent size is 22% for $q = 0.2$ and 30% for the $q = 0.4$ case. The permanent dent size, reduced by 40 and 50% respectively for each case. However, the same thing as in the quasi-static analysis is observed. The denting now is more localized, which could potentially create other kind of problems for the pipeline. Specifically, the localization of denting reduces the energy needed to perforate the pipeline

As can be seen, the results are in a good agreement for all three element types. For smaller pressures, the solid elements present a stiffer behavior in general, resulting in smaller maximum dent depth. This is probably due to the inertia effect that is still significant. However, the unloading path is a bit different as the permanent dent is bigger than the other two cases.

For the case of internal pressure equal to $q = 0.4$, the maximum dent value is almost the same for all three cases with less than 1.5% error. This is a strong evidence that as the pressure increases, the inertia effect of the fluid inside the pipe becomes less important and the pressure term dominates the response. The softening effect is also visible in the

case with $q = 0.2$, verifying once again that this is happening due to the inertia of the fluid and becomes negligible for higher pressures.

Moreover, this means that instead of the time-consuming and relatively unstable solid elements for these kind of applications, acoustic and fluid cavity elements perform good, reducing the CPU time needed significantly as well as the time to model and calibrate the model. The same is derived for different impact velocities.

One thing that cannot be captured when fluid cavity or acoustic elements are used, is the inertia of the fluid itself in a rigid body motion, whereas the solid elements can by definition. This can be tackled, by calculating the total mass of the enclosed volume and assign one or more virtual masses to it, equal to the total mass of the fluid.

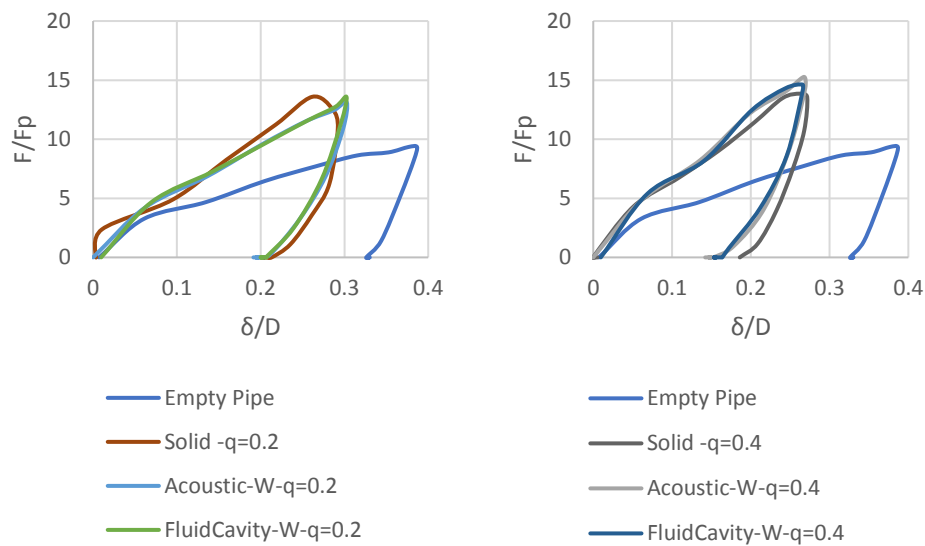


Figure 6.8 Force- dent diagrams for internal pressure level equal to (a) $q = 0.2$ and (b) $q = 0.4$

6.4 Conclusions

By performing this pipe-fluid interaction investigation, some useful results have been derived. Due to the fact that the quasi-static analysis does not take into account inertia effects or incompressibility of the fluid it is important to verify our findings by doing a more accurate analysis.

For this reason, several different modeling techniques and elements have been used for each problem. The effect of the gas or a liquid in the pipe is obvious, as it increases the resistance of the whole system against local deformation. For unpressurized pipes where only the incompressibility of the fluid and its inertia are computed, the resistance is increasing, but in the cost of localizing the deformation more.

The same applies for the case of pressurized fluid inside the pipe. However, after investigating the behavior of the system, it has been found that as the pressure increases, inertia phenomena such as “added mass” effect become less important and can be safely

excluded. In the following table, some concentrated conclusions about the elements used to model the fluid are presented.

Modeling	Solid Elements	Acoustic Elements	Fluid Cavity Elements
Added Mass	***	***	-
Incompressibility	***	***	***
Pressure	**	***	***
Deviatoric Behavior	***	-	-
Large Deformations	**	**	***
CPU Time	*	**	***
Liquid Inertia	***	*	-
- = Not available	* = Poor	** = Good	*** = Excellent

Table 6-4 Summarized conclusions on different modeling of the pipe fluid and their capabilities.

7. Soil Modeling

7.1 Introduction

In the previous chapters, the fundamental characteristics of pipe denting have been thoroughly investigated in both quasi-static and dynamic analysis. Yet, these analyses are just conservative approximations of the true conditions that exist in real life. One of the main goals of this thesis is to quantify the effect of soil and the medium inside the pipe on the denting behavior of the system. With other words, it is important for the industry and the research community to understand how energy is dissipated during the impact of an object to a marine pipeline.

However, to do so a more detailed model is needed that properly and efficiently takes into account the contribution of the different parameters in the pipeline response. Thus, the soil, the medium and the infinite length (hundreds of kilometers) of the pipe has to be modeled.

The soil modeling, is without a question the most difficult and most uncertain parameter of this study. The importance of the soil is great in the dissipation of the impact energy. In the present thesis, an effort to model the soil correctly without wrong assumptions has been made in order to capture these effects. But since, this is not the primary goal of this study some simplifications and engineering judgement had to be implemented wherever needed.

A realistic soil model needs very sophisticated material failure models, proper soil profile distributions and most important adequate modeling of the pore pressures within the different soil types (clay, sand).

The biggest uncertainties are the shear modulus of the soil, the internal friction angle, the cohesion, the plasticity index and the over consolidation ratio. These uncertainties not only relate to the lack of data but they also relate to the dynamic response of soil to an impact. The international research community still debates about these matters, which leaves no choice but to make logical assumptions in order to determine the safety level of an impact incident.

One other parameter that has its own value, is the water pore pressure and in general, how the water moves through the pores of the soil under a high-speed loading. This is a very complex phenomenon that needs enhanced models which will properly account for mass conservation equations and all the possible trajectories of the water through and out of the soil.

7.2 DNV Treatment

Just recently DNV has issued a new recommended practice (RP-F114) for pipe-soil interaction problems. The soil in this guideline is described in terms of equivalent linear and non-linear springs for lateral, axial and vertical resistance.

Specifically, for dynamic loading, DNV-RP-F114 still does not give a lot of information. The only recommendation that can be found in DNV codes regarding dynamic behavior of soil is in the RP-F105 for free spanning pipelines. There linear dynamic springs can be evaluated by the proposed formulas. However, the case always with the usage of springs is that it is just an approximation. Thus, using them can be very tricky in problems where contact matters. Also, the provided stiffness is concentrated in nodes and not in the total length of the examined pipeline. Two approaches are proposed which present differences between them.

DNV dynamic springs are using the following for the evaluation of their stiffness:

- Type of soil (sand or clay).
- Specific Weight
- Drained or Undrained Conditions
- Strain magnitude dependence of Shear modulus
- Over consolidation Ratio for Clays

As expected, these springs have values higher than the equivalent static ones. However, since they are just linear they do not account for any plastic deformation and thus dissipation of energy in that form.

7.3 Soil Properties

As aforementioned, the soil properties are governed by huge uncertainties. To this end, the DNV codes along with published research, will be used to determine a realistic range of all the possible soil parameters. Generally, sand and clay behave totally different, as clay is always considered undrained whereas sand under static loads are considered drained. Impact loading cannot under any circumstance be considered static which means, that static soil parameters are not valid anymore. However, it is very difficult to assess the dynamic soil properties and simplified approaches should be used due to lack of reliable experiments or results on the matter.

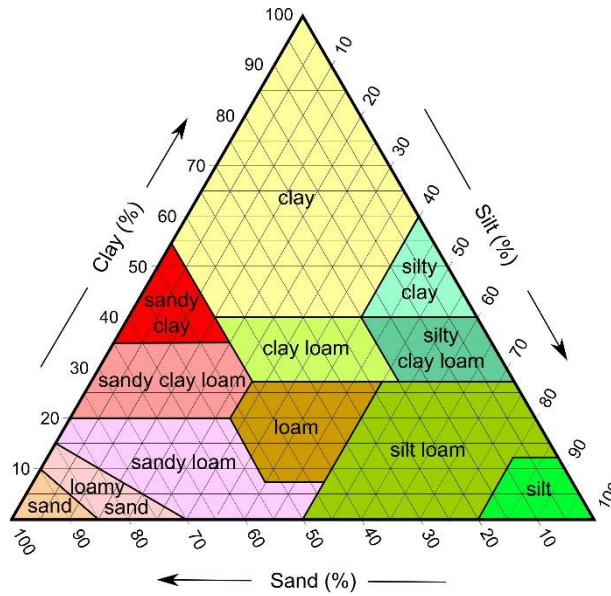


Figure 7.1 Soil types by clay, silt and sand composition as used by the USDA (Wikipedia.com)

7.3.1 Soil Basic Properties

Basic parameters, such as the soil submerged and saturated density have been gathered by both the available literature and DNV-RP-F105.

Clay	Su (kPa)	γ (kN/m ³)	γ' (kN/m ³)	v (-)
Very Soft	< 12.5	14.0 - 17.0	4.0 - 7.0	0.45
Soft	12.5 - 25	15.0 - 18.0	5.0 - 8.0	0.45
Firm	25 - 50	16.0 - 21.0	6.0 - 11.0	0.45
Stiff	50 - 100	17.0 - 22.0	7.0 - 12.0	0.45
Very Stiff	100 - 200	20.0 - 23.0	10.0 - 13.0	0.45
Hard	>200	20.0 - 23.0	10.0- 13.0	0.45

(a)

Sand Type	ϕ (°)	γ (kN/m ³)	γ' (kN/m ³)	v (-)
Loose	28 - 30	18.5 - 21.0	8.5 - 11.0	0.35
Medium	30 - 36	19.0 - 22.5	9.0 - 12.5	0.35
Dense	36 - 41	20.0 - 23.5	10.0 - 13.5	0.35

(b)

Table 7-1 Soil Properties for (a) clay and (b) sand as given by DNV-RP-F105

7.3.2 Young's and Shear Modulus

Another important parameter of soil behavior is the Young and Shear elastic modulus. Some representative values for static loading are presented below:

Type of Soil	Es (MPa)
Clay	
Very Soft	2.0 - 15.0
Soft	5.0 - 25.0
Medium	15.0 - 50.0
Hard	50.0 - 100.0
Sandy	25.0 - 250.0
Sand	
Silty	7.0 - 21.0
Loose	10.0 - 24.0
Dense	48.0 - 81.0
Sand and Gravel	
Loose	48.0 - 148.0
Dense	96.0 - 192.0
Silt	
	2.0 - 20.0

Table 7-2 Soil elastic moduli for different types (Code of Practice for foundations, Hong Kong government).

The engineering community, still debates on the behavior of Young's and Shear modulus under high-loading rate (Omidvar et al). DNV recognizes that there is a difference which is produced only when small strains are observed. The same conclusion has been adopted by the earthquake engineering society. However, this is believed not to be entirely true.

Earthquakes, are low-frequency excitations which usually cause small strains in the soil medium. Thus, it can be safely assumed that a strain-rate approach can be simplified to small strains. However, when high frequency excitations such as impact, pile driving or explosion are considered, strain-rate might exist for large strains. This means, that by considering the DNV approach, we would omit the increased strength of the soil due to the large deformations that follow the impact. The general trend applies for both sands and clays, however the effect of the high-speed loading can differ significantly as sands

have an additional stiffness due to the pore overpressure. However, this is a complicated problem as the dissipation of water through the pores under such a loading condition is not straightforward and thus very difficult to predict efficiently.

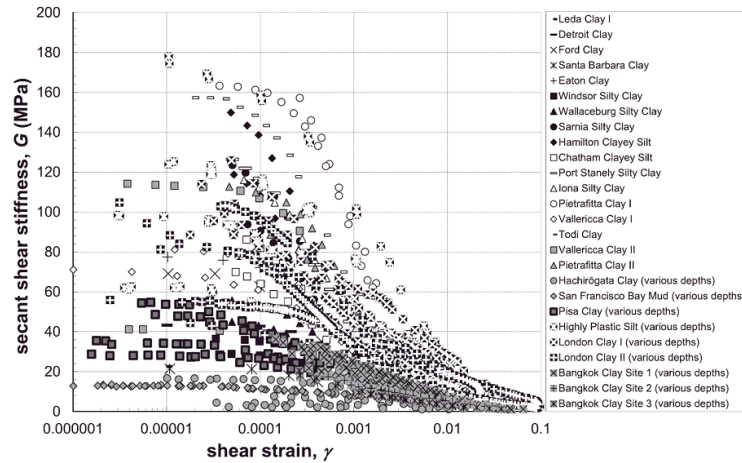


Figure 7.2 Shear modulus of different soil versus the developed shear strain (Vardanega et al, 2013)

Since this is a matter under investigation for the geotechnical society at the moment and rigorous experiments are needed in order to verify this, a realistic range will be used in the present thesis in order to capture all the relative phenomena. Thus, dynamic and static values for the G and E will be considered separately as a logical approximation.

7.3.3 Undrained Shear Strength of Clays

DNV, also gives a range of values for the undrained shear strength of soils as presented earlier. A distinction is being made between the hardness of the clay and usually these values are being used for preliminary design.

Since this is a parametric study approximate values are used, assumptions for the soil profile and the corresponding undrained shear strength will be made. The undrained shear strength increases linearly with depth and thus some profiles will be considered for the present thesis.

Besides, the Shear modulus strain-rate dependence, undrained shear strength has been reported to also have strain-rate dependence. The value, due to a relatively fast loading in clays has been observed to increase up to 50% - (Lunne and Andersen, 2007). Having said that, the author of this thesis is not aware of any constitutive model that has been developed to describe this strain-rate dependency. Thus, yet again, reasonable assumptions and investigations have to be made for the undrained shear strength values.

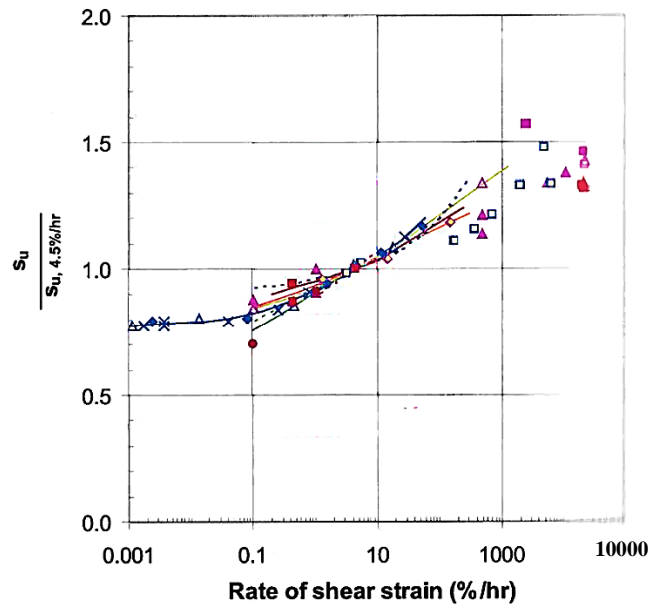


Figure 7.3 Static shear strength of several clays as function of rate of shear strain. (Lunne and Andersen, 2007)

In the offshore industry, some empirical relationships have been developed in order to correlate clay material properties based on the undrained shear strength in order to make fast approximations of the soil conditions on site. In a recently published paper from Statoil, an equivalent elastoplastic model with hardening has been used. In this model, Young's modulus, yield stress and hardening are calculated based on the values of the undrained shear strength. The fitting is based on experience and measurements of many years and it is considered by the authors accurate enough to predict soil behavior near the surface. However, it exhibits very small differences than the equivalent Mohr-Coulomb elastic-perfectly plastic model.

Parameter	Value
Young's Modulus	(100-300) S_u
Yield Stress	$0.8S_u$
Hardening Modulus	$0.008S_u$

Figure 7.4 Statoil's equivalent elastoplastic material model for clays (Oosterkamp, 2017)

7.3.4 Undrained Sand Behavior

As aforementioned, the behavior of sand during an impact will be a transient one. This means that due to the pore pressure build up and escape during the impact there is not a constant behavior over time of the sand. On the other hand, it is known that for clays drainage occurs in much more time.

Considering these, the determination of the detailed model must be used in order to predict accurately the water flow in such a high-speed loading scenario. This is a purely geotechnical problem which is out of the scope of this thesis, as it concentrated mostly on the behavior of the system and not of the soil itself.

Omidvar et al (2012), have performed a series of high speed impact experiments on loose and dense sands, in order to determine the stress-strain behavior at high strain rates (HSR) where the saturation and the confinement pressure are taken into account.

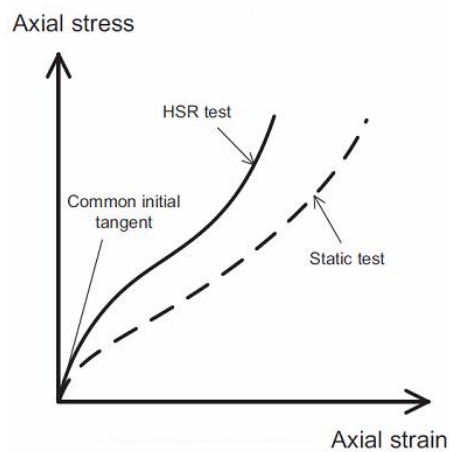


Figure 7.5 Schematic representation of the effect of high strain rate on the stress-strain response of sand in uniaxial compression (Omidvar et al, 2012)

Uniaxial compression and triaxial tests exhibit a marked increase in stiffness due to HSR loading. The Dynamic modulus ratio in uniaxial compression tests increases gradually with increasing strain rate, with a ratio in excess of 2 reported for strain rates exceeding 10/s. Similarly, the dynamic modulus ratio of sand in triaxial shear increases up to twice the static value in dense sand under high confinement and HSR loading. The strain to peak decreases by up to 2% in HSR triaxial tests.

Although limited experimental data can be found on the matter, the authors have concluded that the degree of saturation is an important contributing factor in a high strain rate uniaxial compression response. As aforementioned, it is expected that there will be not enough time for the dissipation of the excess pore pressures resulting in an undrained or partially undrained behavior of the sand. For fully saturated sands, it is observed that the stiffness is dramatically increased due to the highly incompressible water in the pores. For dry sands where pores are filled with air the behavior is a lot softer compared to a

saturated sand. The transition from soft to stiff response has not been studied in sand under uniaxial compression.

The response of partially saturated sand under HSR loading depends on the applied stress level, and the degree of saturation. The response of partially saturated sand is schematically represented below, depicting the two effects of increasing the degree of saturation on the response, i.e., softening of the initial response, and a stiffer response at higher strains with increasing degrees of saturation.

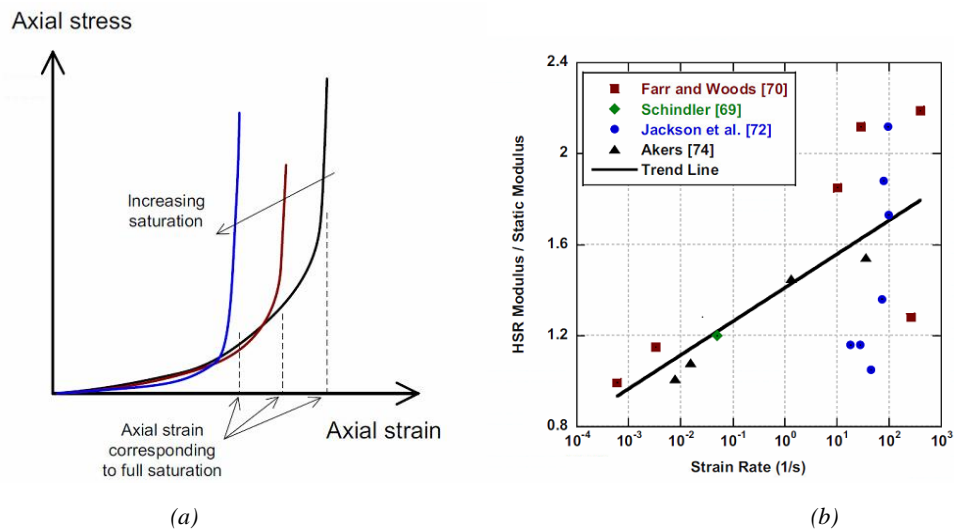
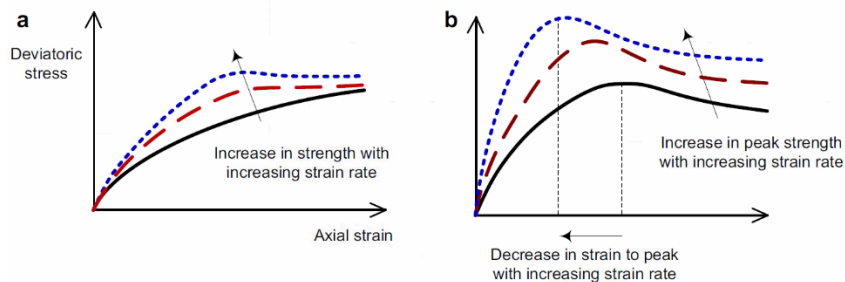


Figure 7.6 (a) Effect of saturation on uniaxial compression response of sand soils (b) Dynamic modulus ratio as a function of strain-rate (Omidvar et al, 2012)

It is evident from all the above information, that sand soil behavior under impact or high strain-rate loading is very complicated. In general, the classic elastic parameters such as the elastic modulus and the Poisson ratio, fail to give a reasonable estimate on the behavior of the sand. More sophisticated models are needed in order to capture the behavior of sand as the pore pressure build up is crucial. Considering the sand to be drained is an over-simplification which will lead in wrong conclusions in the scope of this thesis.



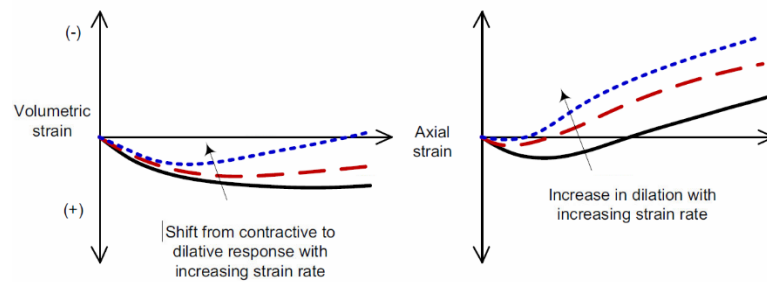


Figure 7.7 Effect of increase in strain-rate on stress-strain response and volumetric strains in (a) loose sand, (b) dense sand. (Omidvar et al, 2012)

Additionally, the Mohr-Coulomb failure model that will be used in the present work is another oversimplification regarding the soil behavior without accounting for the pore pressures that exist. Another thing that is omitted with a simplified model as that, is the hardening and breakage of the sand grains as the load increases which could considerably affect the results of the analysis. Thus, the only thing that can be done in order to simplistic approach the behavior of the sand within the framework of this thesis is to increase the elastic parameters of the sand such as the Poisson ratio and the elastic modulus in order to observe how much the results are affected. Regarding the angle of internal friction not much can be done because there are not enough data to propose a dynamic equivalent value. However, all of these modifications are completely arbitrary and thus the author of this thesis consider this unpractical and unrealistic.

A simplified way to treat the lack of data in the present thesis, sand will be treated as completely undrained where no pore water dissipation is allowed and instead of effective stresses the total stress regime will be used. This means, that the angle of friction is no longer valid to describe the failure of sand and thus the undrained shear strength has to be used. Of course, sand is not characterized by the undrained shear strength and thus certain assumptions have to be made in order to convert the drained sand parameters to equivalent undrained.

Generally, some semi-empirical guideline from DNV, PRCI (Pipeline Research Council International) and from industry experience exist in order to derive the undrained shear strength of sand for certain occasions. Additionally, the author of this thesis has carried out simplified calculations based on the Mohr-Coulomb failure criterion considering the loading case to be a uniaxial compression with insufficient time for increase of the horizontal stresses in order to approximate the undrained shear strength as a function of the depth.

- PRCI proposes that when subjected to dynamic load, the soil strength can be treated as if the soil were a cohesive material ($\phi = 0$) with an undrained shear strength equal to approximately 20% of the effective overburden stress.
- DNV, proposes four different relationships distinguishing passive and active loading of the soil. A further distinction is being made regarding the way the passive or active failure is achieved (increase/decrease of horizontal or vertical effective stresses).

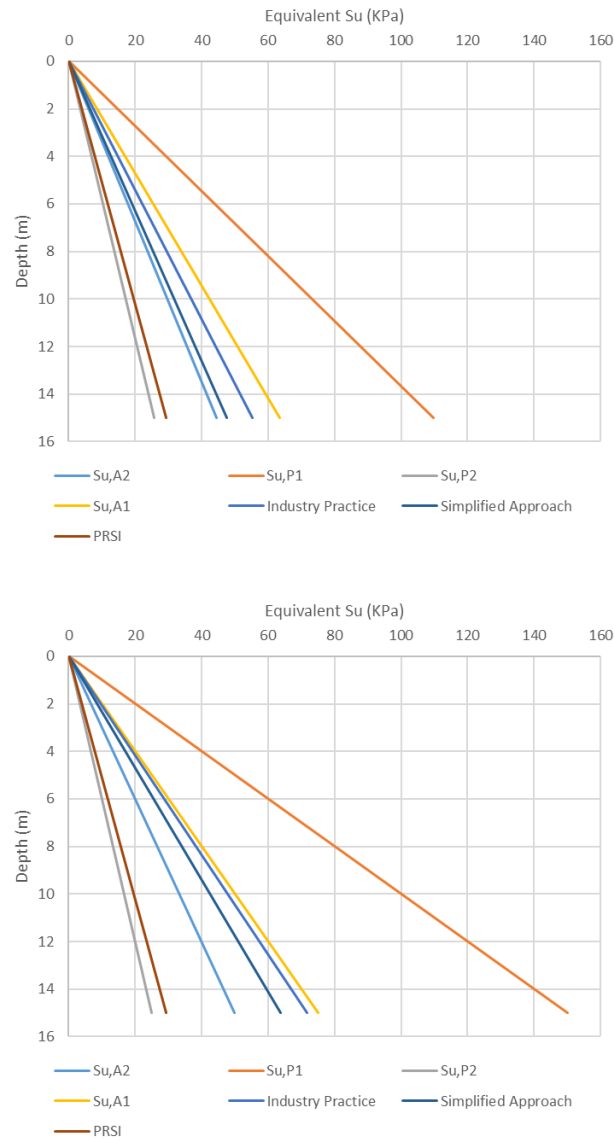


Figure 7.8 Equivalent undrained shear strength profile of sand for different approaches. Top diagram represents a sand with $\phi = 25^\circ$ and bottom $\phi = 30^\circ$. For both sand $\rho = 2000\text{kg/m}^3$

As can be seen from the above derivations, for two different sands, most of the proposed theories predict equivalent S_u values that do not differ significantly. Only one curve from DNV ($S_u, P1$) gives more than 100% difference. Additionally, in the surface no initial cohesion is considered, which cannot be known upfront. As will be shown later, the critical depth for the impact scenario is roughly the first 4-5 meters where the calculated values are relatively small compared to what would be expected. This happens due to the small overburden pressure at small depths, which reduces the equivalent confinement stresses around a soil element. It should be also highlighted again, that sand does not behave as a linear-perfectly plastic material as clay does, but rather as a linear-plastic material with hardening due to fracture and compaction of the grains.

7.4 Failure Models

One of the most important parameters in soil simulations is the failure model. In the literature, numerous models can be found. Some of them, like Mohr-Coulomb give relatively good approximations given their easy implementation. Other models, are semi-empirical which mean they are based on developed theories but they are also calibrated according to conducted experiments. These models, are usually difficult to be used in a parametric analysis like the present thesis, since they use experiments to determine certain coefficients. Moreover, these models are usually developed for a site-specific soil condition which has been encountered either due to failure either due to a priori investigation of the geotechnical properties.

For the purposes of this thesis, the Mohr-Coulomb model will be used in order to get a first approximation of the soil behavior due to impact. More, specifically for clay soils zero internal friction angle will be considered and for sands zero cohesion. This, leads practically on working with total stresses regime in clays and with the effective stress principle for sands.

In general, Mohr-Coulomb is not considered the optimal failure model as it does not account for any hardening or stress history but it is sufficient in order to determine if there is a need for a further investigation of the soil itself. Additionally, the other proposed models require high-level geotechnical knowledge and implementation, like the use of experimental data to fit several coefficients which is out of the scope of this thesis.

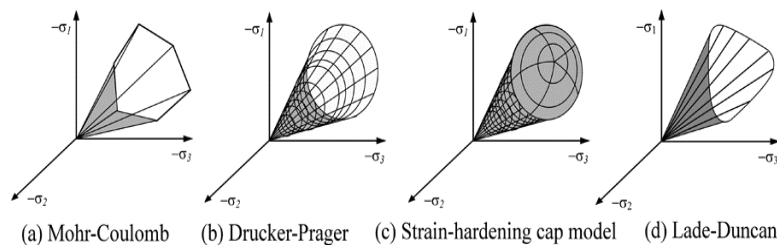


Figure 7.9 Soil failure models' comparison. (Contreras et al, 2012)

Another model that has been used in the literature when investigating dynamic response of soil is the Drucker-Prager model. The extended Drucker-Prager models are used to model frictional materials, which are typically granular-like soils and rock, and exhibit pressure-dependent yield (the material becomes stronger as the pressure increases). They are also used to model materials in which the compressive yield strength is greater than the tensile yield strength, such as those commonly found in composite and polymeric materials. In general, they allow for volume change with inelastic behavior. The classic Drucker-Prager model, can be directly related to a Mohr-Coulomb failure surface by projecting the failure surface on the deviatoric plane.

A modification of the classic Drucker-Prager model is the Strain-Hardening Cap model or the Modified Drucker-Prager model, which intends to model cohesive geological materials that exhibit pressure-dependent yield, such as soils and rocks. It is based on the addition of a cap yield surface to the Drucker-Prager plasticity model, which provides an

inelastic hardening mechanism to account for plastic compaction and helps to control volume dilatancy when the material yields in shear. However, in order to properly implement this model laboratory triaxial tests are needed in order to determine a number of coefficients for the cap yield surface and the transition piece. As it can be easily understood, this is neither possible or within the goals of this thesis and thus it is only mentioned for the sake of completion and for future research purposes.

7.5 Wave Propagation in Soil

One major difference of soil modeling between soil modeling in quasi static problems and dynamics, is the wave propagation that is generated due to the dynamic excitation. Propagating waves can affect the results of the analysis and the behavior of the soil a lot. Two different waves propagate during a dynamic excitation of the soil.

- Acoustic waves

- Shear waves.

Acoustic wave propagation through porous media is affected by the properties of the pore fluid and the matrix material. Acoustic velocity and travel times are extensively used for imaging of subsurface strata, and to predict petrophysical properties such as porosity, fluid type and saturation. Usually, in soils and rocks the acoustic or pressure wave travels 10 times faster than the shear wave velocity.

According to the elastic wave theory, it is possible to predict the wave velocity for a homogeneous medium when the elastic modulus and Poisson ratio is known. This can be formally written as follows:

$$c_{shear} = \sqrt{\frac{G_{max}}{\rho}} \quad (7.1)$$

Where G_{max} is the dynamic shear modulus of the soil and ρ which is the saturated density of the soil. Accordingly, for the acoustic (sound) or pressure waves in a linear medium:

$$c_{sound} = \sqrt{\frac{K_b + \frac{4}{3}G_{max}}{\rho}} \quad (7.2)$$

However due to plastification of the material, the acoustic velocity of the wave changes and can be calculated as follows for a perfectly plastic material:

$$c_{sound,pl} = \sqrt{\frac{K_b}{\rho}} \quad (7.3)$$

Where K_b is the soil bulk modulus which equals to:

$$K_b = \frac{2G_{max}(1+\nu)}{3(1-2\nu)} \quad (7.3)$$

Due to the fact that soil is not a homogeneous medium but rather a porous one, the aforementioned equations predict relatively good the velocities only when a Poisson ratio equal to 0.495 is used in the calculations. The reason is that the soil does not experience volumetric change due to the small vibrations of the waves. For clay the order of magnitude of these velocities is about 200m/s for the shear waves and 1500 m/s for the acoustic/pressure waves.

Generally, sound propagation in porous media is a research topic to this day, as the exact value of the wave velocity is important in seismographic and other identification operations of the geomorphology.

The wave propagation is an aspect of this thesis that is to be investigated. It is of interest to observe until which depth the pressure waves effect the soil, before their pressure drops to negligible levels. This will give a better understanding on the soil depth that actually contributes to the impact problem and the energy dissipation.

7.6 Soil Finite Element Model

7.6.1 Soil Domain Dimension and Boundary Conditions

The dimensions of the soil domain have been chosen after an iterative procedure in order to achieve converged results and minimized CPU time. Specifically, the length of the model is determined primarily by the length of the pipe. This is because the pipe length needs to be sufficiently big in order not to have the need of an axial feed-in spring, which practically means that the far end of the pipe will not move axially. Regarding, the soil cross section the dimensions have been chosen in order to obtain optimal absorption of the propagated waves.

For the present thesis, a soil half circle cross section of 15m radius will be considered. After some preliminary analyses, it has been found that within this range the important phenomena can be captured without the loss of valuable information. The most important parameter is to secure that the soil domain will not suffer from reflecting waves that can alter the final solution. As aforementioned, pressure waves travel with speeds up to

1500m/s. So, it is essential to cancel or absorb these waves. This problem can be treated in three different ways in a FEM analysis:

- Increase the size of the model enough so the waves will not be able to reflect and reach the area of interest on time. This solution, might be the simplest in terms of implementation, but it might also be costly in CPU time as more elements are needed especially for stiff soils where waves travel a lot faster.
- Add damper elements at the boundaries of the soil domain, which will dissipate energy depending on the incoming frequency of the waves. However, the calibration of such elements is rigorous and not very handy for a parametric study like the present thesis as the wave frequency is not known beforehand.
- Add infinite elements at the boundaries of the soil domain. Infinite elements, are used in boundary value problems defined in unbounded domains or problems in which the region of interest is small in size compared to the surrounding medium. They are usually used in conjunction with finite elements and can have linear behavior only. This way we can provide “quiet” boundaries to the finite element model in dynamic analyses so that the generated waves will not be reflected but instead they will be propagated to infinity. This is achieved through the effect of a damping matrix where at the same time the stiffness matrix of the element is suppressed.

Infinite elements at the boundaries away from the impact seem to be the ideal solution for this study. The reason is, that because several soil profiles and properties will be used during the analysis the wave propagation speed and transmitted pressure will change constantly. If a big enough model was to be used, then each time it would need new dimensions which is not practical or computationally efficient.

Infinite element performance is high for one dimensional problems where plane waves impinge orthogonally at the model boundary. Therefore, they offer very high absorption for 1D problems. For more complex problems, such as the case of 3D ground vibration modelling where the wavefield is a combination of surface and body waves, propagating at a range of frequencies, performance is lowered. One reason for this loss in performance is that the waves are not impinging orthogonally at the absorbing boundary thus causing higher levels of reflection. Infinite elements absorb the wave energy in an optimum way when the wave propagation direction is perpendicular to the infinite element’s surface. If the wave falls under a non-orthogonal angle the infinite element, the wave is partially reflected and thus noise is added to the results. This is of utmost importance when constructing the soil domain.

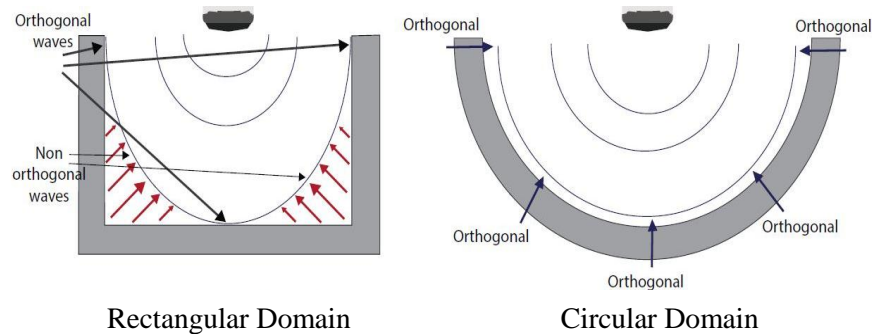


Figure 7.10 Schematic representation of acoustic waves and how the soil domain shape affects their absorption. (D. Connolly, 2013)

An initial consideration, was to create a rectangular domain and assign infinite elements in each side. However, as it can be depicted below, this did not allow the waves to be fully absorbed. It has been observed, that near the edges big stress concentrations occurred along with stationary waves. Of course, such a thing cannot be acceptable as the results of the analyses can be easily compromised.

To overcome this drawback, a circular domain has been considered. The infinite elements lie on the outer diameter of this domain and have a thickness equal to the thickness of the finite domain. By implementing, this shape of a domain the absorption of the waves has become optimal and the noise in the results has been almost erased. Now, the waves will always “hit” the infinite elements orthogonally.

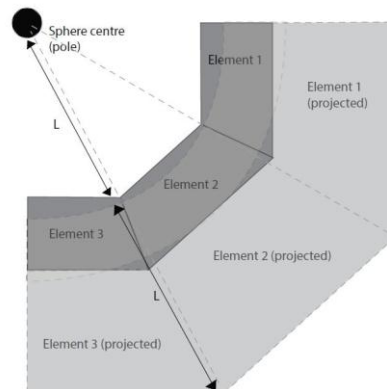


Figure 7.11 Connection detail of finite with infinite elements at the boundaries (D. Connolly, 2013)

However, for soil the boundary conditions in the symmetry plane are slightly different. The difference is due to the fact that soil cannot transfer moment directly. Thus, by not allowing the symmetry plane to rotate we would make a physical interpretation mistake. Symmetry boundary conditions will be applied on the sides of the soil domain that intersect with the impact point or alternatively the sides that lie on the symmetry axes.

7.6.2 Meshing

The soil medium consists of two major parts, namely the finite and the infinite part. As the names suggest, the finite part will consist of finite elements and will be used to describe the model at the impact region, whereas the infinite part will consist of infinite elements that will be used to describe the infinite extent of the soil domain in a region far from the impact.

For the finite part of the soil model, typical C3D8R, solid elements will be used in order to properly capture all the relevant phenomena. Moreover, the mesh strategy that will be followed will be the following: Due to the expected distortion of the mesh near the impact region, careful meshing must be done. Specifically, at the impact region fine mesh is being used for a 5m radius around the pipe. Outside of this refined region, larger elements are used since distortion is not expected there and their only purpose is to transfer the generated pressure waves away from the structure without causing reflection.

For the infinite part, CIN3D8R acoustic infinite elements will be used. These elements, are not available in Abaqus CAE and can be only used by writing a code. As aforementioned, they can only have linear behavior and the numbering of their nodes must be carefully selected because this is how the program understands the direction of the infinity. Schematically all the aforementioned can be seen here:

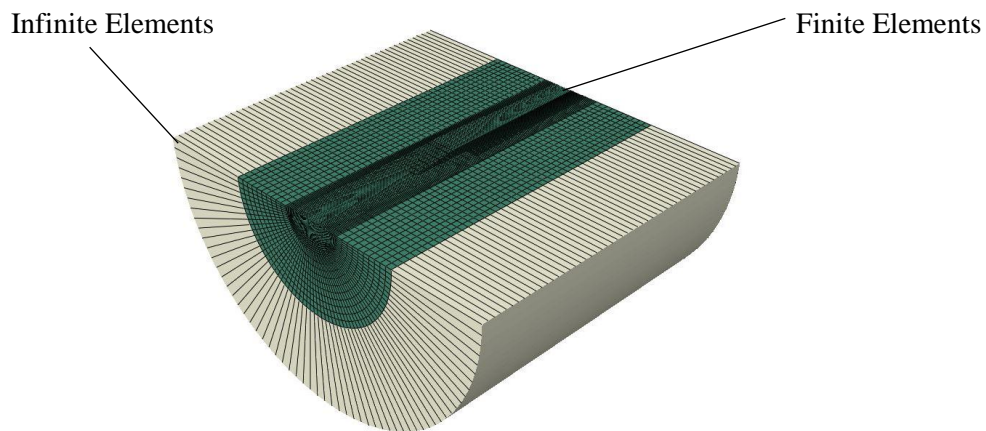


Figure 7.12 Final finite element soil model

7.6.3 Geostatic Stress Field

As soon as the domain has been set-up and the properties of the soil have been selected within the aforementioned range for offshore soils, one more step is needed before the full analysis can be conducted. The geostatic stress field must be established in order for soil to gain its full properties, as the depth increases the soil resistance increases due to triaxial conditions.

For each soil, domain the specific density and the expected geostatic vertical stresses are imported to the model along with the lateral earth coefficient of 0.5 in order to obtain the full geostatic stress field. Special attention is needed in order for the soil not to fail under the gravity load. This can happen if the imported soil parameters are less than the minimum required. This can result in excessive deformations and non-convergence of the solver. The final geostatic vertical stress field for a vertical slice of the domain is depicted below:

Clays will be treated differently in this step comparing to sands. More specifically, both soils have saturated density near 1700 – 2000 kg/m³, and this is the density that is required in the dynamic analysis in order to capture the inertia effect of the soil and the water that is inside the pores in its entirety.

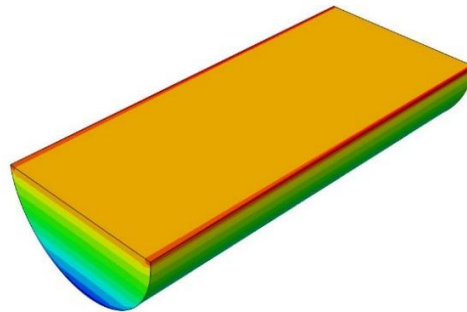


Figure 7.13 Geostatic stress field.

However, as it is widely known, sands work with effective stresses and clays with total stresses. This means, that the initial geostatic field cannot be the same for the two soils. To overcome this, within the Abaqus framework a calibration of the gravity acceleration for the case of the sand must be made. The acceleration must be reduced in order to obtain the effective stress field with the saturated density.

Page intentionally left blank

8. Pipeline – Soil Interaction

8.1 Introduction

In this chapter, the effect of the soil bed flexibility will be investigated mainly for clays. Specifically, the contribution of the soil in the kinetic energy dissipation will be quantified. Additionally, the effect on the dent size and depth will be also investigated in order to reach to useful conclusions when studying problems of this nature. Strain-rate yielding or liquid inside the pipe will not be considered in this study, as the only the contribution of the soil is to be quantified here. In the end of the chapter an effort will be made to model sand separately. A combined analysis with liquid, soil and strain-rate dependencies will be presented in the next chapter.

The reason this study is considered, is due to the fact that the soil plasticity is not considered whatsoever in the DNV guidelines. It is important to observe how much the stiffness and the plasticity of the soil contribute to this end. Several soil profiles will be considered mainly for clays, from very soft to very stiff.

Soil plasticity, allows the pipeline to move globally like a whole body, instead of localizing the deformation strictly in the dent. As the soil becomes stiffer, the pipeline cannot penetrate into the soil globally, which means that all the energy will have to be accumulated by the dent, coming close to the case of a rigid bed.

Another parameter that will be investigated, is the velocity of the object that hits the pipeline. As the velocity increases, due to the inertia of the whole pipeline, global deformation is more difficult to take place. Instead, more energy is expected to be dissipated locally.

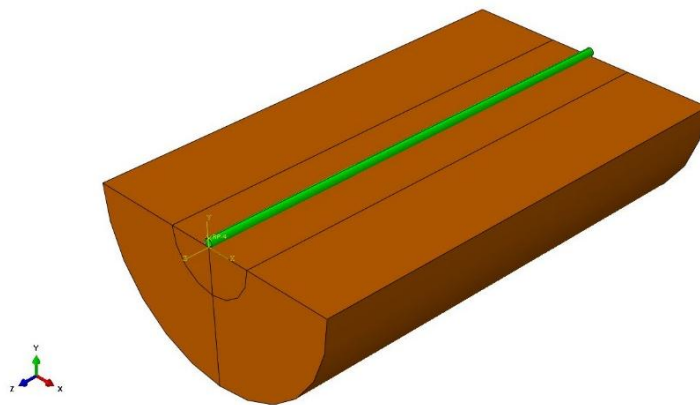


Figure 8.1 Pipeline-soil interaction model

8.2 Analysis Procedure

Now that both the pipeline and the soil finite element models have been created, the impact analysis can be performed. In order to do this correctly certain steps have to be followed in the correct order when the analysis runs in order to capture the phenomenon as realistic as possible. Here the assumption that the external pressure is equal to the internal will be made. The model length has been chosen accordingly to reduce any axial displacement or rotation in the far end of the pipeline, in order to capture the infinite length condition. For the soil domain a 5% structural damping has been considered. The procedure of the explicit analysis can be summarized in the following steps:

- Establish Geostatic stresses in soil due to self-weight.
- Lower and establish contact between pipeline and soil to avoid convergence errors in the interface due to excessive overclosure.
- Introduce gravity force to pipeline and to possible contents to obtain the equilibrium and the initial settlement of the soil. Consider two cases:
 - Empty pipe with concrete coating with a Dynamic Amplification Factor (DAF) equal to 1.3 – 2 to account for the pipe laying operation and a reduced strength soil profile to account for the remolded soil.
 - Filled pipe with concrete coating and with a full-strength soil and with no DAF included.
 - Pick the case with the biggest settlement as initial condition for the analysis.
- Apply internal or external pressure on the contents of the pipeline (if present).
- Drop the rigid object on the pipeline with an initial velocity and mass to initiate the impact.
- Measure the acceleration of the dropped object and the displacements of two opposite nodes in the symmetry cross-section to obtain the dent deformation.

8.3 Investigation of Soil Profiles.

In this section, the effect of different soil profiles in the dissipation of energy will be studied for an empty pipe. As aforementioned, the soil profiles have been selected based on realistic values and realistic correlation between the Young's modulus, the undrained shear strength profile and the density of the soil for static conditions. Here, no internal fluid or any kind of pressure has been added to the model in order to purely investigate the soil contribution and no strain – rate dependency of the yield stress has been considered.

It has to be stated again, that due to the use of a simplified Mohr-Coulomb failure criterion, the soil behaves as an elastic – perfectly plastic material with no hardening effects. Of course, in reality soil has a hardening effect depending on its stiffness, porosity, density and confinement. This makes a priori the results non-conservative as the effect of plasticity becomes more prominent. However, it is still a good approximation to investigate if the effect of the soil in the dissipation of the energy is important enough to be investigated more thoroughly in a geotechnical – oriented research. Due to absence of data regarding a law that takes account strain-rate phenomena for soils, by using a range of soft to very stiff clays we can bound the solution. This means that a soil that can be characterized as soft for static conditions can behave as stiff under dynamic conditions with its elastic modulus and shear strength increased.

Indenter	Energy Input	Velocity	Indenter Mass
Type A	670 kj	10 m/s	13400 kg

Table 8-1 Base case input parameters

Two cases have been considered, one where the pipeline is unburied and one where the pipeline is buried to a depth equal to 0.5D.

Name	E (z = 0) (MPa)	E (z = 15) (MPa)	Poisson Ratio	Su (z = 0) (MPa)	Su (z = 15) (MPa)	Soil Density Saturated (kg/m ³)
Soil 1	1.5	10.5	0.4995	0.005	0.035	1700
Soil 2	4.5	13.5	0.4994	0.015	0.045	1700
Soil 3	7.5	16.5	0.4992	0.025	0.055	1700
Soil 4	15	24	0.499	0.05	0.08	1700
Soil 5	30	39	0.498	0.1	0.13	1700
Soil 6	60	69	0.497	0.2	0.23	1700

Table 8-2 Considered clay soil profile properties for the analysis.

8.3.1 Unburied pipeline

In this section, the case of an unburied pipeline with no trenching that lies on the surface will be investigated. The aforementioned velocity mass combination will be used in order to obtain results. Different soil profiles will be considered as shown mainly for clay soils. The softer soil is Soil-1 and the stiffness increases with the numbering, so that Soil-6 is the stiffest soil of the current investigation.

As expected, for the softer soils, both the maximum and permanent dent size is a lot smaller than the rigid bed case. With increasing stiffness, these values increase as well approaching the upper limit of the completely rigid bed that has been previously investigated as can be seen below.

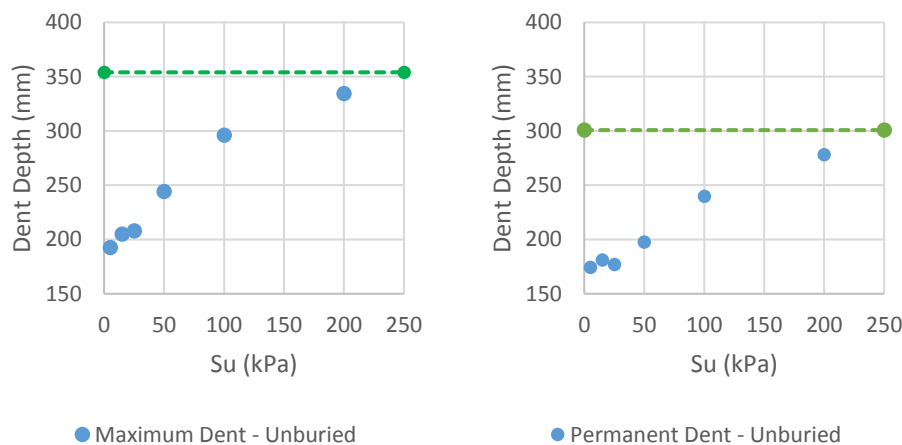


Figure 8.2 Maximum and permanent dent sizes for different surface values of S_u . The values from the rigid bed analysis are marked with dashed lines respectively.

For the softer soil, the reduction in maximum dent size is roughly 45% compared to the rigid bed value, whereas the permanent dent size is 42%. For the Soil-5 which represents a stiff clay the respective percentages are 15% and 21%. The effect of the soil on the dent size is obvious. However, these results must be treated with caution as the hardening of the soil is not taken into account.

Whereas, for the pipe – fluid interaction or pipe – pressure analysis the load-dent curve has changed, here the curve remains the same. The reason is very fundamental in the understanding of the behavior of the system. In the fluid – pipe interaction, the liquid provides an extra stiffness in the denting area as it acts against the dent providing negative work. Thus, the external force (and consequently the energy) that is needed from the indenter increases.

However, for the pipe – soil interaction, the physics are different. Due to the soil plasticity, the distribution of the energy changes, meaning that now only a fraction of the kinetic energy will be absorbed as a denting deformation. The rest of it will be absorbed as a rigid body motion of the pipe itself into the soil and as plastic deformation of the soil

itself. This means that the denting deformation is a product of only the work done by the indenter and thus there is no reason for the load – dent curve to change. This can be verified by integrating the resulting load – dent curves in order to measure the energy that is absorbed each time as denting deformation.

Moreover, the energy calculated here is the energy that will be absorbed as a maximum denting deformation using the familiar equation from chapter 3:

$$Absorbed\ Energy = \frac{\psi \cdot K}{100} = W(\delta) = \int_0^{\delta_{max}} F(\delta) d\delta \quad (8.1)$$

Where ψ , is the fraction of Kinetic Energy absorbed as maximum dent deformation such as:

$$\psi = \frac{W(\delta_{max})}{K} \cdot 100 \leq 100 \quad (8.2)$$

However, as explained earlier the tube does not retain the maximum dent depth, but it reaches an equilibrium at the permanent dent depth. This is due to the fact that the pipeline acts like a non-linear spring. Even though, it might go beyond the elastic region, there will be always a linear spring-back effect when the external load equals to zero. Thus, due to the unloading a portion of the deformation energy becomes kinetic energy of the indenter as it is being pushed away.

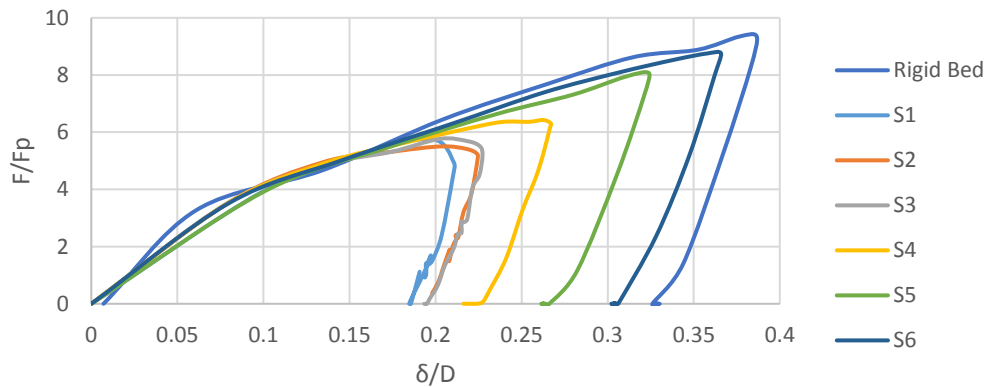


Figure 8.3 The force-dent curve does not change when soil is introduced. However, the area that occupies reduced as it represents the energy absorbed.

Indeed, as the soil becomes stiffer the energy absorbed as maximum dent deformation increases. This is in accordance with the physics of the specific analysis. The very soft soil will undergo large plastic deformations before reaching equilibrium, which dissipates a lot more energy than a stiff one. The very stiff clay has a very small effect on the energy dissipation as it absorbs roughly 90% of the impact energy for a 10 m/s velocity. This

behavior is most probably close to a sand behavior, as sand is usually a lot stiffer than the clay in offshore environments under dynamic loading.

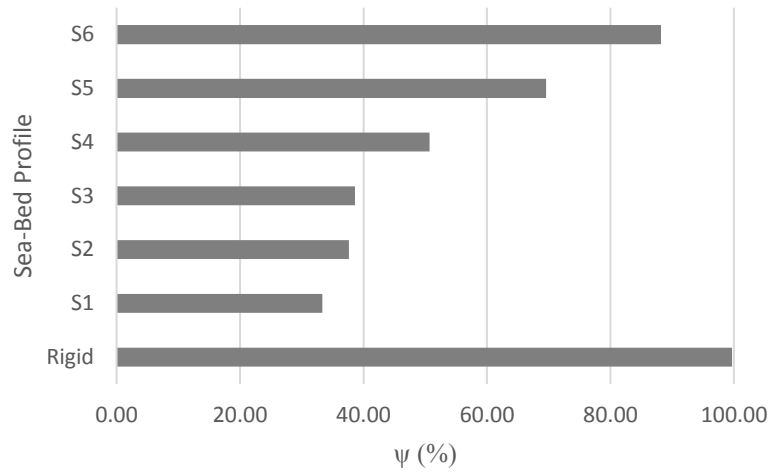


Figure 8.4 Absorbed energy as a fraction of the kinetic energy for the different clay profiles.

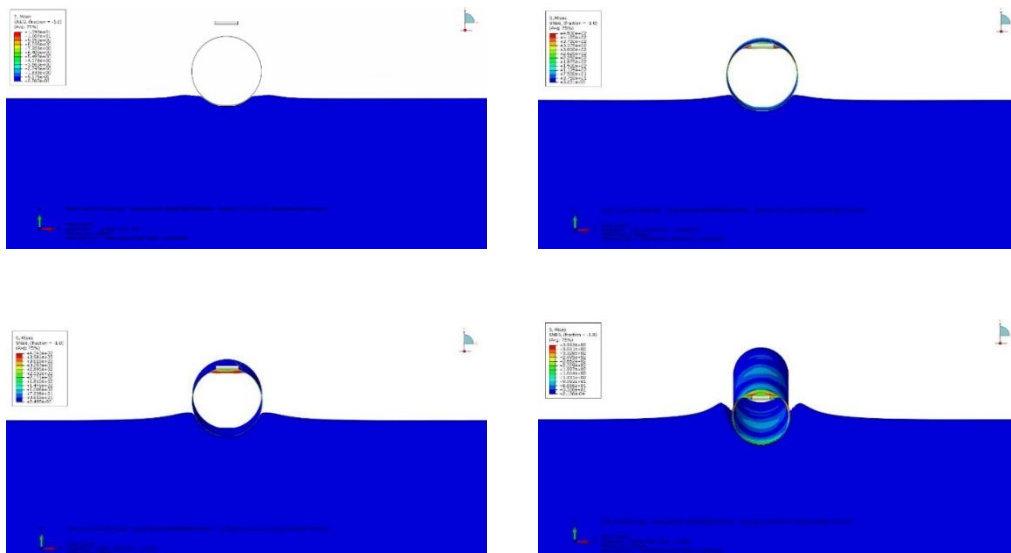


Figure 8.5 Pipeline - soil interaction, deformed cross-section for different time intervals. The penetration into the soil is visible.

8.3.2 Half-Buried Pipeline

Now, that some initial estimations have been derived from the case of unburied pipeline the same analyses will be performed for a half-buried pipeline which also occurs in reality as trenching might be needed for various reasons.

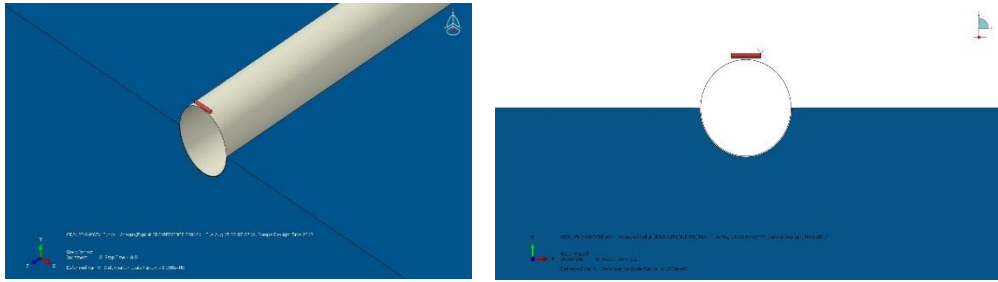


Figure 8.6 Half-buried pipeline model set-up.

The trenching is expected to provide more stiffness to the pipeline, as it will confine it and will resist in the ovalization due to its passive resistance. Additionally, a bigger area of the pipe is in contact with the soil when it wants to move vertically. This means, that the energy will dissipate in a different manner than before which will affect the dent depth eventually as the penetration will be reduced. Again, the same soil profiles will be investigated but for a half-buried pipeline now with an object with $V = 10$ m/s and $M = 13.4$ mt.

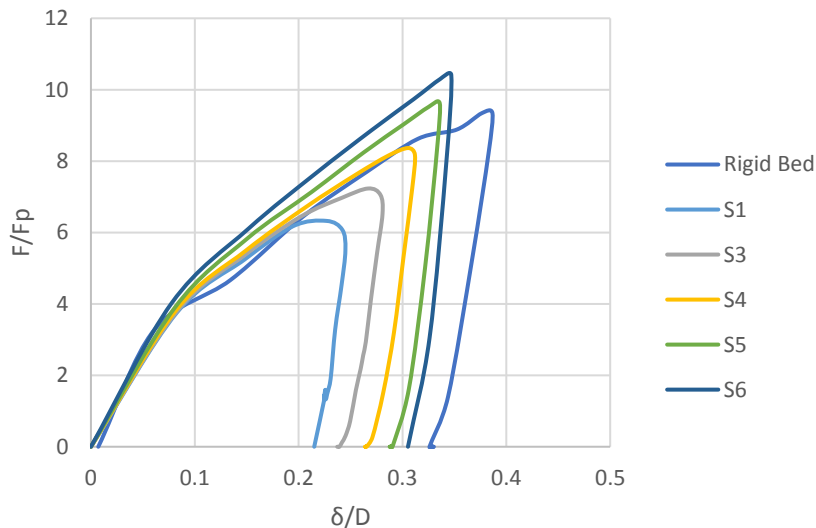


Figure 8.7 Force-dent diagram for half-buried pipeline. As the soil stiffness increases, the residual stiffness of the diagram increases as well due to the confinement from the soil at the sides.

One interesting result has emerged from the half-buried analysis. Due to the passive resistance of the soil on the side of the pipeline not only the energy dissipation has

changed but the loading-dent curve has showed increased stiffness as well. This can be explained from the fact that the soil is resisting to the cross section ovalization and thus the circular shape becomes harder to change in an oval one. This practically means that the soil resistance has a negative work against pipeline ovalization and because of that the force-dent curve has an increased stiffness.

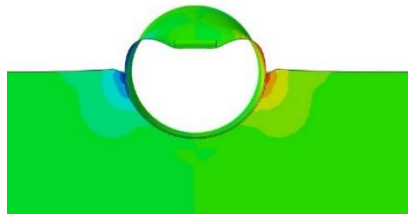


Figure 8.8 Soil lateral movement for the half-buried pipeline

This verifies the conclusion that the load-dent curve and relation is affected only by external factors that produce positive or negative work on the denting itself or the ovalization that comes along with it. However here the effect of the soil on the side of the pipeline is double, as it dissipates energy and at the same time provides an external pressure so that the cross-section is not excessively deformed. This is not observed for surface pipelines as there is not such a force existing.

Again, there is a significant reduction in denting deformation compared to the rigid bed case but it is increased when compared to the unburied pipeline case for each soil respectively. Despite that, the dissipation of energy is still in significant levels but as expected reduced compared to the unburied pipeline. The amount of energy that is absorbed as denting deformation is now increased by 30-40% compared to the unburied case, as can be shown below:

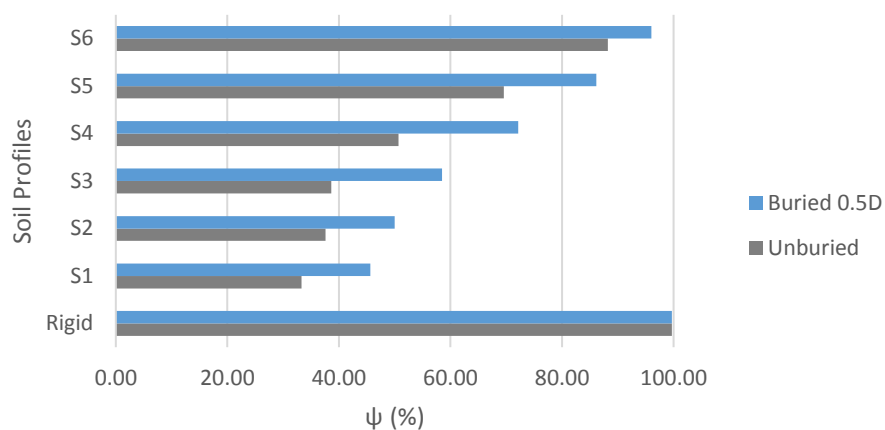


Figure 8.9 Maximum absorbed kinetic energy fraction for buried and half-buried cases.

As for the denting itself, a same pattern is observed in both the unburied and half-buried pipeline as the stiffness of the soil increases. For very stiff soil, the values match and there is not an actual contribution of the burial to the denting behavior. This can also be verified if the absorbed energy is compared for the two different cases.

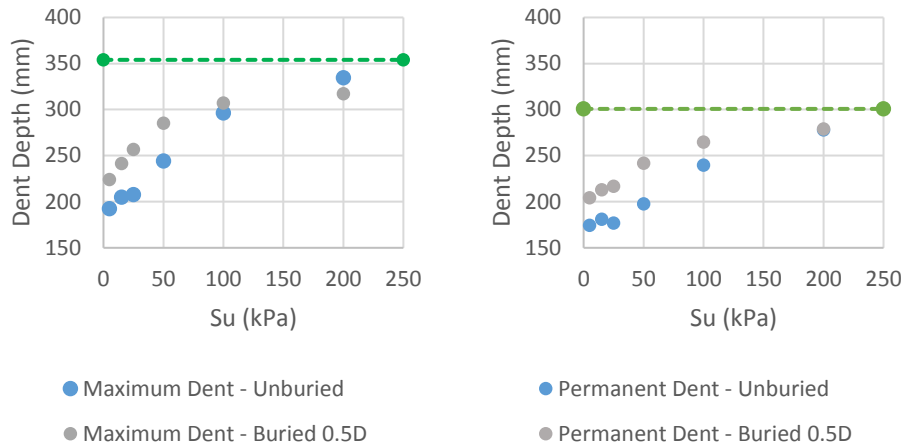


Figure 8.10 Maximum (left) and permanent (right) dent size for unburied and half-buried cases and different soil profiles. With dashed line, the values for the rigid bed case are marked as the upper limit.

8.4 Effect of Velocity

Now that the contribution of soil in the kinetic energy dissipation has been proven for an average velocity of 10m/s and an energy input of 670 kj, a sensitivity analysis will be carried out in order to determine the effect of the velocity in the energy dissipation. By considering this simplified two springs – two masses system, it is expected that the energy absorbed by the denting will be larger as the velocity increases.

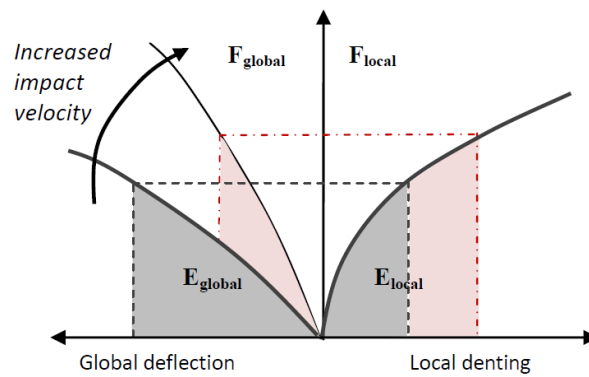


Figure 8.11 Schematic representation of conversion of energy between global deflection and local denting (Alsos et al, 2012)

The following input cases are considered for a range of velocities between 5 and 20 m/s. The mass is derived by solving the kinetic energy equation.

Energy	Velocity (m/s)	Mass (kg)
670 kJ	5	53600
	10	13400
	15	5956
	20	3350

Table 8-3 Considered velocity-mass input cases for the sensitivity analysis

Again, both buried and unburied pipelines will be considered for two soil profiles, Soil-1 and Soil-5 in order to better understand the effect of the velocity.

8.4.1 Soft Soil

As anticipated, for both the unburied and the half-buried pipelines, there is a velocity dependence. More specifically, for large velocities due to the inertia of the pipe, a bigger portion of the kinetic energy is absorbed locally.

This happens because, due to the speed at which the phenomenon occurs there is not enough time for the whole pipe to mobilize and move into the soil due to its inertia. Thus, before starting to move a significant fraction of the energy takes the form of local dent deformation and as the impact progresses, the pipeline will start moving into the soil where the rest of the energy is dissipated.

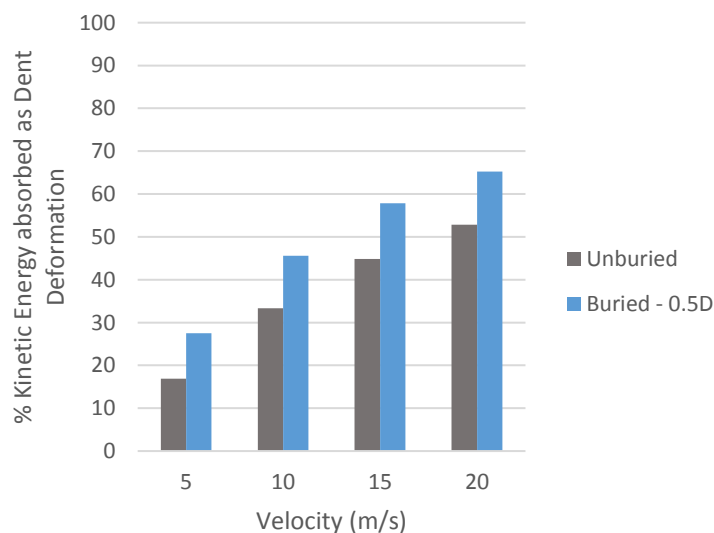


Figure 8.12 Absorbed kinetic energy - velocity diagram for unburied and half-buried cases.

Indeed, the results match with the initial considerations. Of course, the results have smaller differences as the soil becomes stiffer and approaches the rigid bed assumption where all the energy is dissipated only locally.

For the half-buried pipeline, the slope of the line that describes the absorbed energy – velocity relationship graph is steeper than the one for the unburied case. This practically means, that buried or half-buried pipelines are more sensitive to velocity changes which might result to a big difference in both the dent size and the absorbed energy fraction. This is a critical conclusion for the assessment of damage to pipelines, because it is obvious that both the foundation and the velocity of the falling object can completely alter the behavior of the dented pipeline.

As can be seen from the graphs below, there is an almost linear relationship between the absorbed energy for the maximum dent deformation and the increase of the velocity. These results, are completely against the DNV considerations, where for the same kinetic input energy the same dent depth always occurs. It is obvious that there is a big influence of velocity in the results which should be accounted when damage assessment has to be made.

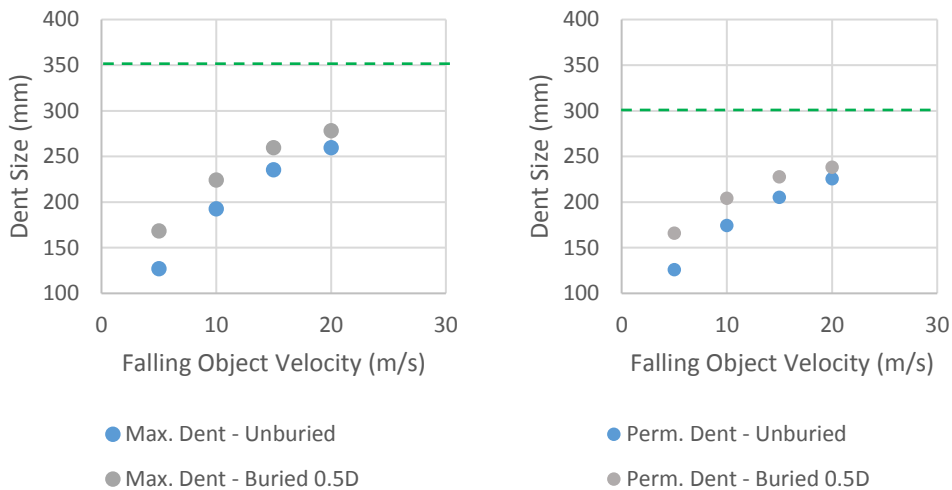


Figure 8.13 Maximum and permanent dent size for different velocity input for buried and half-buried cases. With dashed lines, the equivalent values from the rigid bed case are marked.

8.4.2 Stiff Soil

For the stiffer soil profile – Soil5, as expected it is generally insensitive to the velocity of the falling object, as the fraction of kinetic energy absorbed is in the same order of magnitude.

Moreover, when the pipeline is considered half-buried, there is no influence at all of the velocity as the soil is stiff enough not to allow any kind of global deformation in the form of body motion.

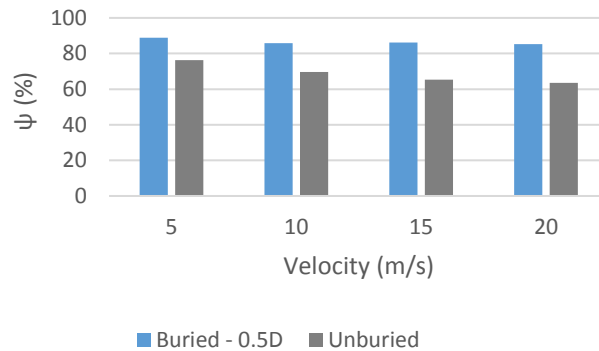


Figure 8.14 Fraction of kinetic energy absorbed versus the impact velocity for soil profile-5.

However, for the unburied case it has been observed something initially unexpected. Specifically, as the velocity increased the absorbed energy was slightly bigger for the low-velocity impact. When comparing the absorbed energies and the respective dent depths the difference between for $V = 5\text{m/s}$ and $V = 20\text{m/s}$ was about 10%.

By conducting an investigation on the reasons that led to these results, the following have been found. When the object hits the pipeline, a pressure wave is generated that travels initially through the steel pipe entering after the soil medium. As it is already known, the speed of the wave is constant and it is a function of the elastic properties and the density of the material each time. Thus, despite how fast the indenter hits the pipe the generated wave always travels with the same speed in each medium respectively.

However, the amplitude of the pressure wave that is propagated is not constant. It depends on how fast the loading occurs and also on the ratio of the impacted masses. It has been observed, that due to the difference of the impact velocities and mass ratio, the different pressure amplitude results in slightly higher-pressure wave amplitude when the velocity is increased.

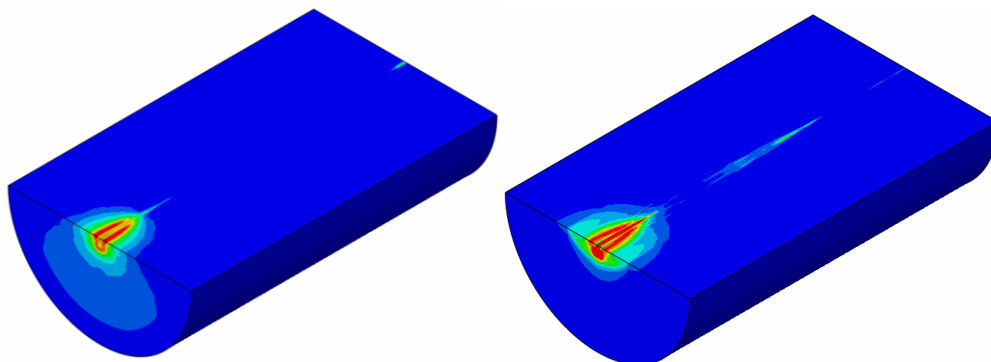


Figure 8.15 Wave propagation in soil medium for the unburied pipeline case for 5 and 20 m/s impact velocities respectively.

Additionally, the pressure wave amplitude decays with depth due to the loss of the energy transfer in the form of deformation and vibrations of the soil. So, this is strongly affected by the initial value of the pressure at the source where the wave is generated,

here the pipeline. This means, that the wave increases the stresses on the underlying soil significantly until a certain depth. It is straight forward, that for higher velocity, a higher-pressure amplitude is generated which will affect the soil deeper, plastifying it. This plasticity, allows more global deformations to the pipe as there is less resistance, leading to a bigger energy dissipation and consequently smaller dent. However, the difference in energy absorption and dent size are very close, which consequently means that practically velocity does not have a big impact in stiff soils. Moreover, the impact duration for a 5m/s velocity is about three times larger than the corresponding duration for the 20m/s

On the contrary, the low-velocity impact generates slightly smaller amplitude pressure waves which will decay in shallower soil depths. This means, that there is less plastification of the soil and thus, the total resistance of the soil against any vertical movement is bigger compared to a higher velocity impact. Of course, as mentioned many times in this report, this soil model is simplistic and only wants to display the significance of the soil in the energy dissipation of an impact. For all the above to be verified completely, a more sophisticated model is needed for the soil that will account for pore pressures and soil hardening.

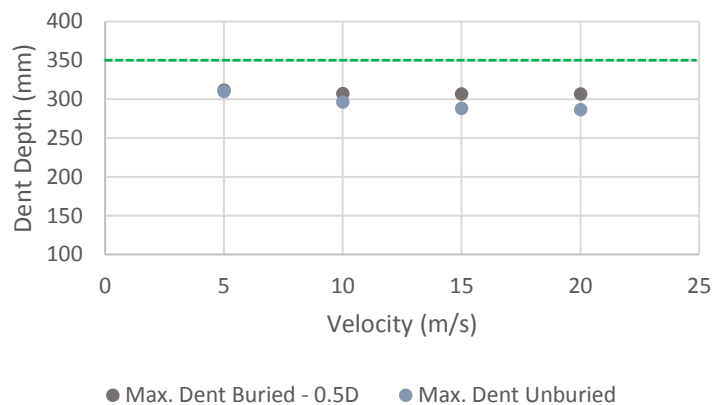


Figure 8.16 Maximum dent size for different velocities in the stiffer soil case for unburied and half-buried cases. With dashed line, the equivalent value for the rigid bed case is marked.

8.5 Conclusions.

Concluding, the pipeline – soil interaction impact analysis is a rather complicated problem, as it combines impact dynamics and wave propagation through non-linear mediums. It is evident that, velocity and mass ratio between the system components are extremely important. This means, that impact problems cannot be treated only by the product of velocity and mass which is the kinetic energy of the falling object. It must also be highlighted that the main feature through which energy is dissipated is the soil plasticity. Without plasticity, the soil bed behaves totally different and the effect of energy dissipation is reduced significantly. Moreover, this chapter provides just an estimate of the soil contribution because the soil dynamic behavior is not treated directly but by considering soil profiles of increased stiffness. It is thus important that more sophisticated models will be implemented for a more detailed estimation of the pipeline damage under impact scenarios.

Page intentionally left blank

9. Combined Model

9.1 Introduction

In this chapter, an effort has been made to combine all the previous models in order to approach reality as much as possible. The reason behind this investigation is that due to the non-linear behavior of the phenomenon, the results of each individual analysis cannot just be added together.

It is important to observe and measure how the combined system of pipeline-fluid-soil will behave together when impacted by a falling object. Moreover, the strain-rate effects of yielding of steel will be incorporated to the model as it has been shown that they are important for pipelines.

9.2 Soil – Filled Pipe Model

In this section, the pipeline – soil interaction problem will be investigated again, but now the effect of internal fluids will be taken into account. As already explained, when the content of the pipeline is gas there is not mass neither an incompressible fluid but only a pressure that exists on the inside of the pipe.

On the other side, modeling of fluid such as water or oil needs to take into account the incompressibility of the fluid, its mass and of course the pressure under which it operates. In this investigation, it is interesting to observe how the additional inertia coming from the fluid, will affect the global displacement of the pipe when the soil will be soft enough to allow significant penetration.

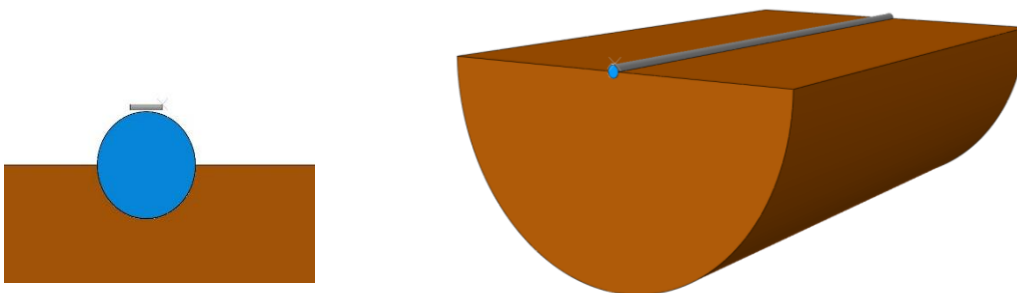


Figure 9.1 Pipe-fluid-soil interaction model set-up

9.2.1 Soil – Gas Model

Initially a gas filled pipeline will be investigated. For the same energy input, as before (670kj) and for a constant pair of velocity and mass, different pressure levels will be examined ($m = 13400\text{kg}$, $V = 10\text{ m/s}$). Moreover, as in the pipe-soil interaction chapter, the effect of the velocity in the behavior of a pressurized gas pipeline will be investigated, where the gas content will be modeled with fluid cavity elements as before. Soil profile 3, will be used here.

As already investigated, the existence of internal pressure is expected to reduce both the maximum and permanent dent depth but at the same time localizing the deformation more than without pressure, leading to smaller perforation energies. Now that the bed is not rigid but flexible and plastic deformations might occur, a percentage of the energy is expected to dissipated as has happened with the empty pipe case.

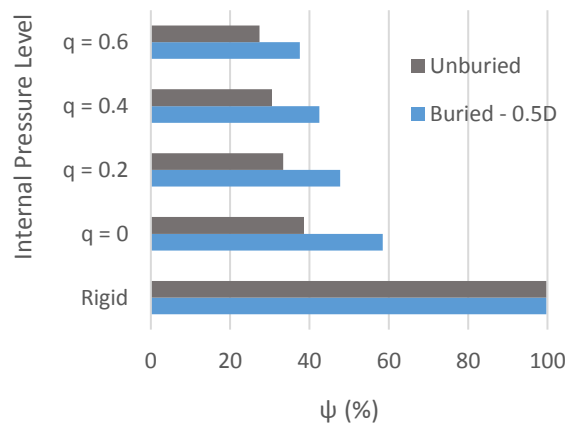


Figure 9.2 Absorbed energy versus the internal pressure level for buried and half-buried pipelines.

It has been observed, that as the pressure level increases not only the maximum and permanent dent size decreases but the maximum absorbed energy locally decreases as well. For the rigid bed case, the absorbed energy was always the same for the gas - pipeline system regardless of the pressure level. By closely investigating the behavior in these analyses, it seems that as the pressure increases, the global deformation increases. As for the dent size, very small differences are observed between the unburied and the half-buried cases compared to previous analyses for empty pipes.

This happens because the added resistance from the pressure practically makes the pipe stiffer against denting converting the local deformation into global. This can be easily understood, if the pipe is considered to be more “rigid” against cross sectional deformations as the pressure increases, which means that no local deformation can occur and consequently all the energy will be converted into global deformation and penetration. Of course, in this case the cross-section is not completely rigid and thus denting will occur as well. This is a very interesting observation that can be easily examined if survey data from existing pipelines are gathered. This can also be observed

by looking the longitudinal deformation of the pipe's upper surface. Due to the pressure, there is a very small longitudinal deformation compared to the empty pipeline case, thus this area as well will experience reduced local deformations but the global deformation will increase.

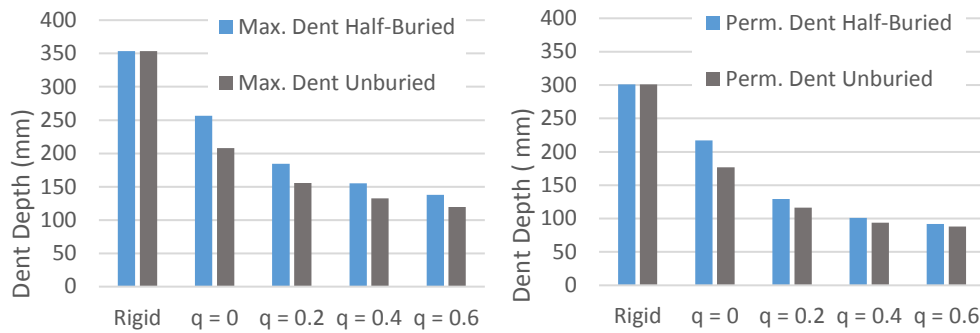


Figure 9.3 Maximum and permanent dent depth for different pressure levels of gas for half-buried and unburied case

Additionally, it has been observed that the propagated waves pattern has changed compared to the case of empty pipe resting on soil (Figure 9.5). However, it is rather difficult to exactly follow the wave behavior due to the plasticity of the soil which complicates the understanding of the phenomenon. Even when no plasticity was considered, the pattern was different as expected. It is obvious that the internal pressure distributes the energy differently between the pipeline and the soil. Specifically, it has been observed that when pressure exists the pressure waves inside the soil are spread more equally on the longitudinally and on the side of the pipe.

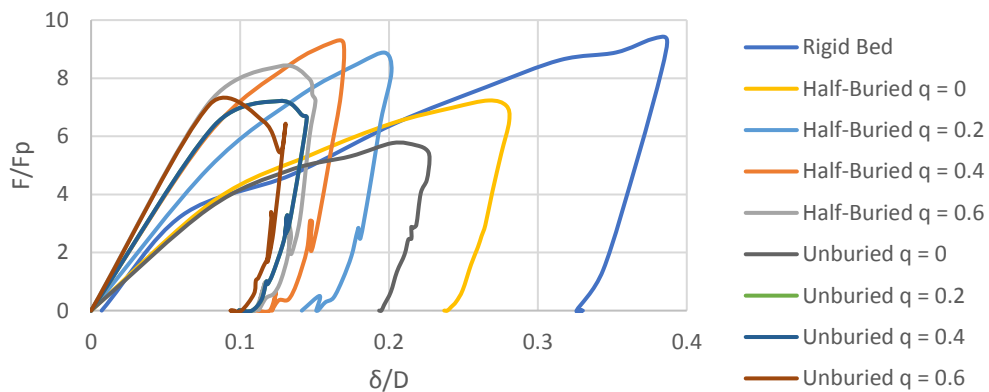


Figure 9.4 Force-dent diagrams for different pressure levels for buried and half-buried pipeline

As can be seen in figure 9.4, for the unburied pipeline for pressure levels larger than $q = 0.4$, this softening behavior is observed, which means that the force exerted by the indenter and the denting deformation are no longer in phase. As mentioned earlier this has to do with the fluid inside the pipe and the gradient of the pressure inside and not with

the soil as this has not been observed when the pipeline was empty. This is very clear especially for $q=0.6$ when the pipeline is unburied. The effect of the soil is limited to the fact that the area covered each time by the force-dent curve is reduced compared to the rigid bed case, which indicated the dissipation of energy into the soil and into global deformation of the whole pipeline.

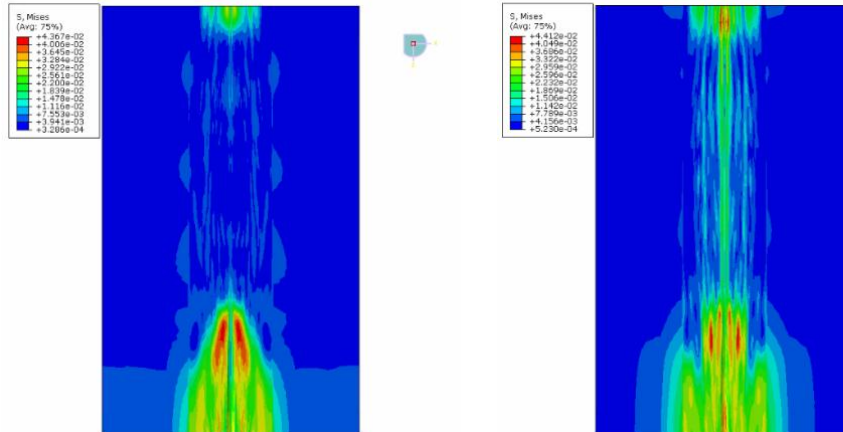


Figure 9.5 Top view of Von Mises stress field for (a) empty pipe (b) pressurized pipe with $q = 0.4$ at $t = 0.16$ sec. For the pressurized pipeline case, the stresses are more spread out both longitudinally and laterally than the empty pipe case resulting in a larger dissipation of energy globally.

Regarding the velocity dependence, it has been shown in chapter 6, that the behavior of a pressurized gas for the velocities examined is not affected. Now that soil is introduced, a velocity dependence is expected due to the soil flexibility and deformation. A fixed pressure level of $q = 0.4$ will be considered in the analysis. As can be seen from the following figure, the internal pressure effect is constant for the examined range of velocities. This means, that compared to an empty pipe or a pipe which has an equivalent pressure equal to zero (external equals internal), the percentage of energy absorbed is increased with increased velocity, but it is reduced compared to an empty pipeline case.

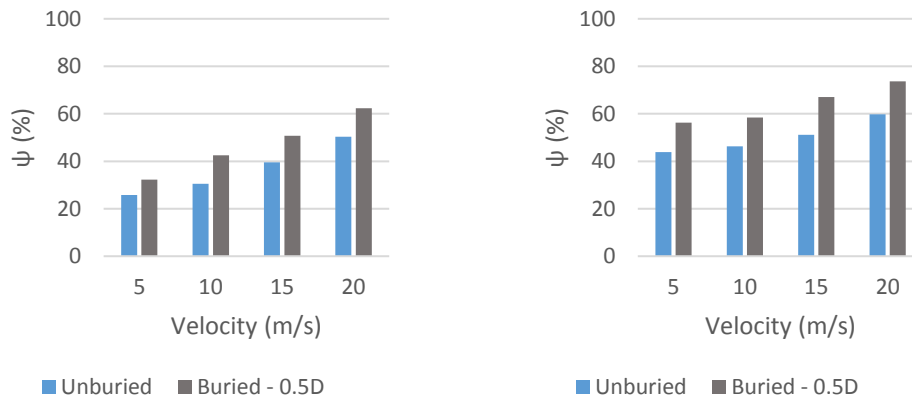


Figure 9.6 Absorbed energy comparison for pressurized (left) and unpressurized (right) pipelines on soil

9.2.2 Soil – Liquid Model.

Now that the case with only internal pressure has been investigated, a comparison will be made with the equivalent liquid model for a water filled pipeline. Again, different pressure levels for the same input kinetic energy and velocity will be investigated. A comparison will be made with the equivalent gas filled half-buried pipeline where fluid cavity elements were used.

Generally, when pressure is introduced it seems that the water filled pipeline absorbs a bigger amount of energy than the equivalent gas pipeline. This happens probably due to the inertia of the fluid inside the pipe, which resist to the global displacement of the pipeline and thus more energy goes to dent. However, the difference is very small.

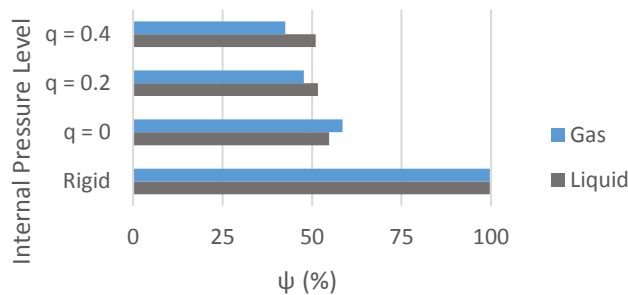


Figure 9.7 Energy absorption for gas and water filled pipeline resting on soil for different pressure levels.

However, as far as the dent depth and the deformation profile of the pipeline are concerned, no significant difference is observed for both the maximum and permanent dents. Only for the unpressurized case a larger difference is observed. This matches well with the observations that were made previously, as the pressure dominates any inertia effect of the fluid when it reaches these levels. Moreover, the phase difference between force and denting has been reduced significantly compared to the rigid bed case.

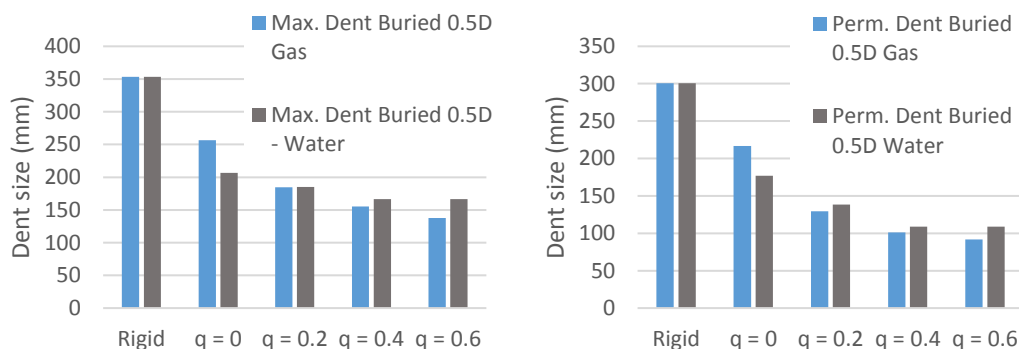


Figure 9.8 Maximum (left) and permanent (right) dent depths for a half-buried pipeline filled with gas or water.

9.3 Soil – Strain-Rate Yielding Model

As already proven, the strain-rate yielding for mild steel pipes is rather important when impacted with velocities from 5-15 m/s as shown by Palmer. To make this whole investigation more realistic the pipeline soil model will be used here but with the addition of the strain-rate sensitive material according to the Cowper-Symonds law.

The analyses have shown, that there is not a big effect of the yielding on the absorbed energy from the soil. The difference can be considered negligible. However, as expected the dent size is significantly lower. The reason is that the most important feature of the denting which is the yielding of the material happens in higher stresses as already shown in both the quasi-static and dynamic analysis chapters.

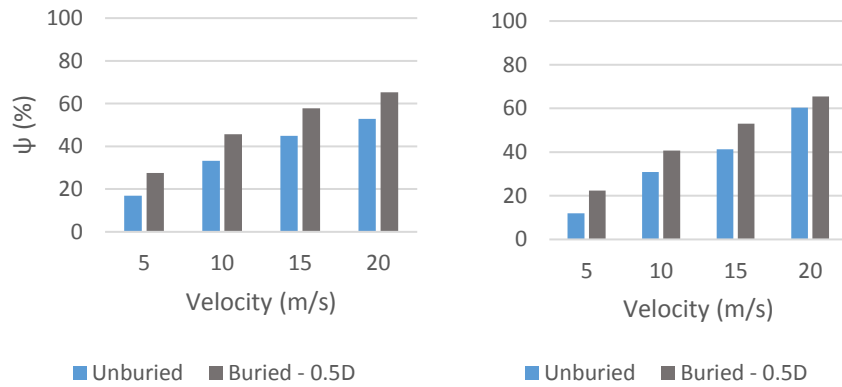
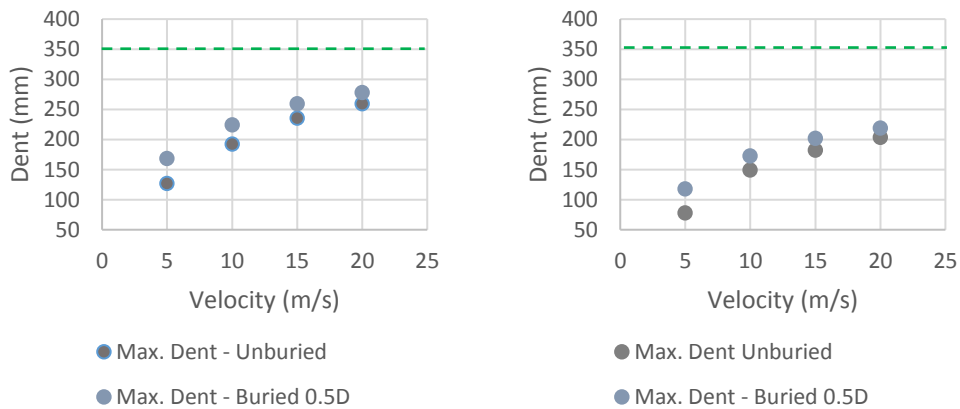
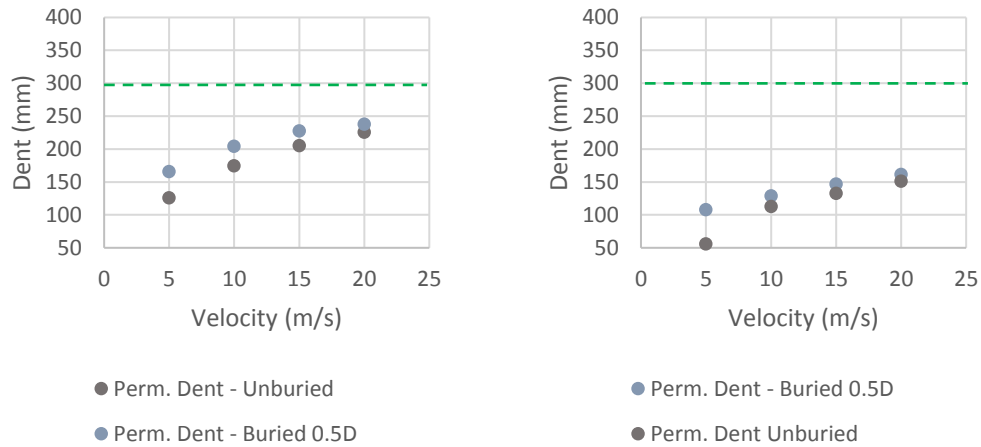


Figure 9.9 Energy absorption for Soil-1 profile, for (a) no strain-rate yielding and (b) strain-rate yielding of steel.

Moreover, both the maximum and permanent dents are smaller compared to the case where no strain-rate is taken into account. The velocity dependence in the dent size still holds, as it is not affected too much from the material itself but rather from the supporting conditions of the pipeline, in this case the soil. This means, that the energy absorbed by the pipe is not affected significantly by the material properties.



(a)



(b)

Figure 9.10 (a) Maximum and (b) Permanent dent depth for Soil-1 profile without (left) and with (right) strain-rate yielding of steel. Equivalent values from empty pipe rigid bed analysis are marked with a dashed line.

9.4 Conclusions

In this chapter, that the medium is introduced in the pipeline-soil model, the effect of energy propagation in the behavior of the system is more visible. When gas or liquid under pressure exist in the interior of the pipe, the pressure wave generated from the impact are transmitted in a different manner than for the empty pipe case. The effect of pressure in the denting again has the same effects, as the denting is more localized but at the same time it requires more energy to obtain a certain dent depth. It is also clear now, that the force – dent relationship is affected only by parameters that actually produce positive or negative work for the dent deformation and the ovalization that comes with it. This means, that generally soil does not have an effect on the force-dent curve but it only determines how much energy will be consumed as denting, whereas fluid will produce work and thus will alter the force – dent relationship. As for the strain-rate it only increases the yielding stress of the material, altering in a different manner the force-dent curve without affecting the absorption of energy significantly.

Page intentionally left blank

10. Conclusions and Recommendations

10.1 Conclusions

In this thesis, an effort has been made to understand in depth the physics of denting behavior of marine pipelines when impacted by an object. Starting from a simple quasi-static FEM model fundamental observations and conclusions regarding the material the internal and external pressure and the shape of the falling object have been derived for the behavior of a pipeline against dent.

Continuing, a more sophisticated dynamic explicit model has been set-up in order to study the denting behavior against a real impact load instead of an infinitely slow. In this model, the effect of fluid inertia and incompressibility was also investigated. Finally, the role of the soil in the energy dissipation during an impact scenario was investigated, where a parametric study has been carried out.

10.1.1 Static - Dynamic analysis differences

After verifying the quasi-static model with available experiments in the literature mainly from Karamanos, a comparison has been made by conducting the same simulations in a dynamic manner where inertia of the pipe and the velocity and the mass of the indenter was also taken into account for a pipeline resting on a rigid bed, excluding any strain-rate effects on the material yielding stress.

The results from the dynamic analysis of a semi-infinite pipeline have showed bigger maximum and residual dent depths for the same equivalent kinetic energy input. Moreover, the longitudinal deformation for the dynamic loading has shown a more localized dent. The force-dent curve for the dynamic case has exhibited a reduced stiffness compared to the quasi-static case. The aforementioned were not observed for tubes with significantly smaller lengths and fixed ends.

For semi-infinite tubes, low-frequency damping seems to be critical for the response of the system. If it is not accounted, then the system responds with reduced stiffness compared to the quasi-static case. However, it is rather difficult to determine the value of damping that in the end has to be used for the system, as this need necessarily experimental verification.

The dent behavior was relatively insensitive for a given energy input and different velocities that ranged from 5 – 25 m/s. However, when the pipeline was impacted with a velocity of 60 m/s (216 km/h) the dent behavior totally changed. This range of velocities is out of the scope of this thesis as they are unrealistically high and have only been studied for completion of the results.

10.1.2 Contribution of Material

Following the simple dynamic case, the Cowper-Symonds law has been implemented in order to take into account strain-rate sensitive material yielding. Palmer et al, have reported that the strain-rate yielding is important when dealing with mild steel pipelines and impact is investigated.

Indeed, an implementation of this model has been carried out for the same experimental set up without any fluid, internal pressure or bed flexibility effects. The results have shown a significant reduction in both maximum and permanent dent depths compared to both the simple dynamic analysis and the quasi-static one.

The reason behind this significant reduction, is that yielding is what dominates the denting. Thus, an increase in yielding stress even if this happens momentarily gives an additional resistance to the system. Of course, measuring the exact strain-rate is a very difficult task and the Cowper-Symonds law just gives an empirical outline on how the yielding stress behaves. Concluding, neglecting the strain-rate sensitivity of yielding stress for mild steel pipelines would result in unrealistically high denting values which might lead to wrong conclusions of an integrity analysis.

10.1.3 Contribution of Fluid

The most realistic scenario would be that a marine pipeline will be operating when an impact occurs. However, DNV does not consider any effect of the internal pressure or the contents in general of the pipe in order to give a conservative estimate. To this end, analyses using a set of different finite element models has been carried out in order to obtain results that would give confidence.

The analyses have proven, the significance of the contents in the reduction of the maximum and permanent dent during an impact scenario. The force – dent curve of the pipeline exhibits an increased stiffness which is due to the work of the internal fluid that resists in the denting. For fluid filled pipelines, as the operating internal pressure increases the effect of the added mass of the fluid becomes negligible.

All the aforementioned however, come at a cost. More specifically, despite the additional stiffness of the pipeline against denting, the deformation profile of the dent is very localized, as the pressure holds the area away from the impact point intact. This means, that if a perforation damage analysis is conducted, it will be found that the pipeline can perforate or punctured with a smaller energy compared to the value that would be needed if it was empty. However, if the energy is less than the perforation energy, this means that the dent size will be significantly smaller compared to an empty pipe. Last but not least, the maximum exerted force on the pipeline is out of phase with the maximum denting deformation. This happens, because of the fluid movement inside the pipe, which has reported in full scale experiments from Yu and Jeong (2015) when conducting experiments for the puncture of pressurized tank cars. Last but not least, as the pressure increases inside the pipeline, the effect of added mass from the internal fluid can be neglected.

10.1.4 Contribution of Soil

The main goal of this thesis was to determine the effect of soil on the energy dissipation for an impact scenario. DNV conservatively neglects the effect of plasticity of the soil resulting in unrealistically high expected dent sizes. Due to the plastic deformation of the soil, the kinetic energy that initially would be absorbed as dent deformation in its entirety, will now be converted also in global deformation of the pipe.

This means, that a segment of the pipeline will penetrate into the soil. As expected, as the soil stiffness and the yield stress of the soil increase the dissipation of the energy in the form of plastic deformations decreases. For a very stiff soil, the dent deformation approaches the rigid bed case. Different soil profiles from very soft to very stiff have been considered in this investigation in order to account for a potential stiffer behavior of the soil when loaded dynamically.

For softer soil profiles, for a given kinetic energy of the falling object, the effect of the velocity has been investigated. Specifically, as the velocity increases due to the inertia of the pipe a global displacement of the pipe into the soil does not have time to occur, resulting in an increased dent depth compared to a case with lower impact velocity. This is rather important, as by knowing the velocity of the falling object a better approximation of the dent depth can be achieved and of course this means that the energy input only is not enough to estimate the response of the pipe but the mass and the velocity of the object are necessary as well.

Last but not least, the effect of a half-diameter trenched has been investigated to observe how the behavior of the pipe will change by this extra confinement. It has been observed that the absorbed energy in the form of dent deformation has increased and consequently the maximum and permanent dents. Although the absorbed energy increased, the effect of energy dissipation is still significant for soft soils and cannot be neglected. The effect of velocity still stands for the trenched pipeline.

10.1.5 Overall

In total, the following can be concluded for the denting behavior of a pipeline:

- The force-dent relationship of a pipeline depends on the geometrical characteristics of both the pipe and the falling object.
- Denting cannot be treated as a quasi-static problem as it has been shown that neglecting inertia and strain-rate leads to wrong conclusions. For semi-infinite tubes low-frequency damping is critical for the dynamic response, but is rather difficult to predict accurately.
- For a given configuration, the material yielding can alter the force-dent relationship as it is the most significant parameter of the pipe's resistance
- Regarding the pipeline contents, this preliminary study has shown that when pressurized the added mass effect is negligible compared to the additional stiffness gained by the pressure field. The inertia of the fluid affects the behavior of the pipeline globally as it resists more to a global penetration into the soil.
- The force-dent relationship for a given geometrical configuration, can only be changed when there is contribution from an external factor such as: fluid added mass, internal pressure, external pressure or soil passive resistance when the pipeline is confined which will add resistance to the system, requiring more (or less) energy to be spend to obtain the same dent depth.
- The bed flexibility effects do not change the force-dent relationship but rather remove energy from the system leading to reduced excited force and consequently reduced deformations. Thus, the resistance of the pipeline against denting does not change.
- When soil is taken into account, the local deformation is converted partially to global deformation. The decrease of local deformation is proportional to the velocity magnitude. With smaller velocity, the decrease of dent deformation in the pipeline is
- By taking into account all contributing parameters in an integrity assessment for a pipeline that was subjected to impact, it is possible to reduce the predicted damage level significantly as proposed by DNV.

10.2 Recommendations

The present thesis, has utilized some simplistic but accurate models to predict the behavior of the pipeline, the fluid and the soil when an impact might occur. Although some of these models, have been verified by experiments in the literature assumptions have been made to use them in the scope of the present thesis. Thus, in order to achieve results which will reflect reality as much as possible further research is needed in some of these topics.

Unsymmetrical Denting and Damage Model:

The present thesis and all known published literature are dealing with the case of an axisymmetric denting. In reality, the impact between the dropped object and the pipe will never be totally symmetrical and centered. Thus, an investigation on the effect of the position of impact has to be carried out, where torsion will be also induced in the system making the problem more complex. Additionally, a damage model should be introduced in the currently developed FEM model in order to capture any fracture or perforation that might take place for large strain values of the dented pipeline.

Experimental data

More relative experimental data are needed for assessing the damage of marine pipelines that go to infinity and no boundary conditions are practically active. The effect of external pressure in the dynamic denting of a pipeline has to be investigated. Moreover, the damping of the structure when subjected to impact would be very interesting to measure.

Soil Modeling.

As already mentioned, the soil behavior under dynamic impact loading is governed by large uncertainties. Regarding, clay the hardening of the soil has not been taken into account due to the lack of experimental data which describe hardening. However, the use of the Mohr-Coulomb model excluding pore pressures from the model is an approximation of the actual situation.

Thus, a detailed geotechnical oriented research on the matter is needed, where state of the art soil failure models with pore pressure will be implemented. The same applies for sand, where Omidvar has shown that its dynamic behavior is totally different than the static drained assumption and thus grain fracture and compaction has to be incorporated.

Fluid Modeling

In the present thesis, the fluid has been modeled within the Lagrangian framework, which neglects any material flow or dragging forces in the fluid itself. The results have been verified against an acoustic element fluid model where very good agreement was found. This approach has certain limitations when fluid has to be modeled instead of gas. To this end, it would be interesting to verify the findings of this thesis with a more detailed

Coupled Eulerian Lagrange model or even a Computational Fluid Dynamics simulation in order to capture the effect of the flow inside the pipe and go beyond the assumption that the fluid inside the pipe is stationary and confined in a fixed volume. Also, a multi-phase flow would be quite interesting to be investigated which is closer to the reality of operating pipelines.

DNV treatment

Finally, the author of this thesis believes that DNV should incorporate the effect of both soil plasticity and internal/external pressure when making an assessment. The very conservative assumptions used may lead to overestimation of the damage of a pipeline.

Moreover, it has been observed that DNV standards need to be integrated better, as some of the theory presented into one is not applied in the other. Especially for the impact analysis of a pipeline from a dropped object it is recommended that the following recommended practices should be combined to give a more realistic approach on the matter. Proposed DNV practices for integration:

- **DNVGL-RP-F105** Free spanning pipelines: Dynamic soil response.
- **DNVGL-RP-F107** Risk assessment of pipeline protection: Denting relationship, concrete coating contribution.
- **DNVGL-RP-F111** Interference between trawl gear and pipelines: Soil contribution in reducing energy input of an impact, formula for permanent dent calculation.
- **DNVGL-RP-F114** Pipe-soil interaction for submarine pipelines: Detailed modeling guidelines for soil and relative phenomena to be taken into account.
- **DNVGL-RP-C204** Design against accidental loads: Dissipation of strain energy between object and in place structure based on stiffness.

11. References and Bibliography

- 1) DNV-OS-F101-Submarine pipeline systems
- 2) DNV-RP-C204 – Design against accidental loads.
- 3) DNVGL-RP-F105 Free spanning pipelines
- 4) DNVGL-RP-F107 Risk assessment of pipeline protection
- 5) DNVGL-RP-F109 On-bottom stability design of submarine pipelines
- 6) DNVGL-RP-F111 Interference between trawl gear and pipelines
- 7) DNVGL-RP-F114 Pipe-soil interaction for submarine pipelines
- 8) Campbell, J. D. and J. Duby (1956). "The Yield Behavior of Mild Steel in Dynamic Compression." *Proceedings of the Royal Society A: Mathematical, Physical and Engineering Sciences* 236(1204): 24-40.
- 9) Hou, Z., et al. (2015). "Seafloor Sediment Study from South China Sea: Acoustic & Physical Property Relationship." *Remote Sensing* 7(12): 11570-11585.
- 10) Jones, N. and R. S. Birch (2010). "Low-velocity impact of pressurized pipelines." *International Journal of Impact Engineering* 37(2): 207-219.
- 11) Karamanos, S. A. and K. P. Andreadakis (2006). "Denting of internally pressurized tubes under lateral loads." *International Journal of Mechanical Sciences* 48(10): 1080-1094.
- 12) Karamanos, S. A. and C. Eleftheriadis (2004). "Collapse of pressurized elastoplastic tubular members under lateral loads." *International Journal of Mechanical Sciences* 46(1): 35-56.
- 13) Kawsar, M. R. U., et al. (2015). "Assessment of dropped object risk on corroded subsea pipeline." *Ocean Engineering* 106: 329-340.
- 14) Longva, V., et al. (2013). "Dynamic simulation of subsea pipeline and trawl board pull-over interaction." *Marine Structures* 34: 156-184.

- 15) Macdonald, K. A., et al. (2007). "Assessing mechanical damage in offshore pipelines – Two case studies." *Engineering Failure Analysis* 14(8): 1667-1679.
- 16) Mao, D., et al. (2015). "Deepwater Pipeline Damage and Research on Countermeasure." *Aquatic Procedia* 3: 180-190
- 17) Omidvar, M., et al. (2012). "Stress-strain behavior of sand at high strain rates." *International Journal of Impact Engineering* 49: 192-213.
- 18) Radovic, M., et al. (2004). "Comparison of different experimental techniques for determination of elastic properties of solids." *Materials Science and Engineering: A* 368(1-2): 56-70.
- 19) Vardanega, P. J. and M. D. Bolton (2013). "Stiffness of Clays and Silts: Normalizing Shear Modulus and Shear Strain." *Journal of Geotechnical and Geo-Environmental Engineering* 139(9): 1575-1589.
- 20) Yang, J. L., et al. (2009). "Experimental study and numerical simulation of pipe-on-pipe impact." *International Journal of Impact Engineering* 36(10-11): 1259-1268.
- 21) Yu, H. and D. Y. Jeong (2016). "Impact dynamics and puncture failure of pressurized tank cars with fluid–structure interaction: A multiphase modeling approach." *International Journal of Impact Engineering* 90: 12-25.
- 22) Zeinoddini, M., et al. (2013). "Response of submarine pipelines to impacts from dropped objects: Bed flexibility effects." *International Journal of Impact Engineering* 62: 129-141.
- 23) Mellem T, Spiten J, Verley R, Moshagen H, Trawl board impacts on pipelines, In: *Offshore mechanics and arctic engineering conference*, Vol. V, OMAE, 1996. p. 165–78.
- 24) T.-D. Park, S. Kyriakides On the collapse of dented cylinders under external pressure *International Journal of Mechanical Sciences*, 38 (1996), pp. 557-578
- 25) S.R. Reid, T.Y. Reddy Effects of strain hardening on the lateral compression of tubes between rigid plates *International Journal of Solids and Structures*, 14 (1978), pp. 213-225
- 26) T. Wierzbicki, M.S. Suh Indentation of tubes under combined loading *International Journal of Mechanical Sciences*, 30 (3/4) (1988), pp. 229-248

- 27) M. Zeinoddini, J.E. Harding, G.A.R. Parke Dynamic behavior of axially pre-loaded tubular steel members of offshore structures subjected to impact damage *Ocean Engineering*, 26 (1999), pp. 963-978
- 28) Hibbit HD, Karlsson BI, Sorensen P. Theory Manual, ABAQUS, version 6.3, USA, 2003.
- 29) Tang Y.H., Yu H., J.E. Gordon, D.Y. Jeong, A.B. Perlman, Analysis of Railroad Tank Car Shell Impacts Using Finite Element Method Proceedings of the 2008 IEEE/ASME Joint Rail Conference, JRC2008-63014 (2008)
- 30) Yu H., Tang Y.H., J.E. Gordon, D.Y. Jeong Modeling the effect of fluid-structure interaction on the impact dynamics of pressurized tank cars Proceedings of ASME International Mechanical Engineering Congress & Exposition, November (2009)
- 31) A. Palmer, A. Neilson, S. Sivadasan, Pipe perforation by medium-velocity impact, *International Journal of Impact Engineering*, 32 (2006), pp. 1145-1157
- 32) A. Palmer, M. Touhey, S. Holder, M. Anderson, S. Booth Full-scale impact tests on pipelines *International Journal of Impact Engineering*, 32 (2006), pp. 1267-1283
- 33) Sam Helwany, *Applied Soil Mechanics with Abaqus*

